RESEARCH

udot.utah.gov

Utah Department of Transportation - Research Division
4501 South 2700 West - P.O. Box 148410 - SLC,UT 84114-8410

Report No. UT-1X.XX

DESIGN AND EVALUATION OF EXPANDED POLYSTYRENE GEOFOAM EMBANKMENTS FOR THE I-15 RECONSTRUCTION PROJECT, SALT LAKE CITY, UTAH

Prepared For:

Utah Department of Transportation
Research Division

Submitted By:

University of Utah
Department of Civil and Environmental Engineering

Authored By:

Steven F. Bartlett, Ph.D., P.E.
Evert C. Lawton, Ph.D., P.E.
Clifton B. Farnsworth, Ph.D., P.E
Marie Perry Newman

October 2012

DISCLAIMER

The authors alone are responsible for the preparation and accuracy of the information, data, analysis, discussions, recommendations, and conclusions presented herein. The contents do not necessarily reflect the views, opinions, endorsements, or policies of the Utah Department of Transportation or the U.S. Department of Transportation. The Utah Department of Transportation makes no representation or warranty of any kind, and assumes no liability therefore.

This page intentionally left blank

ACKNOWLEDGMENTS

The authors acknowledge the Utah Department of Transportation (UDOT) for funding this research, and the following individuals from UDOT on the Technical Advisory Committee for helping to guide the research.

We also acknowledge the contributions of Syracuse University in installing and gathering some of the field performance data given in this report.

This page intentionally left blank

TECHNICAL REPORT ABSTRACT

1. Report No.	2. Government Accession No.	3. Recipient's Catalog No.
UT- 1X.XX	N/A	N/A

4. Title and Subtitle	5. Report Date
DESIGN AND EVALUATION OF EXPANDED POLYSTYRENE GEOFOAM EMBANKMENTS FOR THE I-15 RECONSTRUCTION PROJECT, SALT LAKE CITY, UTAH	October 2012
	6. Performing Organization Code

7. Author(s)	8. Performing Organization Report No.
Steven F. Bartlett, Evert C. Lawton, Clifton B. Farnsworth, Marie Perry Newman	

9. Performing Organization Name and Address	10. Work Unit No.
Department of Civil and Environmental Engineering University of Utah 110 Central Campus Dr. Salt Lake City, Utah 84112	5H06615H
	11. Contract or Grant No. 06-9156

12. Sponsoring Agency Name and Address	13. Type of Report & Period Covered
Utah Department of Transportation 4501 South 2700 West P.O. Box 148410 Salt Lake City, UT 84114-8410	Final
	14. Sponsoring Agency Code Project ID Code TB98.029a

15. Supplementary Notes

Prepared in cooperation with the Utah Department of Transportation and the U.S. Department of Transportation, Federal Highway Administration

16. Abstract

The report discusses the design and 10-year performance evaluations of Expanded Polystyrene (EPS) Geofoam embankment constructed for the I-15 Reconstruction Project in Salt Lake City, Utah between 1998 and 2002. It contains methods to evaluate the allowable stress in the EPS from live (traffic) and dead loads. It also contains numerical modeling of the pressure and deformation data collected as part of the long-term monitoring effort. Based on these data, this report demonstrates that the design criteria in regards to creep and settlement were met. In addition, the seismic stability of free-standing EPS embankments is evaluated and recommendations are made regarding how to improve their seismic performance. A simplified design methodology is presented to evaluate the embankment for interlayer seismic sliding.

17. Key Words	18. Distribution Statement	23. Registrant's Seal
Expanded Polystyrene, Geofoam, Light-weight embankment, Rapid Construction	Not restricted. Available through: UDOT Research Division 4501 South 2700 West P.O. Box 148410 Salt Lake City, UT 84114-8410 www.udot.utah.gov/go/research	N/A

19. Security Classification (of this report)	20. Security Classification (of this page)	21. No. of Pages	22. Price
Unclassified	Unclassified	zzz	N/A

This page intentionally left blank

TABLE OF CONTENTS

LIST OF TABLES

This page intentionally left blank

LIST OF FIGURES

This page intentionally left blank

UNIT CONVERSION FACTORS

SI* (MODERN METRIC) CONVERSION FACTORS

APPROXIMATE CONVERSIONS TO SI UNITS

Symbol	When You Know	Multiply By	To Find	Symbol
		LENGTH		
in	inches	25.4	millimeters	mm
ft	feet	0.305	meters	m
yd	yards	0.914	meters	m
mi	miles	1.61	kilometers	km
		AREA		
in^2	square inches	645.2	square millimeters	mm^2
ft^2	square feet	0.093	square meters	m^2
yd^2	square yard	0.836	square meters	m^2
ac	acres	0.405	hectares	ha
mi^2	square miles	2.59	square kilometers	km^2
		VOLUME		
fl oz	fluid ounces	29.57	milliliters	mL
gal	gallons	3.785	liters	L
ft^3	cubic feet	0.028	cubic meters	m^3
yd^3	cubic yards	0.765	cubic meters	m^3
	NOTE: volumes greater than 1000 L shall be shown in m^3			
		MASS		
oz	ounces	28.35	grams	g
lb	pounds	0.454	kilograms	kg
T	short tons (2000 lb)	0.907	megagrams (or "metric ton")	Mg (or "t")
		TEMPERATURE (exact degrees)		
°F	Fahrenheit	5 (F-32)/9 or (F-32)/1.8	Celsius	°C
		ILLUMINATION		
fc	foot-candles	10.76	lux	lx
fl	foot-Lamberts	3.426	$candela/m^2$	cd/m^2
		FORCE and PRESSURE or STRESS		
lbf	poundforce	4.45	newtons	N
lbf/in^2	poundforce per square inch	6.89	kilopascals	kPa

APPROXIMATE CONVERSIONS FROM SI UNITS

Symbol	When You Know	Multiply By	To Find	Symbol
		LENGTH		
mm	millimeters	0.039	inches	in
m	meters	3.28	feet	ft
m	meters	1.09	yards	yd
km	kilometers	0.621	miles	mi
		AREA		
mm^2	square millimeters	0.0016	square inches	in^2
m^2	square meters	10.764	square feet	ft^2
m^2	square meters	1.195	square yards	yd^2
ha	hectares	2.47	acres	ac
km^2	square kilometers	0.386	square miles	mi^2
		VOLUME		
mL	milliliters	0.034	fluid ounces	fl oz
L	liters	0.264	gallons	gal
m^3	cubic meters	35.314	cubic feet	ft^3
m^3	cubic meters	1.307	cubic yards	yd^3
		MASS		
g	grams	0.035	ounces	oz
kg	kilograms	2.202	pounds	lb
Mg (or "t")	megagrams (or "metric ton")	1.103	short tons (2000 lb)	T
		TEMPERATURE (exact degrees)		
°C	Celsius	1.8C+32	Fahrenheit	°F
		ILLUMINATION		
lx	lux	0.0929	foot-candles	fc
cd/m^2	$candela/m^2$	0.2919	foot-Lamberts	fl
		FORCE and PRESSURE or STRESS		
N	newtons	0.225	poundforce	lbf
kPa	kilopascals	0.145	poundforce per square inch	lbf/in^2

*SI is the symbol for the International System of Units. (Adapted from FHWA report template, Revised March 2003)

This page intentionally left blank

EXECUTIVE SUMMARY

The Utah Department of Transportation (UDOT) has made extensive use of Expanded Polystyrene (EPS) geofoam block for several major embankments in Salt Lake Valley, Utah. Constructed between 1998 and 2001, the Interstate 15 (I-15) Reconstruction Project involved the widening of interstate embankments within a 27-km corridor with limited right-of-way. Approximately, 100,000 m^3 of EPS block was placed at various locations to minimize postconstruction settlement of deep, compressible lake deposits. This report discusses the design, construction and long-term performance of the EPS fill constructed for the I-15 Reconstruction Project. Geofoam embankments had the best overall settlement performance of the geotechnologies monitored (Farnsworth et al., 2008).

To limit damage and long-term creep deformation of geofoam embankment, the compressive stresses caused by the combination of live and dead loads must be limited to acceptable levels. The I-15 Reconstruction Project geofoam embankments were designed using the draft European Standard of 1998. To limit long-term creep deformation of the geofoam block to non-damaging levels, the working stress level due to dead load (i.e., self-weight of overlying material) was limited to 30 percent of the compressive resistance for Type VIII geofoam. Also, an additional 10 percent of the compressive resistance was allowed to account for live traffic loads; hence the total load combination of dead and live load could not exceed 40 percent of the compressive resistance at 10 percent axial strain, or about 40 kPa (Bartlett et al., 2000).

The postconstruction settlement monitoring shows that the I-15 geofoam embankments are performing as designed, thus validating the 1998 European Standards, which have been updated in 2011 (EPS White Book, 2011) and are further described and compared with other EPS design guidance in this report. Long-term field measurements from the I-15 Reconstruction Project show that the creep settlement will not exceed the 50-year postconstruction deformation limit of 1% creep strain (Negussey and Stuedlein, 2003). In addition, construction settlement measurements show that the EPS embankment undergoes about 1 percent settlement during construction due to gap closure between the block and elastic deformation of the geofoam

embankment from the placement of the load distribution slab and overlying roadway materials (Bartlett et al. 2001).

Experience has shown that extra care is required when placing earthern fill in areas of geofoam placement. For example at the 3300 South Street geofoam location, the foundation soil settled only about 15 mm when the EPS block and pavement were constructed. However, the face of the EPS embankment settled an additional 25 mm in a 5-year period because a 1.5-m earthern toe berm was constructed along the base of the wall (Farnsworth et al., 2008). Because of this, total postconstruction settlement (foundation settlement and geofoam creep) is expected to be about 50 mm at the wall face for a 10-year postconstruction period.

Numerical modeling was also used to estimate the complex stress distribution and the displacements (i.e. strain) that developed in some of the geofoam embankments. The proposed numerical approach used a bilinear elastic model to produce reasonable estimates of gap closure, block seating and the subsequent elastic compression of the geofoam embankment at higher stress levels. Such estimations are important for modeling and designing geofoam embankments and potential connections with other systems. The calculation of the complex stress distribution and displacements that develops in a geofoam embankment has application to settlement, lateral earth pressure against retaining and buried walls, slope stability and seismic design of geofoam embankments.

EPS geofoam can also be used to construct earthquake resilient infrastructure in areas with high seismicity because of its extremely low mass density and relatively high compressibility when compared with traditional backfill materials. This report also summarizes recent research regarding the seismic design and construction of EPS geosystems to improve the resiliency of embankment and slopes. The evaluations suggest that interlayer block sliding may be initiated in some free standing geofoam embankments and the amount of sliding displacements depends on the amplitude and long-period characteristics of the inputted strong motion. Therefore, shear keys, or other structural/mechanical restraints, are recommended for free-standing EPS embankment systems where the seismically-induced sliding displacement is potentially damaging to the geosystem.

1.0 INTRODUCTION

From 1998 to 2001, the Utah Department of Transportation (UDOT) and a large construction consortium reconstructed Interstate Highway 15 (I-15) in the Salt Lake Valley prior to the start of the 2002 Winter Olympic Games. Utah's rapidly growing population and traffic flow necessitated the widening of the freeway from 6 lanes to 12 lanes, but the awarding of the Winter Games gave momentum to the project and placed a rigid and challenging time constraint on its completion. During a 3.5-year period, 26 km of urban interstate were reconstructed, which included 144 bridges and 160 mechanically stabilized earth (MSE) retaining walls. To achieve the accelerated schedule, designers implemented geotechnical technologies including: a lime cement column (LCC) supported embankment, accelerated drainage with prefabricated vertical drains (PVD), multi-staged embankment construction with geotextile reinforcement, two-stage MSE walls, and lightweight embankments including scoria and geofoam. This reconstruction project earned the ASCE 2002 Outstanding Civil Engineering Achievement Award (Negussey et al., 2003).

The widened I-15 alignment required the placement of large embankments (8 to 10 m high) atop soft clayey foundation soils. These soils had the potential to produce primary consolidation settlement exceeding 1 m at many locales. In some areas, preexisting utility lines crossed beneath the freeway and would be damaged by the settlement caused by new embankment construction. To allow these utilities to remain in-service without costly relocation and delays, the design team chose to use expanded polystyrene (EPS) geofoam for embankment construction. The placement of this extremely lightweight material, with a density of 18 kg / m^3, allowed rapid construction of full-height embankments in a short period of time without costly utility relocations.

As the project progressed, UDOT Research personnel and researchers from the University of Utah and Syracuse University placed geotechnical instrumentation adjacent to and in the geofoam embankments at several locations to monitor the construction and post-construction performance (Bartlett and Farnsworth, 2004). This report discusses the design, field performance monitoring and numerical modeling of I-15 geofoam embankments on the I-15

Reconstruction Project in Salt Lake City, Utah (Bartlett et al., 2001; Negussey et al., 2001; Negussey and Studlein, 2003). At select locations, geotechnical instrumentation was placed atop and within the geofoam in order to measure the vertical and horizontal stresses that develop in the geofoam embankment and underlying soils and to record the amount of vertical displacement related to the static loading and long-term creep of the geofoam. Pressure cell, magnet extensometer and optical survey data from the above instrumentation arrays have been collected for approximately 10 years since the start of embankment construction.

This report provides a summary of these data and discusses the design used for the I-15 Reconstruction Project. It compares the I-15 design methodology with current design guidance developed in Japan, Europe and the United States. It also compares the measurements from geofoam instrumentation arrays with numerical modeling results to estimate the vertical and horizontal stress distribution and vertical displacement that developed during the static loading of I-15 geofoam embankments. It also discusses the evaluation of the seismic stability of geofoam embankments subjected to strong ground motion from nearby, large earthquakes typical for the tectonic regime found in Utah.

The design and modeling of the performance data described herein was performed using *FLAC* (Fast Lagrangian Analysis of Continua), a general finite difference program developed by Itasca (2005) for geomaterials. The *FLAC* models are compared with analytical solutions and field measurements to verify the numerical solutions. The modeling was used to develop a better understanding of the complex vertical and horizontal stress distributions and displacements that develop in these composite systems.

2.0 SUMMARY OF DESIGN METHODS FOR ALLOWABLE STRESS FOR EPS

To limit damage and long-term creep deformation of geofoam embankment, the compressive stresses caused by live and dead loads must be limited to acceptable levels. This section of the report describes the current methods of evaluating the allowable stress in the EPS embankment based on design guidance from Japan, Europe and the United States. A design example is also included to aid future engineers involved in the design and construction of EPS systems.

2.1 I-15 Reconstruction Project (Bartlett et al. 2000)

The design of the I-15 Reconstruction Project geofoam embankments is more fully described in Bartlett et al., 2000. The I-15 Reconstruction Project design team specified geofoam with no more than five percent regrind content. Although both Type VIII and Type II geofoam (ASTM C-578) were approved, only Type VIII geofoam was used (Table 2-1). (The nominal density of Type VIII is essentially equivalent to EPS18 (18 kg/m^3.) The blocks installed on the I-15 project were 0.8 m high by 1.2 m wide by 4.9 m long. The blocks, as manufactured, met the specified ± 0.5 percent dimensional and 5% flatness tolerances and trimming was not necessary. The overall design considered the nominal compressive resistance at 10 percent strain for Type VIII geofoam using ASTM-C-578-95 (Table 2-1).

Project-specific compressive testing was done on Type VIII geofoam supplied by ACH Foam of Murray, Utah formerly known as Advanced Foam Plastics (Figure 2-1). This testing showed that the Type VIII geofoam exceeded the requirements of ASTM-C-578-95, which was required in the project specifications. At 10 percent compressive strain, the compressive resistance for the I-15 geofoam varied between 100 to 122 kPa (14.5 to 17.7 psi) as performed on 5-cm (2-inch) cube samples (Figure 2-1), which is somewhat higher than the nominal values given in Table 2-1. In addition, the corrected initial Young's moduli from these same compressive tests were in the range of 2.9 to 5.1 MPa. (Bartlett et al. 2000).

Table 2-1 Typical EPS Properties from ASTM-C-578-95 (from Bartlett et al. 2000)

Physical Property	ASTM Test Procedure	Type VIII Accepted Value	Type II Accepted Value	Tolerances
Density	D1622	18 kg/m^3	22 kg/m^3	± 10 %
Compressive Resistance	D1621	90 kN/m^2	104 kN/m^2	minimum @ yield or 10 percent axial deformation
Flexural Strength	C203	208 kN/m^2	276 kN/m^2	Minimum
Water Absorption	C272	3	3	< % by volume

The I-15 Reconstruction Project geofoam embankments were designed using the draft European Standard of 1998. To limit long-term creep deformation of the geofoam block to non-damaging levels, the working stress level due to dead load (i.e., self-weight of overlying material) was limited to 30 percent of the compressive resistance for Type VIII geofoam, or about 30 kPa based on a compressive resistance of 100 kPa at 10 percent strain (Figure 2-1). Also, an additional 10 percent of the compressive resistance or 10 kPa was allowed to account for live traffic loads; hence the total load combination of dead and live load could not exceed 40 percent of the compressive resistance at 10 percent axial strain, or about 40 kPa. No partial load factors were applied to the dead and live loads. Adherence to these allowable load criteria were believed to result in no more than 2 percent creep strain in 50 years as outlined by the draft European Standard (1998).

Subsequent monitoring of EPS embankment over a 10-year period shows that this creep performance goal has been met by the I-15 Reconstruction Project design and construction methodologies. Instrumentation was installed at several geofoam embankment locations to monitor the construction and post-construction performance. Pressure cell measurements show that the vertical stress (i.e., dead load) from the overlying pavement system induced in the geofoam embankment varies between about 20 to 35 kPa. Long-term creep measurements project that construction and post-construction vertical strain will be less than 2 percent in 50 years, as discussed later in this report.

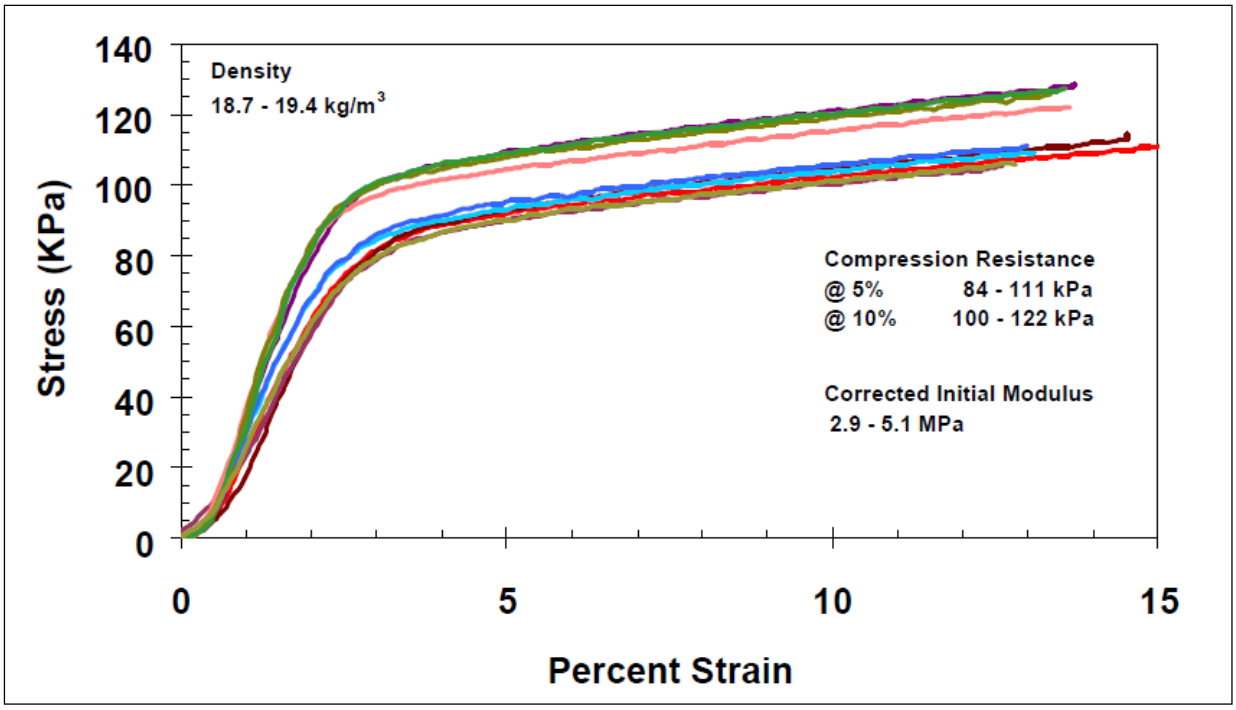

Figure 2-1 Compressive Resistance (Stress) Versus Strain for I-15 Type VIII Geofoam (from Bartlett et al., 2000).

2.2 Japanese Practice as Developed by EDO (Tsukamoto, 2011)

The EPS method Development Organization (EDO) was established to promote the technical development and application of EPS geofoam method in Japan. The compressive strength of EPS at 10 percent axial strain geofoam is measured for quality control purposes by using 5-cm (i.e., 2-inch) cubic specimens, which are loaded at a rate of 10% strain per minute. However for design, the allowable stress level in the EDO method is set to 50 percent of the compressive strength at 10 percent axial strain (Table 2-2).

Table 2-2 Unit Weight and Compressive Strength for EDO Geofoam (Tsukamoto, 2011).

	Expanded(EPS)					Extruded(XPS)		
Type	D-30	D-25	D-20	D-16	D-12	DX-35	DX-29	DX-24H
Unit weight (kN/m3)	0.30	0.25	0.20	0.16	0.12	0.35	0.29	0.24
Allowable compressive stress (kN/m2)	90	70	50	35	20	200	140	100
Compressive stress for QC (kN/m^2) 10% strain	180	140	100	70	40	400	280	200

The EDO method specifies the requirements for calculating the stress redistribution above and below the EPS embankment. Live and dead load vertical stress distributions are

calculated for the EPS embankment assuming that the load redistribution angle varies according to the pavement structure and whether or not a concrete load distribution slab (LDS) is present atop the EPS. When a LDS is placed between the pavement and the EPS, the stress redistribution angle is set to 45 degrees for the pavement section and the concrete slab (Figure 2-2). When no LDS is present, this angle is set to 30 degrees in the design calculation. The load distribution angle inside the EPS embankment is set to 20 degrees (measured from the vertical) in the calculation regardless if a LDS is present (Figure 2). The EDO method does not appear to use any additional load factors for the live and dead loads.

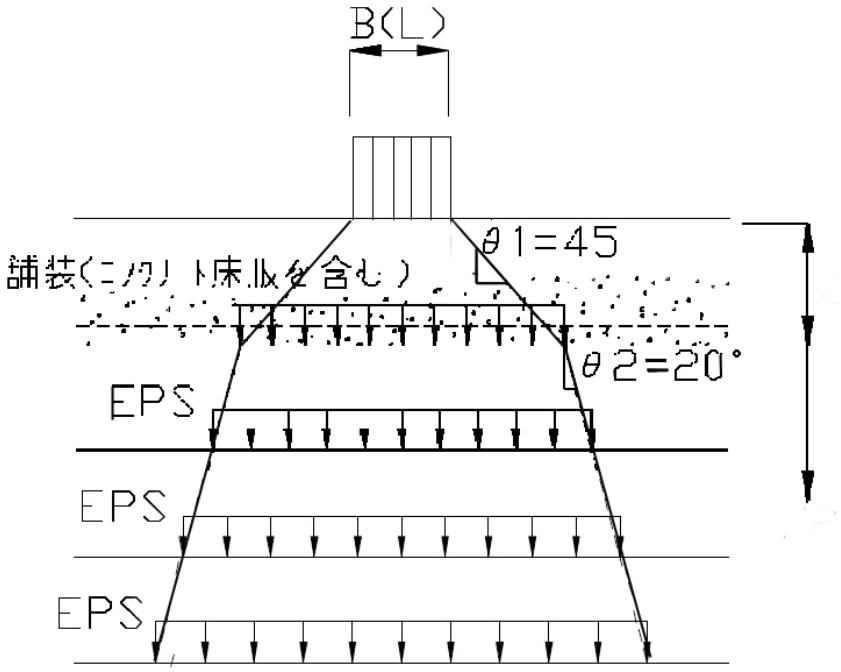

Figure 2-2 Vertical Stress Redistribution Chart for EDO Design Method (from Tsukamoto, 2011).

2.3 European Standards (EPS White Book, 2011)

As a result of the EU policy to strengthen the European Union by encouraging free trade of building products between member countries, product standards for building product groups have been created over the past 20 years. The product standard for EPS in Civil Engineering Applications (EN 14933) was adopted in March 2009.

The EPS product values shown in Table 2-3 represent samples of EPS that have various compressive strengths at 10 percent axial strain using 5-cm cubic samples. For example, the declared compressive strength (i.e., resistance) of EPS100 is 100 kPa at 10 percent axial strain. This is called the "declared short-term value of compressive strength (σ_{10})" (Table 2-3). However the declared values are factored to a design value ($\sigma_{10,d}$) by dividing the declared compressive strength by a material resistance factor (γ_m) of 1.25 and by multiplying this reduced value by additional resistance factors that depend on the type of loading condition. The loading conditions considered by Table 2-3 are: (1) short-term conditions ($\sigma_{10,d}$), (2) permanent conditions ($\sigma_{10,perm,d}$) and (3) cyclic (i.e., traffic) loading ($\sigma_{10,cycl,d}$). The design factor for short-term conditions is 1.0, the design factor of permanent conditions is 0.30, and the design factor for cyclic loading is 0.35.

It should be noted that in the European Standards, σ_{10} is only used to classify EPS products and to obtain reproducible and repeatable test results for factory production control purposes. In addition, the values of σ_{10} shown in Table 2-3 are based on testing of materials over several decades; however, if a EPS producer is able to prove that better results are produced using certified laboratory data, these better results can be used for σ_{10} in the design (EPS White Book, 2011).

Regarding creep deformation resulting from the permanent loading, EPS geofoam is expected to have a compressive creep deformation of 2%, or less, after 50 years when subjected to a permanent compressive stress of less than 30 percent of the compressive resistance at 10 percent axial strain (σ_{10}) (EPS White Book, 2011). For example, the design value for permanent compressive resistance of EPS100 is 0.30 * σ_{10}, or 30 percent of σ_{10}. However, the design value for permanent applications, σ_{10} perm, is also divided by the material factor of 1.25, thus the design value $\sigma_{10,perm,d}$ is 0.3 * 100/1.25 or 24 kPa for EPS 100 (Table 2-3).

Regarding cyclic (i.e., traffic) loadings, European researchers have concluded that with a relative light permanent loading at the top (i.e.,15 kN/m^2), and if the vertical deformation under a cyclic loading remains under 0.4%, then the resulting EPS deformation will be elastic and there

will be no permanent deformation (EPS White Book, 2011). In terms of vertical stress, the maximum safe value due to cyclic loading is 0.35 * σ_{10}. Thus, the design compressive strength of EPS100 under cyclic load $\sigma_{10;cycl;d}$ is 0.35 * σ_{10} / 1.25, or 28 kPa (Table 2-3).

The design criteria for the various load combinations are summarized in the paragraphs below citing the instructions given in the White Book (2011). Some additional comments by the authors of this report have been added in italicized script.

Ultimate Limit state (STR) short term (EPS White Book, 2011)

"Loading combination: Multiply the dead and imposed load with their respective loading factors and combine both loads. Calculate the acting design compressive stress $\sigma_{10;d}$ and compare it with the short term design compressive strength (e.g. 80 kPa for EPS 100). The short term acting stress should be less than or equal to the short term strength."

(Note that this ultimate limit state considers the permanent dead loads, construction-related dead and live loads, and the cyclic (i.e., traffic) loads. The loading factors from the White Book consist of a 1.35 loading factor for permanent loads (i.e., dead loads) and a 1.5 loading factor for cyclic (i.e., traffic) loads. In the STR-short loading combination, the permanent dead load from the pavement section and the traffic loads are also included.)

Ultimate Limit state (STR) permanent (EPS White Book, 2011)

"Loading combination: Multiply the dead load and the permanent part of the imposed load (mostly zero in civil applications) with their respective loading factors and combine both loads. Calculate the acting design compressive stress and compare it with the permanent design strength $\sigma_{10;perm;d}$ (e.g. 24 kPa for EPS100). The permanent acting stress should be less than or equal to the permanent strength."

(Note that in highway applications, the permanent load is the vertical stress corresponding to the weight of the pavement, base, sub-base, LDS and other materials placed atop the EPS. In the

STR-permanent loading combination, only these permanent dead loads are only.)

Ultimate Limit state (GEO) cyclic loads (EPS White Book, 2011)

"Loading: Multiply the cyclic load with the factor $\gamma_Q = 1.50$. Calculate the acting design compressive stress and compare it with the design cyclic strength $\sigma_{10;cycl;d}$ (e.g. 24 kPa for EPS100).

(In the GEO-cyclic load combination, the cyclic loads from traffic are considered and the dead loads are assumed not to exceed 15 kPa. The EPS White Book (2011) does not give guidance regarding cases where the permanent dead loads exceed 15 kPa and traffic loads are present.)

Construction phase (EPS White Book, 2011)

"The worst case scenario [is] to be taken."

Table 2-3 Declared and Design Compressive Resistance Values of EPS in European Code (from EPS White Book, 2011).

Property			EPS product type				
Description	Symbol	Unit	EPS60	EPS100	EPS150	EPS200	EPS250
Declared value short-term compressive strength	σ_{10}	kPa	60	100	150	200	250
Design value short-term compressive strength	$\sigma_{10;d}$	kPa	48	80	120	160	200
Modulus of elasticity	E_t; E_{dyn}	kPa	4000	6000	8000	10000	12000
Declared value permanent compressive strength	$\sigma_{10;perm}$	kPa	18	30	45	60	75
Design value permanent compressive strength	$\sigma_{10;perm;d}$	kPa	14,4	24	36	48	60
Declared value compressive strength under cyclic load	$\sigma_{10;cycl}$	kPa	21	35	52,5	70	87,5
Design value compressive strength under cyclic load	$\sigma_{10;cycl;d}$	kPa	17	28	42	56	70

A sample design calculation with the required loading combinations for EPS 100 (EPS White Book, 2011) is shown in Figure 2-3. The EPS White Book (2011) does not discuss a method for calculating the vertical stress redistribution of the applied surface load with depth, as

was done with the Japanese EDO method (Figure 2-2). However, finite-element numerical modeling has been used extensively in the research associated with the development of European Standards (Duskov, 1997). In addition, EPS roadway projects in the Netherlands have made use of the finite element program PLAXIS^{TM} to estimate the vertical stress distribution in EPS embankments from traffic loadings.

2.4 NCHRP 529 (2004)

NCHRP Report 529 (2004) consists of design guidelines, supporting material and a proposed construction standard for EPS-block geofoam. The project final technical report with four unpublished appendixes is available as *NCHRP Web Document 65. NCHRP Reports 529 and Web Document 65* can be used as additional sources for EPS design, but the implementation of such design procedures/approaches has not been as widely reviewed when compared with methods found in European and Japanese guidance/standards.

In contrast to European and Japanese approaches, the allowable stress (i.e., allowable elastic stress limit in NCHRP 529) is based on the compressive resistance at 1 percent strain (Table 2-4), instead of that at 10 percent strain as is used in other countries. In NCHRP 529, the allowable stress under the combination of dead and live loads is calculated as the stress value corresponding to 1 percent of the initial tangent modulus of the EPS. In NCHRP 529 nomenclature, EPS50 is type of EPS block that has a compressive resistance of 50 kPa at 1 percent vertical strain (Table 2-4). This also means the initial tangent modulus for EPS50 is: 50 kPa divided 0.01, or 5 MPa (Table 2-4). The typical mass density of EPS50 is 20 kg/m^3, which most closely corresponds to the nominal 18 kg/m^3 density of EPS used on the I-15 Reconstruction Project.

As an example a typical road in the "Polders' in the western part of the Netherlands i herewith taken. The road is constructed by removing the peat soil to a depth of aroun 1,5 m; adding EPS 100 kPa blocks to a height of 2 m, putting a sand/gravel combinatio over it to distribute the point loads; it is finished with a double asphalt layer.

Cross section typical Polderroad NL

Loadings:
Permanent loads (γ=1,35)

0,15 m asphalt bitumen layers	0,15 * 2100 kg/m^3 =	3,1 kN/m^2
0,50 m gravel/sand	0,50 * 1800 kg/m^3 =	9,0 kN/m^2
2,0 m EPS 100	2,00 * 100 kg/m^3 =	2,0 kN/m^2
	TOTAL =	14,1 kN/m^2

Traffic load (γ =1,50)
Cyclic and uniformly distributed on EPS = 15,0 kN/m^2

Loading combinations:
STR- short:
1,35 * 14,1 + 1,50 * 15 = 41,35 < 80 for EPS100 ? O.K.
STR-permanent
1,35 * 14,1 = 19,05 < 24 for EPS100? O.K.
GEO-Cyclic
1,50 * 15 = 22,50 < 28 for EPS100? O.K.

Conclusion: The product properties of EPS 100 fulfil the performance requirements

Figure 2-3 Design Example for Calculating Allowable Stress from European White Book.

Dead loads are permanent loads that develop from the self-weight of the pavement section and load distribution slab (if present). Live loads are generally considered to be traffic loadings. In addition, NCHRP 529 requires that load factors be applied to the design live loads. A factor of 1.3 is applied to the traffic load to account for the potential of impact loading. Also, the combination of the dead and factored live loads is multiplied by a factor of 1.2 and compared with the elastic limit stress given in Table 2-4. The same load factor of 1.2 is also recommended for other transient live loadings such as wind, hydrostatic uplift, interblock sliding, and seismic loading used for external stability analyses.

Simplified methods are proposed by NCHRP 59 and Wed Document 65 to calculate the stresses induced in the top of the EPS by the overlying dead and live loads. 1-D stress calculations are recommended using the appropriate unit weights of the pavement and base materials in order to calculate the vertical stress from the dead load (e.g., pavement, base, sub-base materials and load distribution slab placed above the EPS).

For live (i.e., traffic) loads, NCHRP 529 recommends a procedure based on an elastic layered solution (Burmister, 1943) to estimate the vertical stress distribution at the top of the EPS embankment. Burmister's solution is applicable for a uniform surface pressure applied as a circular area on top of an elastic, semi-infinite half-space. It can be applied to a 2-layered system with varying moduli for each layer as long as the modulus ratio between the stiff, upper layer (i.e., pavement system) and the soft, underlying layer is less than 100. However, this moduli ratio is greater than 100 when EPS is used as the underlying layer; hence Burmister's solution does not apply to many roadway sections containing underlying EPS. Thus, the NCHRP 529 recommendation is not applicable for a complex, layered pavement systems consisting of (from top to bottom) pavement/base/load distribution slab/geofoam, such as was used on the I-15 Reconstruction Project. For such layered systems, we recommend that numerical modeling be performed to determine the stress at the top and within the EPS embankment, as discussed in the next section.

NCHRP 529 also recommends simplified methods to calculate the vertical stress redistribution within the EPS embankment from traffic loads. For redistribution of stresses

within the EPS, a 2V:1H distribution is recommended. (This corresponds to a 26.6 degree angle referenced to the vertical direction.)

Table 2-4 Minimum allowable values of elastic limit stress and initial tangent modulus (NCHRP 529).

Material Designation	Dry Density of Each Block as a Whole, kg/m^3 (lbf/ft^3)	Dry Density of a Test Specimen, kg/m^3 (lbf/ft^3)	Elastic Limit Stress, kPa (lbs/in^2)	Initial Tangent Young's Modulus, MPa (lbs/in^2)
EPS40	16 (1.0)	15 (0.90)	40 (5.8)	4 (580)
EPS50	20 (1.25)	18 (1.15)	50 (7.2)	5 (725)
EPS70	24 (1.5)	22 (1.35)	70 (10.1)	7 (1015)
EPS100	32 (2.0)	29 (1.80)	100 (14.5)	10 (1450)

2.5 Sample Size Effects

All of the design methods discussed thus far are based on defining the design stress in the EPS using test results from 5-cm (2 in) cube samples. However, the size of the EPS specimen tested in the laboratory influences the compressive resistance and Young's modulus (Elragi, 2000; Elragi et al. 2000). Elragi (2000) showed that the distribution of vertical strains over the height of a geofoam sample is not uniform and that results from conventional 5-cm cube samples significantly underestimate Young's modulus of geofoam when compared with larger block samples. The main cause for the underestimation in the 5-cm cube samples was attributed to crushing and damage near the geofoam surface and rigid platen loading interfaces used in the laboratory testing.

The testing results shown in Figure 2-4 suggests that the initial Young's modulus for 60-cm cube block of EPS19 is about twice the value obtained from 5-cm cube samples. Therefore, the Young's modulus of full-sized EPS block placed in large embankments may be significantly underestimated using 5-cm cube samples (Elragi, 2000; Neguessey and Stuedlein, 2003). This further suggests that current design methods from the U.S., Europe and Japan, which are based on test results from 5-cm cube samples, may be overly conservative in that they consistently underestimating the real value of Young's modulus for EPS full-sized block used in

embankment construction. Hence, it is likely that there is a larger factor of safety against EPS damage and creep than represented by current design guidance. More study is needed to determime the consequences of this in terms of design procedures.

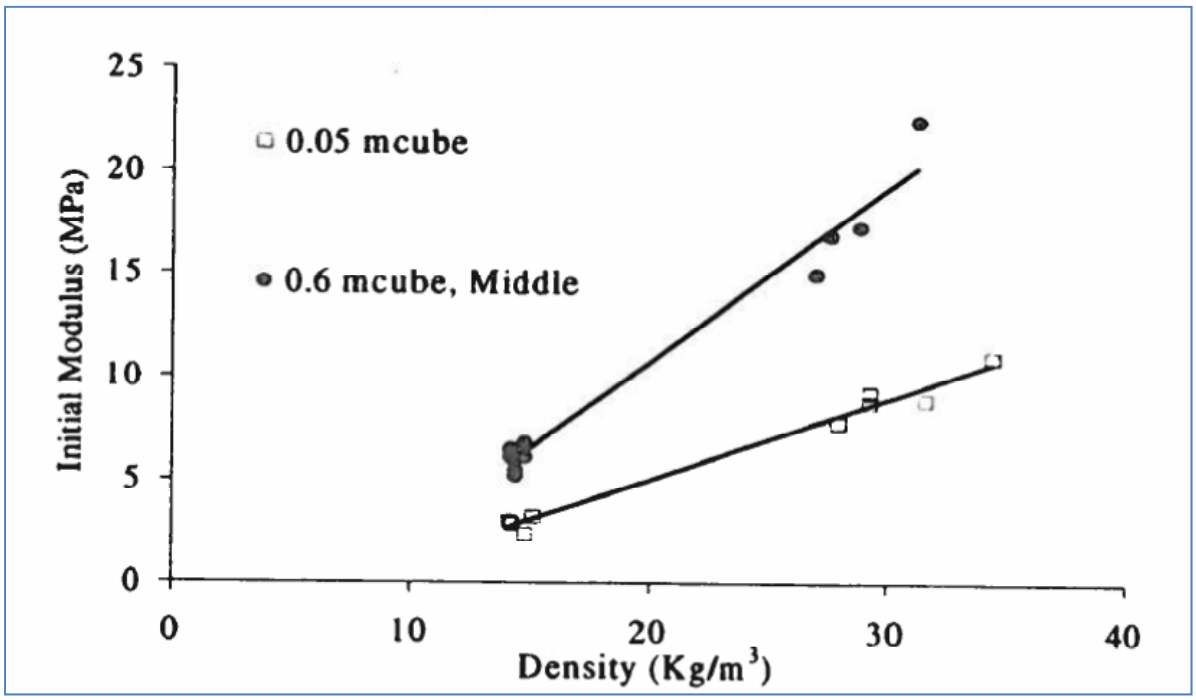

Figure 2-4 Initial Young's Modulus Values for 5-cm and 60 cm Cube Samples as a Function of EPS Density and Sample Size (Elragi et al., 2000).

3.0 ESTIMATION OF LIVE LOADS FOR HS-20 TRUCK LOADING

3.1 Introduction

This section discusses how to estimate the design vertical stress distribution in multi-layered elastic pavement systems caused by an AASHTO HS-20 25-kip dual rear axle tire load placed atop a concrete pavement/EPS system. Later, the design guidance in NCHRP 529 and the European White Book (2011) are used to check the allowable stresses in the EPS from this standard truck loading. In order to calculate the vertical stress induced in the top of the EPS, a 2D finite difference model, i.e., FLAC (Fast Lagrangian Analysis of Continua) (Itasca, 2005) is verified and implemented. The model is a 2D axisymmetrical elastic model with tire loading converted to an equivalent circular load.

In EPS design outlined by NCHRP 529, the vertical stresses imposed by live (i.e., traffic) loads are calculated as though they were static loading using simplified stress distributions that have their origins in foundation design. As discussed in the previous section, NCHRP 529 recommends the use of Burmister (1943) to calculate the vertical stress distribution in the top of the EPS block. Burmister (1943) extended classical elastic theory to multi-layered elastic systems and his solutions have been widely applied in pavement design to calculate the stress induced in pavement systems from tire loadings.

However, for the case where a concrete load distribution slab is constructed atop EPS block, as typically done by UDOT, the modulus ratio of concrete to EPS is approximately 6000 (i.e., the Young's modulus of concrete is approximately 6000 times stiffer than that of EPS); hence Burmister's (1943) solution is not applicable for this case because of the high modulus ratio. (Burimister's (1943) solution was developed for a maximum modulus ratio of 100.) Therefore, the NCHRP 529 recommendation to use Burmister (1943) cannot be strictly followed for a case where a concrete load distribution slab is placed atop EPS. For such situations, we recommend that numerical modeling be done to estimate the vertical stress distribution in the EPS using elastic properties for the various materials, as was done by Duskov (1997); and as is

commonly used in European practice. Such modeling can be used to estimate the vertical stress redistribution through the LDS and into the EPS from live loads.

Numerical modeling is applicable for multilayered systems where the corresponding layer moduli vary significantly. Traditionally, such modeling is done using elastic properties for the various layers, because it is assumed that the applied loading is not significantly large to cause yielding of the pavement, base and EPS, hence the system remains in the elastic range.

3.2 Validation of the Numerical Approach

The numerical modeling approach discussed herein was verified using a layered system example found in the engineering literature (Helwany et al., 1998). The modeling approach was subsequently applied to a layered pavement system with a concrete load distribution slab and underlying EPS. For the validation case, the tire load is converted to an equivalent circular load and applied atop an 2D axisymmetrical model comprised of asphalt concrete, base and subbase (Helwany et al., 1998) (Figure 3-1).

An equivalent FLAC model was developed for this case and the predicted vertical stress profile from the FLAC model (see redline in Figure 3-2) was compared with the results obtained by Helwany et al., 1998 and with Boussinesq's classical elastic solution for a circular footing on a semi-infinite elastic halfspace. The FLAC results closely, if not exactly, match the finite element and elastic solutions. The FLAC code used to produce this validation is presented in Appendix 1.

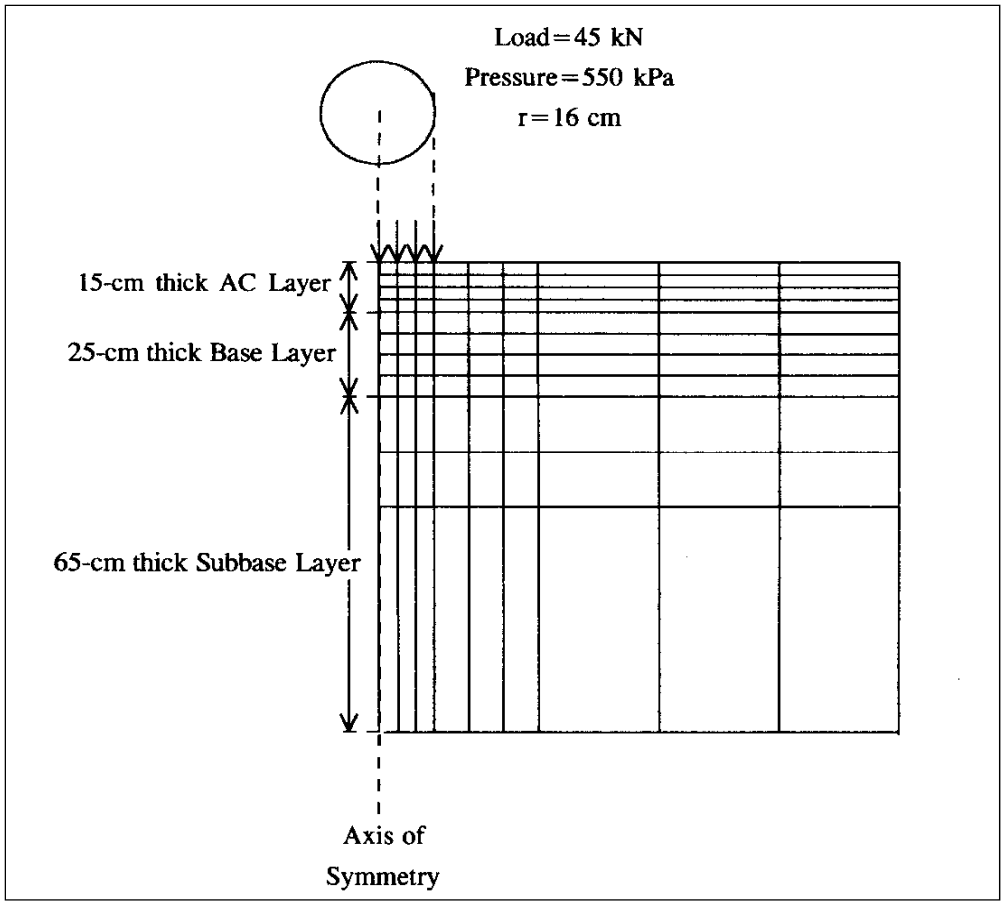

Figure 3-1 FEM Model Developed by Helwany et al., 1998.

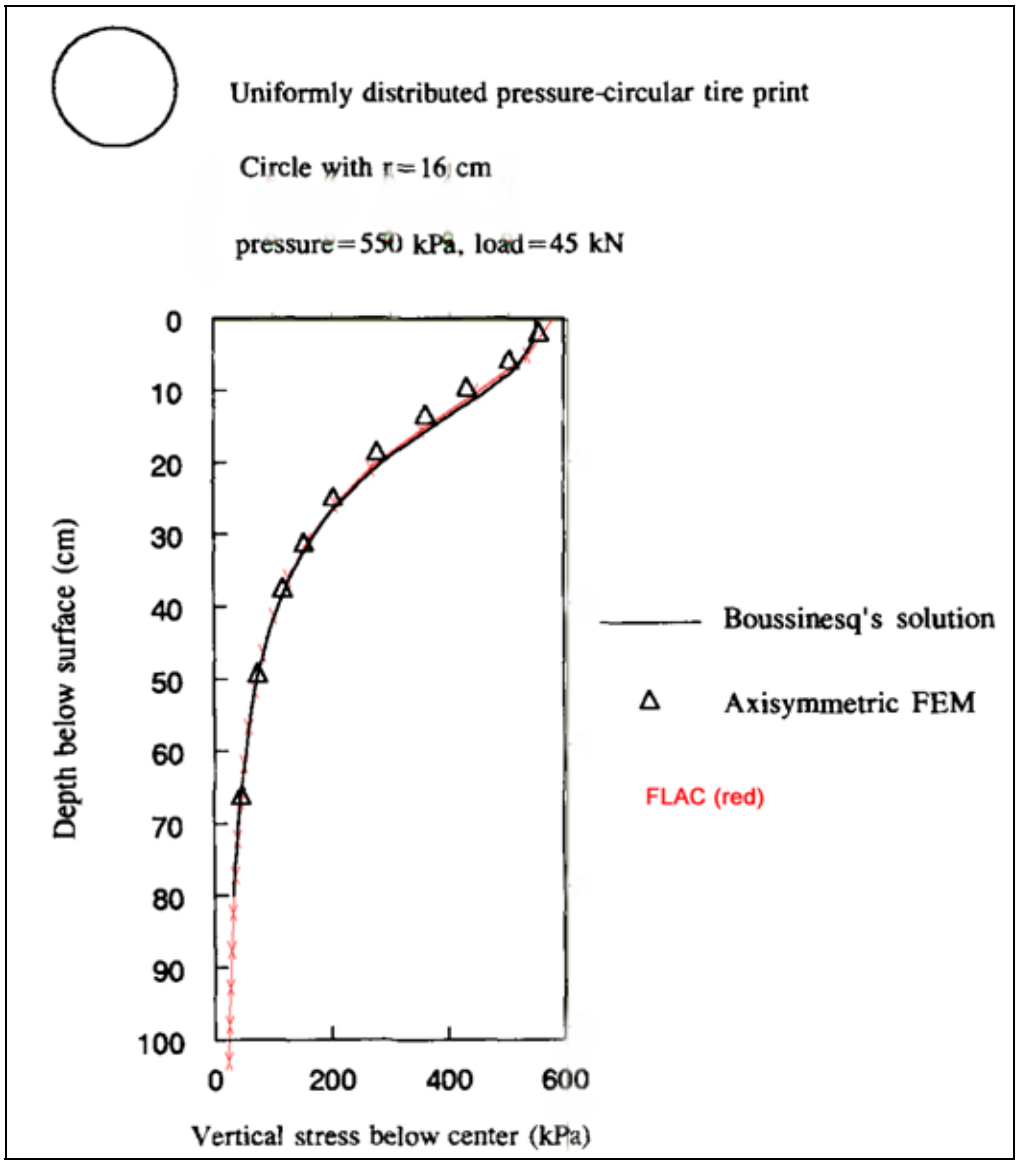

Figure 3-2 FLAC Prediction of Vertical Stress Profile Centerline of Circular Load.

3.3 HS-20 Loading from FLAC

The FLAC model was then modified to estimate the induced stress for a standard truck loading. The example was modified to represent an AASHTO HS-20 25-kip dual tire load (Figure 3-3) placed atop a typical concrete pavement system underlain by EPS19 block. The equivalent circular load for 1 set of dual tires was calculated with Equations 3-1 and 3-2 below.

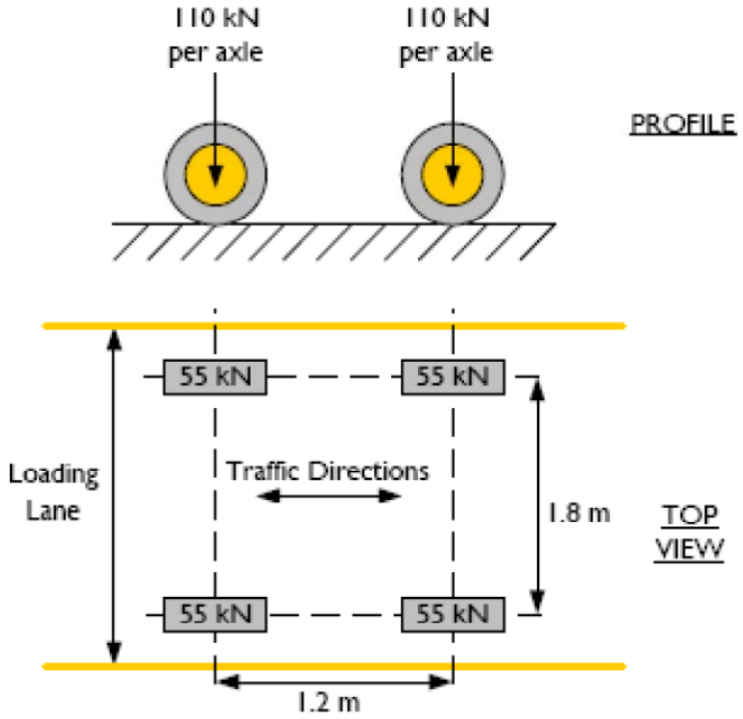

Figure 3-3 25-kip (110 kN) Dual Tire Load

For the case of a single axle with dual tires, the contact area of the dual tires can be estimated by converting the set of dual tires into a singular circular area by assuming that the circle has an area equal to the contact area of the duals, as shown in Equation 3-1.

$$A_{CD} = Q_D/q \tag{3-1}$$

The equivalent circular radius is calculated from:

$$r = (A_{CD}/\pi)^{1/2} \tag{3-2}$$

where: A_{CD} is the contact area of the duel tires, Q_D is the live load on the dual tire, q is the contact pressure on each tire (i.e., tire pressure) and r is the equivalent circular radius. The corresponding calculations for an HS-20 Truck Loading are given in Table 3-1.

Table 3-1 Equivalent Radius for an HS-20 Truck Loading

Dual Tire Loading (single axial/one side)				
QD =	12.5	kips	55.6	kN
q =	90	psi	622.08	kPa
A_{CD} =	138.89	in^2	0.0897	m2
r =	6.649	in	0.1689	m

The grid, boundary conditions and applied load from the FLAC numerical model is shown in Figure 3-4. A 55 kN (12.5-kip) tire load was applied over a circular area with a radius of 0.169 m (6.649 in) and a circular area of 0.0897 m^2 (139 in^2). This produces an equivalent, circular, uniform stress of 622 kPa (90 psi) where the dual tires are applied at the pavement surface. (Note that in an axisymmetrical mode, the radius of the applied surface load appears on the top of the left-side of the model.) The boundary conditions of the FLAC model were fixed in both the vertical (y) and horizontal (x) directions at the base. The outside boundary, which appears on the right-hand side of the model, was fixed in the x-direction. The left-hand vertical edge of the model represents the axis of symmetry, which by definition is also fixed in the x-direction by FLAC. The diameter of the model was set equal to the minimum dimension of a 2-lane roadway with 10-foot shoulders on both sides. The roadway width analyzed was 12+12+8+8 or 40 feet, which was set equal to a radius of 20 feet, or 6.1 m in the numerical model. (Note that in reality the roadway is essentially infinite in the out-of-plane direction. However for a conservative estimate of the traffic loads, the diameter of the model was set equal to 40 feet or 12.2 m, which models the roadway as a finite pavement section with the minimum width of the roadway equal to the diameter of the numerical model.)

Table 3-2 presents the material properties used in the FLAC model for the various layers of the pavement section. The layers shown in Figure 3-5 are appropriate for a 0.3-m thick Portland Concrete Cement Pavement (PCCP) underlain by 0.6-m thick roadway base underlain by 0.15-m thick concrete load distribution slab, underlain by a 2-m thick layer EPS19. These

thicknesses and layer properties were selected to approximate the pavement section used on the I-15 Reconstruction Project.

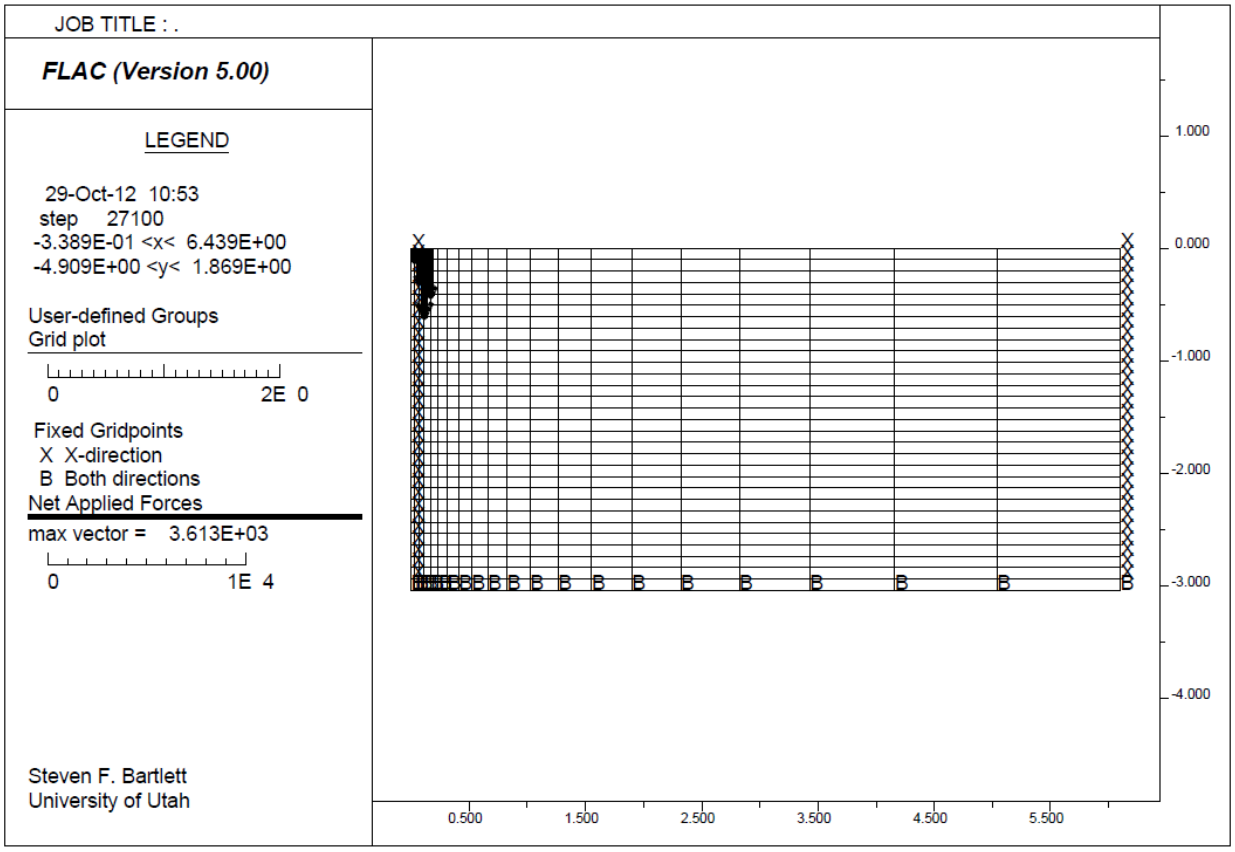

Figure 3-4 FLAC Model for 55 kN (12.5 kip) Dual Tire Loading.

Table 3-2 Properties Used in FLAC Modeling

	ϱ (kg/m3)	γ (lb/ft3)	E (MPa)	v	K (MPa)	G (MPa)	Thickness (m)	$\Delta\sigma_v$ (kPa)
PCCP	2400.5	150.00	25000	0.18	13021	10593	0.075	1.77
Road Base	2160.5	135.00	400	0.3	333	154	0.600	12.72
LDS	2400.5	150.00	25000	0.18	13021	10593	0.075	1.77
EPS19	18.4	1.15	4.0	0.1	1.67	1.82	---	---

PCCP = Portland Concrete Cement Pavement $\Sigma\sigma_v$ 16.25 (kPa)

LDS = Load Distribution Slab 2.35 (psi)

ϱ = mass density, γ = unit weight, E = Young's modulus, V = Poisson's ratio, K = bulk modulus, G = Shear modulus,

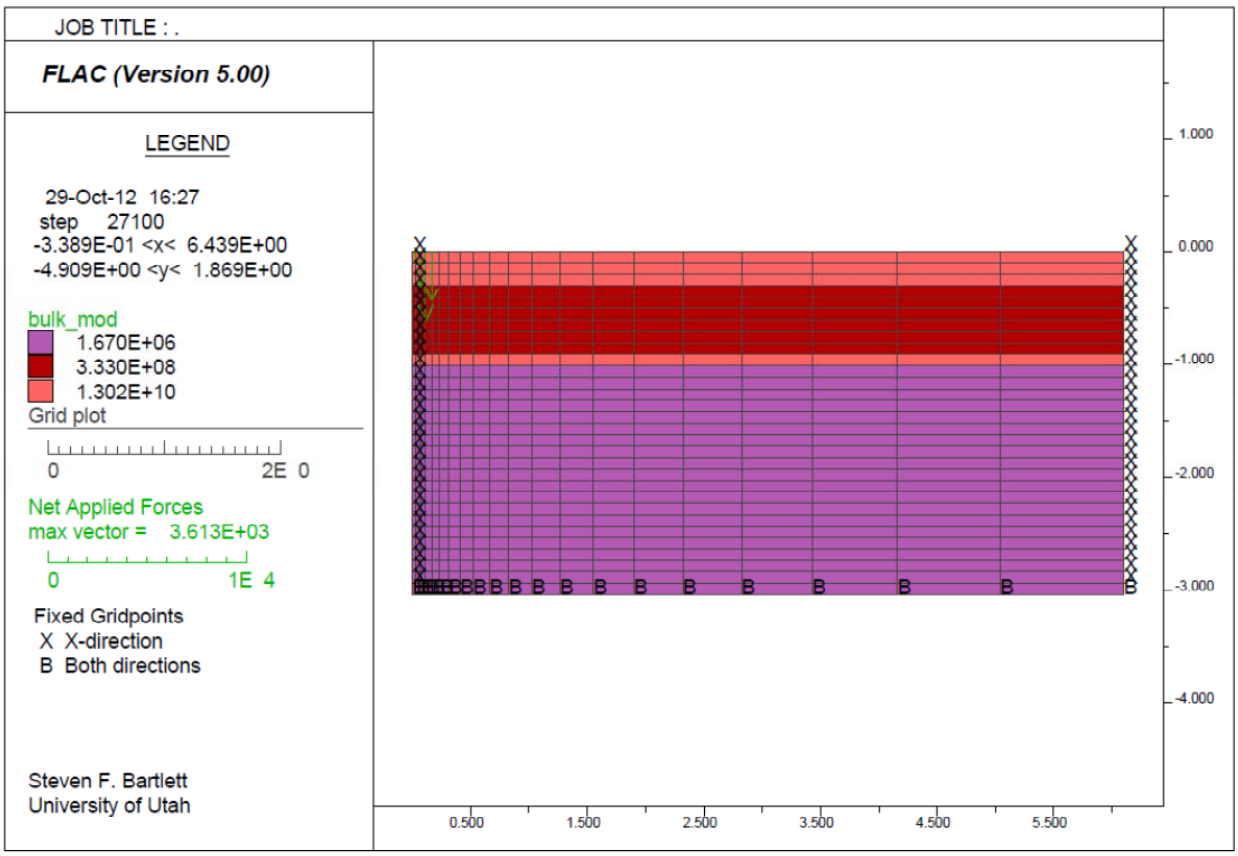

Figure 3-5 Bulk Modulus Plot for Four-layer FLAC Model.

The vertical stress distribution for a 55 kN (12.5 kip) tire load placed on a four-layer pavement system is shown Figure 3-6. This figure shows the vertical stress versus depth for a vertical line placed directly under the center of the loading. Table 3-3 gives the tabulated values for the results shown in Figure 3-6. Values shown in blue in Table 3-3 are located within the EPS. The maximum value at the top of the EPS is about 0.67 kPa. For comparison purposes, the value calculated in the top of the EPS using a homogeneous elastic solution is 21.3 kPa (Table 3-3). Thus, the vertical stress versus depth has been reduced significantly due to the redistribution of stress resulting from the high stiffnesses of the concrete pavement layer and underlying concrete load distribution slab. The relatively low vertical stress calculated in the top of the EPS demonstrates the effectiveness of the concrete pavement and load distribution slab in significantly redistributing the localized surface tire loading.

The vertical stress contribution from the nearby tires must also be accounted for in determing the stress in the top of the EPS for loading condition given in Figure 3-3. This diagram shows 1.8-m horizontal spacing between adjacent tires on the same axle and 1.2-m horizontal spacing between adjacent axials. In addition, the diagonal spacing between opposite tires on adjacent axels is 2.2 m.

To account for these additional localized loadings, superposition of stress based on elastic theory can be used to calculate the total vertical stress contribution from these adjacent tires and axel. Figure 3-7 shows contours of vertical stress (i.e., vertical stress bulb) for the 55 kN loading. This plot indicates that the vertical stress in the EPS diminishes with distance from the applied loading and that the vertical stress is between 0.4 to 0.6 kPa at a distance between 1.2 to 2.2 m from the center of the applied load. Table 3-4 lists the vertical stresses in the top of the EPS (depth z =1.1 m) plotted as a function of horizontal distance (m) from the applied loading. These same values are also plotted in Figure 3-8. Directly under the the applied loading at z = 1.1 m, the stress is about 0.67 kPa, which is consistent with the value at z = 1.1 m given in Table 3-3. Figure 3-8 shows that the vertical stress at z = 1.1 m dimishes with horizontal distance from the applied loading. The stresses at this depth reach a minimum value of about 0.46 kPa at a distance of about 4 m. Beyond this distance, the vertical stress does not vary significantly and is relatively uniform in the top of the EPS (Figure 3-8). In addition, the relatively low stress level of 0.67 to 0.46 kPa shown throughout the top of the EPS in the numerical model can be verified by assuming that the vertical stress is perfectly distributed by the time it reaches the top of the EPS. Thus,

$$\text{Vertical stress} = F / A = 55 \text{ kN} / [(6 \text{ m})^2 \ \pi] = 0.486 \text{ kPa} \qquad (3\text{-}3)$$

This simple calculation confirms the reasonableness of the numerical results. Therefore, based on the vertical stress values discussed in the previous paragraph and given in Table 3-4, the total vertical stress calculated in the top of the EPS located directly under one set of dual tires and resulting from the adjacent loadings of both axels and both sets of tires is:

$$0.67 \text{ kPa} + 0.55 \text{ kPa} + 0.52 \text{ kPa} + 0.50 \text{ kPa} = 2.24 \text{ kPa} = (0.31 \text{ psi}) \qquad (3\text{-}4)$$

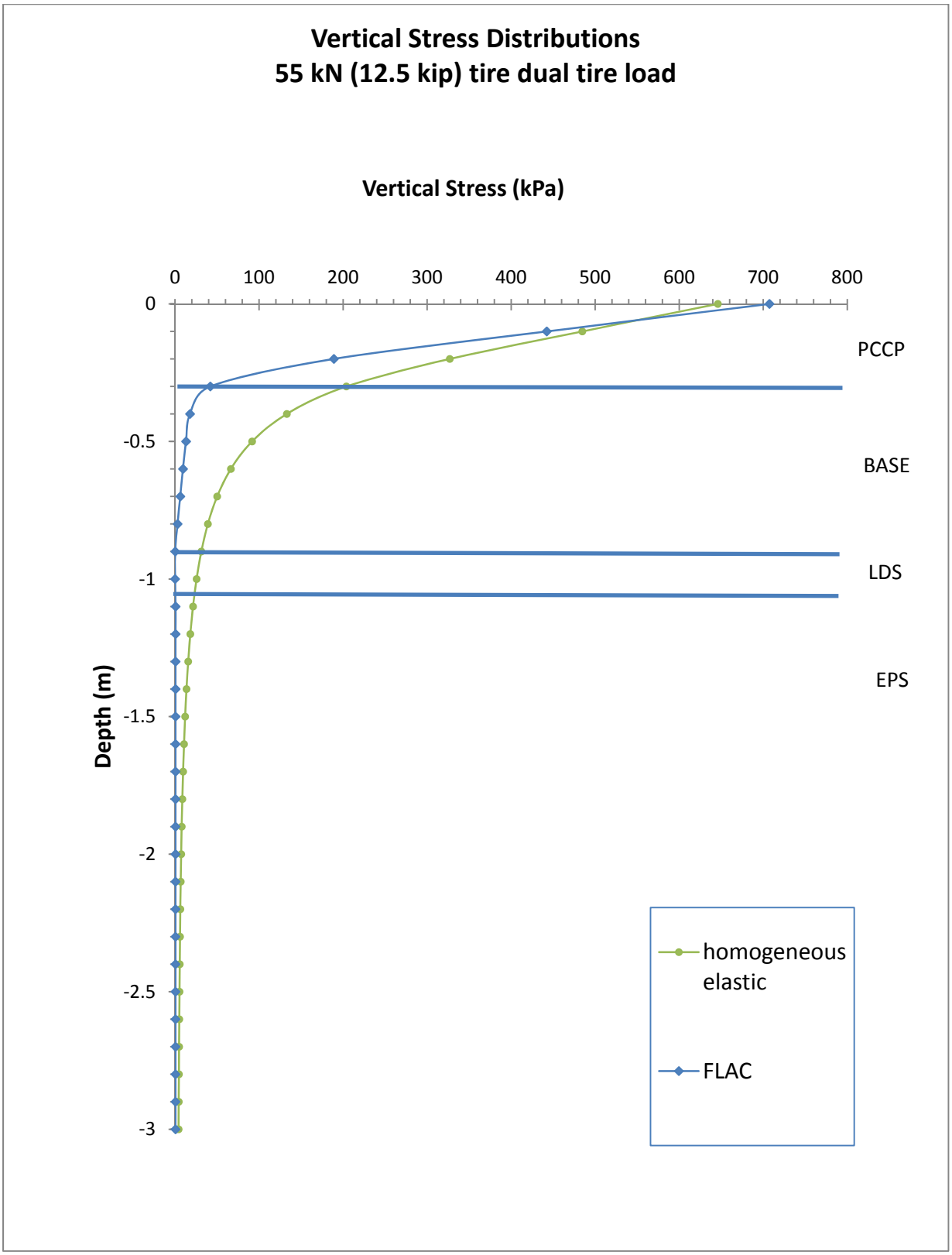

Figure 3-6 Vertical Stress Profiles for 55 kN (12.5-kip) Dual Tire Load for 4-layer System.

Table 3-3 Vertical Stress Profile for 55 kN (12.5-kip) Dual Tire Load for 4-layer System.

	homogeneous elastic	FLAC
Depth (m)	Vertical Stress (kPa)	Vertical (kPa)
0	645.95	707.42
-0.1	484.62	442.33
-0.2	326.93	189.01
-0.3	203.84	41.975
-0.4	132.98	17.803
-0.5	91.668	13.11
-0.6	66.399	9.4548
-0.7	50.086	6.2515
-0.8	39.046	2.996
-0.9	31.27	0.20038
-1	25.609	0
-1.1	21.372	0.67073
-1.2	18.127	0.64346
-1.3	15.594	0.62665
-1.4	13.582	0.61346
-1.5	11.963	0.60264
-1.6	10.644	0.5935
-1.7	9.5585	0.58566
-1.8	8.657	0.57884
-1.9	7.903	0.57287
-2	7.2679	0.5676
-2.1	6.7301	0.56294
-2.2	6.2721	0.55878
-2.3	5.8801	0.55505
-2.4	5.5425	0.5517
-2.5	5.2499	0.54865
-2.6	4.9935	0.54586
-2.7	4.7659	0.54328
-2.8	4.5598	0.54084
-2.9	4.3678	0.5385
-3	4.1815	0.53619

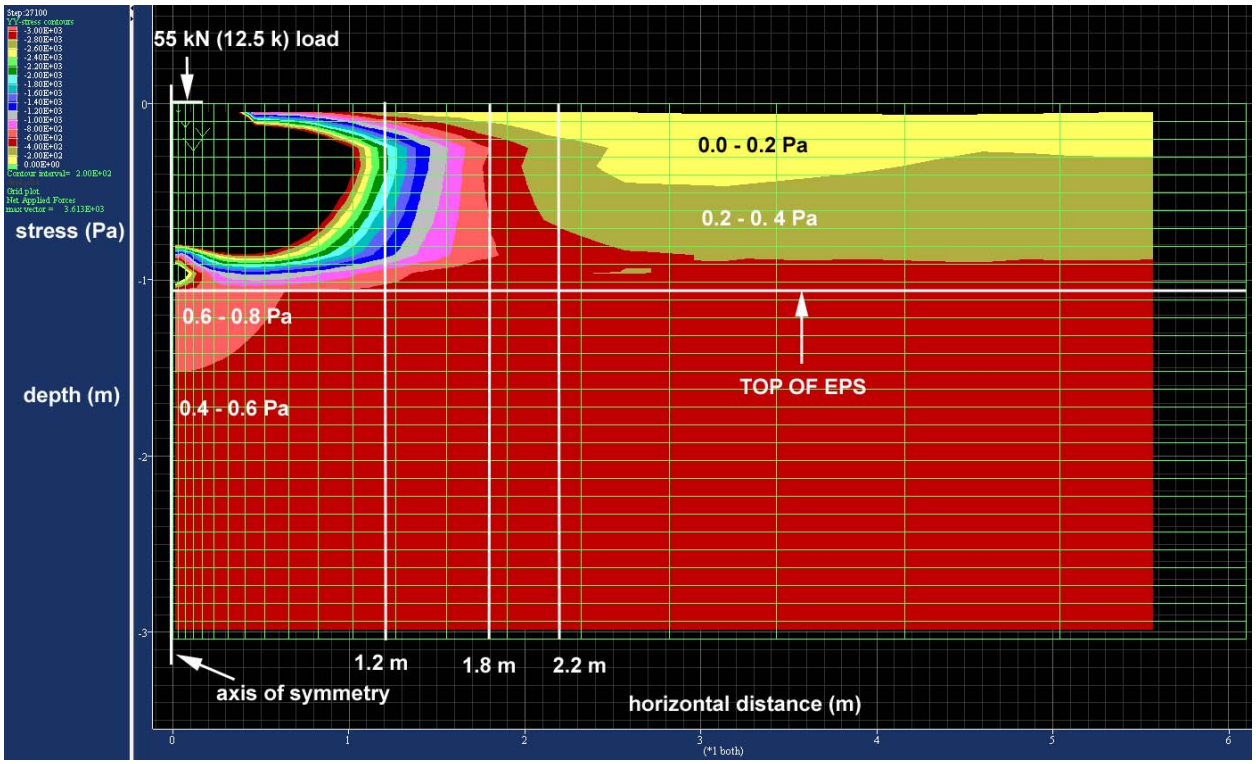

Figure 3-7 Vertical Stress Contours for 55 kN (12.5 kip) Dual Tire Load.

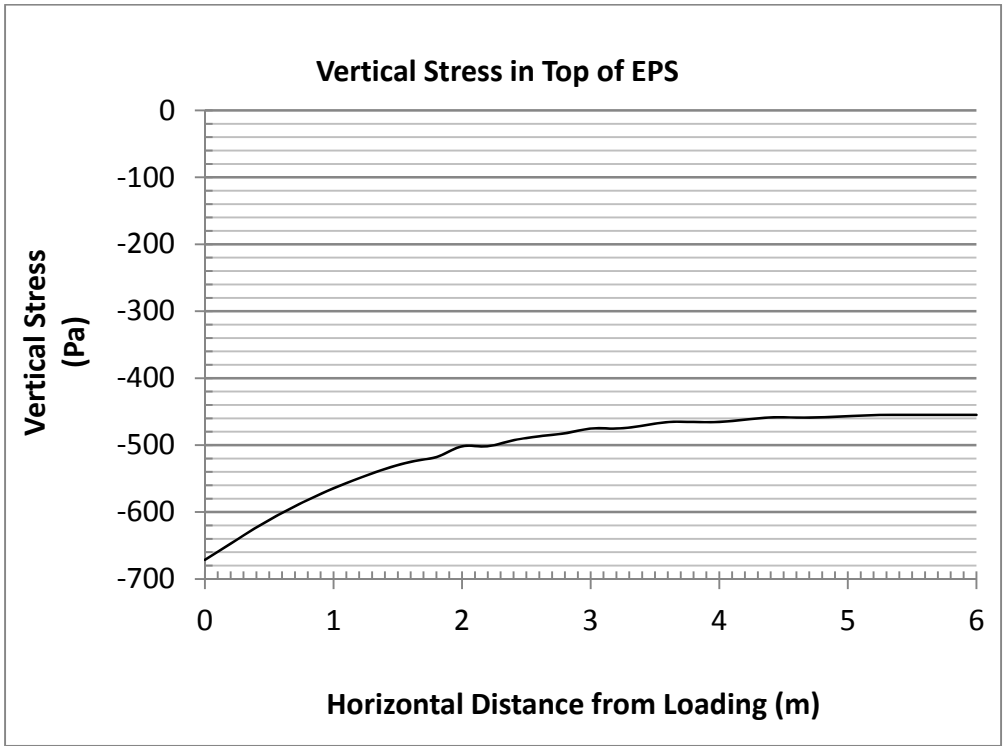

Figure 3-8 Vertical Stress in Top of EPS
As a Function of Horizontal Distance from 55 kN (12.5 kip) Loading

Table 3-4 Vertical Stress in Top of EPS (z = 1.1 m) as a Function of Horizontal Distance from 55 kN (12.5 kip) Loading

Hor. Distance (m)	Vertical Stress (Pa)
0.00E+00	-6.71E+02
2.00E-01	-6.47E+02
4.00E-01	-6.23E+02
6.00E-01	-6.01E+02
8.00E-01	-5.82E+02
1.00E+00	-5.65E+02
1.20E+00	-5.49E+02
1.40E+00	-5.36E+02
1.60E+00	-5.25E+02
1.80E+00	-5.18E+02
2.00E+00	-5.02E+02
2.20E+00	-5.02E+02
2.40E+00	-4.93E+02
2.60E+00	-4.87E+02
2.80E+00	-4.82E+02
3.00E+00	-4.75E+02
3.20E+00	-4.75E+02
3.40E+00	-4.71E+02
3.60E+00	-4.66E+02
3.80E+00	-4.66E+02
4.00E+00	-4.66E+02
4.20E+00	-4.62E+02
4.40E+00	-4.59E+02
4.60E+00	-4.59E+02
4.80E+00	-4.59E+02
5.00E+00	-4.57E+02
5.20E+00	-4.55E+02
5.40E+00	-4.55E+02
5.60E+00	-4.55E+02
5.80E+00	-4.55E+02
6.00E+00	-4.55E+02

This page intentionally left blank

4.0 Comparison of EPS Design Guidance and Performance Monitoring

In order to compare NCHRP 529 guidelines with the current the EPS White Book (2001), a relationship between the NCHRP 529 elastic limit stress at 1 percent strain and the compressive resistance and 10 percent vertical strain used by EPS White Book (2001) is required. This can be reasonably estimated by comparing the elastic limit stress values at 1 percent vertical strain with those at 10 percent vertical strain values as published by ASTM D6817 (Table 4-1).

Table 4-1 Physical Properties of Geofoam (from ASTM D6817).

Type	EPS12	EPS15	EPS19	EPS22	EPS29	EPS39	EPS46
Density, min., kg/m^3(lb/ft^3)	11.2 (0.70)	14.4 (0.90)	18.4 (1.15)	21.6 (1.35)	28.8 (1.80)	38.4 (2.40)	45.7 (2.85)
Compressive Resistance, min., kPa (psi) at 1 %	15 (2.2)	25 (3.6)	40 (5.8)	50 (7.3)	75 (10.9)	103 (15.0)	128 (18.6)
Compressive Resistance, min., kPa (psi) at 5 %	35 (5.1)	55 (8.0)	90 (13.1)	115 (16.7)	170 (24.7)	241 (35.0)	300 (43.5)
Compressive Resistance, min., kPa (psi) at 10 %[A]	40 (5.8)	70 (10.2)	110 (16.0)	135 (19.6)	200 (29.0)	276(40.0)	345 (50)
Flexural Strength, min., kPa (psi)	69 (10.0)	172 (25.0)	207 (30.0)	276 (40.0)	345 (50.0)	414 (60.0)	517 (75.0)
Oxygen Index, min., volume %	24.0	24.0	24.0	24.0	24.0	24.0	24.0

Linear relationships between EPS density and compressive resistance are calculated in Figure 4-1 for both the NCHRP 529 1 percent elastic limit stress and the 10 percent compressive resistance values given in ASTM D6817 using vales from Table 4-1. For EPS20, the predicted compressive resistance corresponding to NCHRP 529 elastic limit stress is 53.4 kPa, as calculated from Figure 4-1. Similarly, the predicted compressive resistance for EPS corresponding to ASTM D6817 at 10 percent vertical strain is 115.2 kPa, as calculated from Figure 4-1. Thus, the NCHRP 529 elastic limit stress is about 46 percent of the compressive resistance value at 10 percent for EPS20.

When these calculations are repeated for EPS30, the NCHRP 529 elastic limit stress is about 45 percent of the 10 percent strain value of ASTM D6817. These results imply that a reduction factor of about 0.45 can be applied to the 10 percent compressive resistance values to obtain the elastic limit stress at one percent strain used in NCHRP 529.

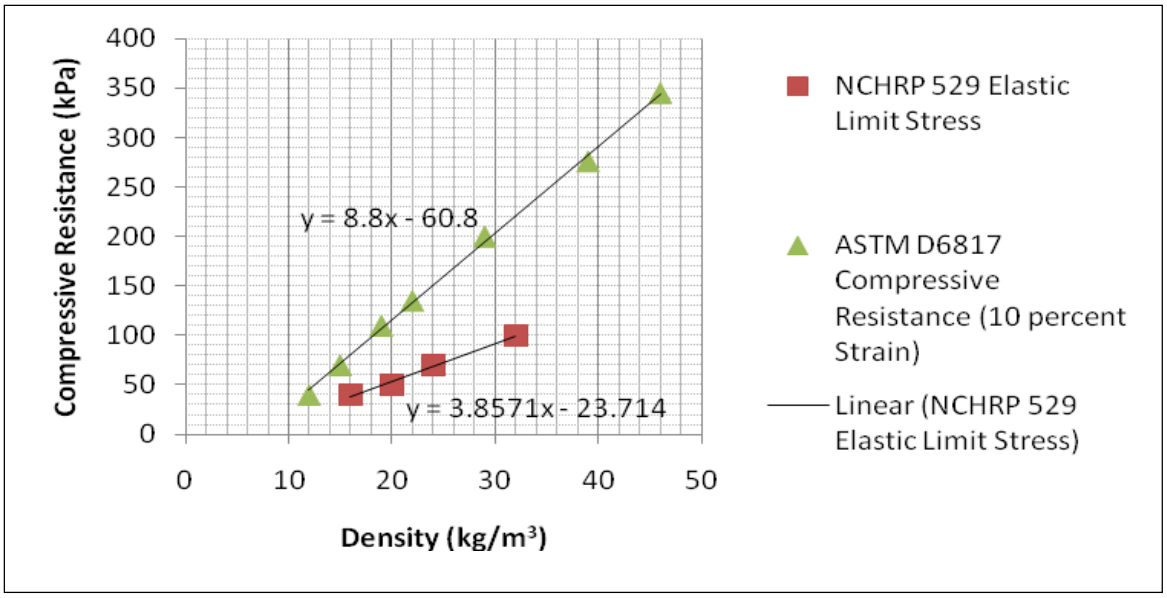

Figure 4-1 EPS Density Versus Compressive Resistance for NCHRP 529 Elastic Limit Stress and ASTM D6817 Compressive Resistance at 10 Percent Vertical Strain

4.1 Design Example

For this example, EPS19 (19 kg/m^3) based on ASTM D6817 will be used for the comparison of design guidance given in NCHRP 529 and the EPS White Book (2011). This density of EPS19 was selected for this example because it is commonly used in highway construction in both the U.S. and Europe, and its density is approximately the EPS density used on the I-15 Reconstruction Project (Bartlett et al., 2001). The nominal compressive resistance at 10 percent vertical strain for EPS19 is 110 kPa from ASTM D6817 (Table 4-1). The estimated elastic limit stress for EPS19 as required by NCHRP 529 is calculated as 110 * 0.45 or 49.5 kPa based on the relations given in Figure 4-1.

Design Example

Dead Loads (DL) = 16.25 kPa (Table 3-2)

Live Load (HS-20) truck = 2.24 kPa (Eq. 3-4)
LL Lane load (HS-20) = 0.65 klf /12 ft wide lane = 0.054 ksf or 2.7 kPa

Using NCHRP 529 and the above loads:

1.2(DL + 1.3LL) = [16.25 + 1.3(2.24 + 2.7)]*1.2 = 27.21 kPa*

The limit state safety factor for this combination using NCHRP 529 is:

FS = 49.5/27.2 = 1.82

Using the EPS White Book (2011) and the same live and dead loads

DL = (1.35)(16.25) = 21.94 kPa

The safety factor for this STR-permanent case is:

FS = (0.3)(110/1.25)/21.94 = 1.20

Note that the 0.3 resistance factor is required for permanent dead loading and the 1.25 factor is the material factor, γ_m, discussed previously

For the traffic loading (i.e., GEO CYCLIC case):

LL = (1.5)(2.24 + 2.7) = 7.41 kPa

The safety factor for the GEO CYCLIC case is:

FS = (0.35)(110/1.25)/7.41 = 4.16

The resistance factor of 0.35 is required for cyclic loading and the 1.25 factor is the material factor, γ_m, discussed previously.

It should be noted that NCHRP 529 places an allowable limit on the combination of live and dead loads, but does not place a limit on the live load exclusively, as required by the EPS White Book (2011). However, if the dead load is relatively small compared to the live load, it may be possible to overstress the EPS, even if the requirements of NCHRP 529 are met. This might be the case for pavement/EPS systems where the overlying pavement section is relatively thin, traffic loads are high and the EPS strength is relatively low. Thus, it is recommended that a separate check of the live load be made consistent with the EPS Whtie Book (2011), as follows:

$$LL_{cyc} = (1.5)(LL) \quad (3\text{-}5)$$

The safety for the live load case is:

$$FS = (0.35)(\sigma 10/1.25)/(LL/1.5) \quad (3\text{-}6)$$

where: σ10 is the compressive resistance of the EPS at 10 percent axial strain, 0.35 is the resistance factor required for cyclic loading by the European standards, and the 1.25 factor is the material factor, γ_m, required by the European standards.

Equation 3-6 can be rearranged and applied to the values of σ10 from ASTM D6817 (Table 4-1) to estimate the maximum allowable live load in the EPS as a function of EPS density (Table 4-2). The maximum allowable live load from is calculated as:

$$LL_{max} = (0.35)(\sigma 10/1.25/1.5) \quad (3\text{-}7)$$

Table 4-2 Recommended Maximum Allowable Live Load Based on EPS White Book (2011)

EPS Density (kg/m^3)	Compressive Resistance σ10 (kPa)	Max. Allowable Live Load (kPa)
12	40	7
15	70	13
19	110	21
22	135	25
29	200	37
39	276	52
46	345	64

The above calculations using NCHRP 529 and EPS White Book (2011) show that EPS19 is acceptable for an AASHTO HS-20 Truck Loading for the typical pavement section constructed on the I-15 Reconstruction Project. However, we note that this project used Type VIII EPS block, which is similar in properties to EPS19. The I-15 Reconstruction design was done according to the draft 1998 European Standards for EPS (Bartlett et al., 2000). Using this earlier standard, the unfactored dead load for the I-15 EPS block was limited to 30 percent of σ10 and the unfactored live load was limited to 10 percent of σ10, which for Type VIII EPS block is a minimum value of 100 kPa (Figure 2-1) (Bartlett et al., 2000). Therefore, the design value for the allowable dead load was about 30 kPa. Correspondingly, the design value for the allowable live load was about 10 kPa for the I-15 Reconstruction Project.

The long-term vertical stress measured in the I-15 geofoam embankments varies from about 20 to 35 kPa, as discussed later, which maximum value is approximately equal to the design allowable dead load stress, as discussed in the previous paragraph. Construction settlement measurements of the EPS embankments from the I-15 Reconstruction Project (Bartlett et al., 2001) show that elastic compression and gap closure of the EPS block produced about 1 percent vertical strain as the load distribution slab and overlying pavement materials were placed atop the EPS during construction. Subsequently, post-construction monitoring shows the EPS embankment has undergone about 0.2 to 0.4 percent of additional creep strain in a 10-year post construction period under a working stress level of about 20 to 35 kPa (Bartlett et al., 2011). Projection of the 50-year creep strain value suggests that it will be less than 1 percent (Bartlett et al., 2011).

Therefore, the 10-year post-construction performance monitoring shows that the design goal of limiting the short-term (i.e., construction) vertical compression to about 1 percent and the long-term creep settlement to an additional 1 percent vertical strain have been met. These measurements confirm that the 1998 methodology (Bartlett et al., 2000) selected to design the I-15 Reconstruction Project geofoam embankments was successful in terms of limiting the construction and creep deformation to acceptable levels.

This page intentionally left blank

5.0 Numerical Modeling of Pressure and Vertical Displacement Data

5.1Introduction

The I-15 Reconstruction Project was predominately a widening of the existing interstate, and wedge-shaped geofoam embankments were constructed adjacent to and atop the pre-existing embankment in areas where buried utilities were present (Figure 5-1). The typical construction cross-section for a geofoam embankment consisted of multiple layers (Figure 5-2). Starting from the bottom, the first layer consisted of a minimum of 0.3 meters of base sand that was graded and leveled for the placement of the approximately 0.82-m high by 1.2-m wide by 4.9-m long geofoam blocks (untrimmed dimensions). Two materials made up the second layer: the preexisting granular embankment, graded at a 1.5H:1V (33.7 degrees) backslope, and the adjacent geofoam, which abuts the existing embankment. Layer three consisted of a 0.150-m thick reinforced concrete load distribution slab, used to protect the geofoam from local overstressing. Layer four was an untreated pavement base course, about 0.610 m thick, and layer five was an unreinforced Portland cement concrete pavement, which was generally 0.356 m thick.

After placement of the geofoam embankment, a full-height tilt-up, prefabricated reinforced concrete panel wall was placed in a slotted strip footing. This wall permanently protects the face of the geofoam embankment from sunlight, collisions, and petroleum spilling down the face of the wall. The panel wall was connected to the load distribution slab with a relatively rigid bar connection and a 0.1-m gap was maintained between the vertical face of the geofoam embankment and the backside of the panel wall.

However, at the 3300 South Street location, the bar connections were damaged by vertical displacement of the geofoam mass, due to the loading from the overlying pavement section. However, these connections were later re-established by drilling through the face of the wall, at the elevation of the load distribution slab, and inserting epoxy cemented dowels into the slab. This re-established a relatively rigid connection that does not allow for differential displacement or rotation at the connection point. The overlying concrete pavement slab was

designed as a “moment” slab and is called so because it cantilevers over the top of the panel wall without causing any vertical load transfer to the top of the panels. The design intent was to minimize any interaction between the panel wall and the overlying pavement; however some interaction has occurred, as discussed later.

Figure 5-1 Typical Geofoam Embankment Construction on the I-15 Reconstruction Project in Salt Lake City, Utah.

5.2 Instrumentation

UDOT and the University of Utah implemented an extensive, 10-year monitoring program of the construction and post-construction performance of the various geotechnologies used on the I-15 Reconstruction Project (Bartlett and Farnsworth, 2004). In the geofoam instrumentation arrays, magnet extensometers were used to measure the vertical compression of the geofoam embankment during placement of the overlying materials and pavement section. The magnet extensometer systems consisted of base plates with annular magnets, polyvinyl chloride (PVC) riser pipe, and a sensing probe. In this system, the plates move freely along the PVC pipe as the geofoam is compressed. To measure settlement, a probe was lowered through

the pipe to measure the displacement of the plate magnets relative to the PVC riser pipe. The location of the plate magnets is shown in Figure 5-3. Conductors within the probe locate the position of the plates and the reading device sounds when the magnet is located (Negussey et al., 2003). A measuring tape attached to the probe makes it possible to read the individual positions of the plates relative to the top of the PVC riser pipe to the nearest millimeter.

Commercially available, 230-mm diameter, stainless steel vibrating wire (VW) total pressure cells rated at 180 kPa measured the vertical and horizontal stresses that developed in the geofoam embankment. The cell is installed with its sensitive surface in direct contact with the overlying material. The stress applied perpendicular to that surface is transmitted to the fluid inside the cell and is measured by a vibrating wire pressure transducer. The output from the transducer is in turn recorded by a data collection box which is programmed with calibration factors that convert the raw transducer readings to pressure. The vendor calibrated the pressure cells prior to installation in their calibration test device and provided the calibration factors. The pressure cell has a low profile (i.e., 11 mm thickness) and stiffness similar to that of typical sand. The resolution of the pressure cell is 0.025% and the accuracy is 0.1%. The pressure cell has a range of 0 to a maximum of 360 kPa, which is twice the measurement range of 180 kPa. Its allowable range of temperatures is -20°C to 80°C.

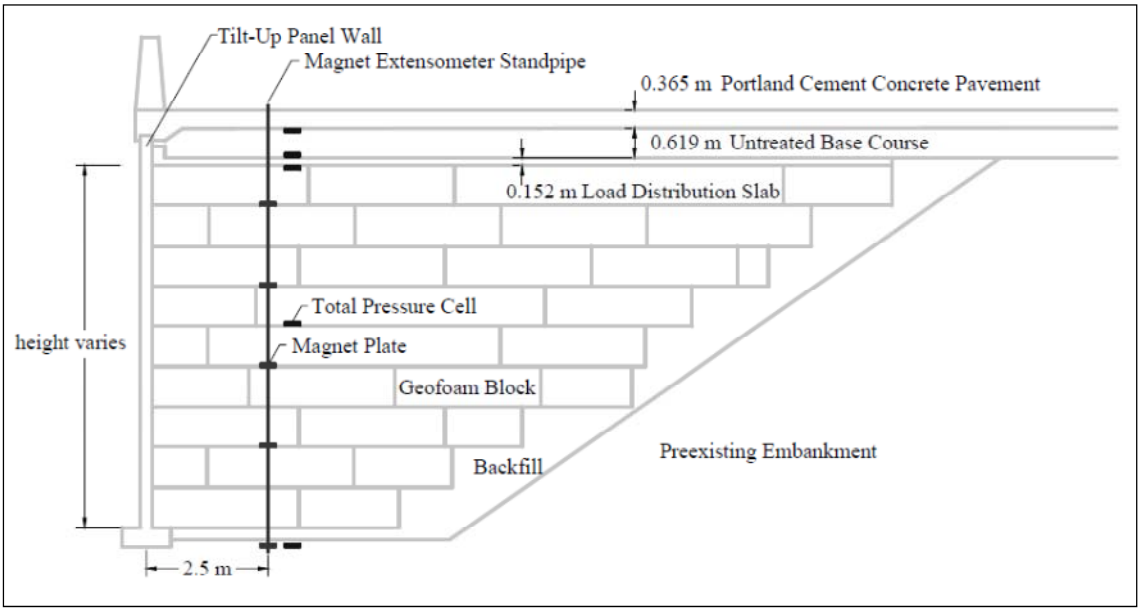

Figure 5-2 Typical Cross-Sectional View and Instrumentation Layout for the Geofoam Instrumentation Arrays at I-15, Salt Lake City, Utah.

5.3 Geofoam Instrumentation Arrays

At the 3300 South Street off ramp, field performance data were collected at three instrumentation arrays: the north array, middle array, and south array (Bartlett et al., 2001). Because the middle and south arrays have the most comprehensive sets of data, we modeled these arrays. The south array is located at project station 25+315 m and is 35 m right of centerline on northbound I-15 mainline alignment; the middle array is located at project station 25+347 and is 36.6 m right of northbound I-15 mainline alignment (Bartlett et al., 2001). At the south array, there are nine layers of geofoam, yielding a total geofoam height of about 7.4 m. There are eight layers of geofoam at the middle array, producing a total geofoam height of about 6.6 m.

UDOT researchers installed magnet extensometer plates underneath the first geofoam layer in the basal bedding sand and at every other block layer interface at the middle and south instrumentation arrays. Pressure cells at the 3300 South Street middle and south instrumentation arrays were placed in four vertical positions, as shown in Figure 5-3. Where pressure cells rested on a geofoam block, hand-carved grooves accommodated the cylindrical pressure transducer. Also, a thin veneer of sand was placed in the circular cut that was carved into the geofoam to fill and level slight imperfections in the cut and to ensure that the pressure sensitive side of the pressure cell was flush with the top surface of the underlying block. In addition, the bottom surface of the overlying block was trimmed and placed in intimate contact with the pressure sensitive side of the pressure cell. No sand was placed on the contact surface between the overlying block and the pressure sensitive side of the pressure cell.

Additional pressure cells were deployed in and underneath geofoam embankment along eastbound Interstate 80 at the State Street off ramp. (Note that a small portion of Interstate 80 was reconstructed as part of the I-15 Reconstruction Project.) **Error! Reference source not found.**5-4 shows a profile view of a full-height geofoam embankment that abuts against a pile-supported bridge that crosses Main Street on the western end of the State Street off ramp. Geofoam embankment supports the Main Street bridge eastern approach slab and the adjacent pavement section of the State Street off ramp. Further to the east, this ramp and the underlying geofoam embankment diminish in height until the ramp matches the grade of the adjacent State

Street. At these locations, pressure cells were installed at the Main Street bridge east abutment and at three additional locations in the State Street off ramp: a west instrumentation array, a middle instrumentation array and an east instrumentation array. At the Main Street bridge eastern abutment, pressure cells were oriented horizontally and vertically to measure the vertical and horizontal stresses that developed at the face of the concrete abutment and in the adjacent geofoam block (Figure 5-4). Three vertically oriented flush-mounted pressure cells were cast in the face of the concrete abutment at the same elevation to measure horizontal stresses transferred to the abutment face from the abutting geofoam. Two additional pressure cells, one oriented vertically and the other oriented horizontally, were inserted in the adjacent geofoam blocks at the same elevation as the flush-mounted pressure cells to measure the horizontal and vertical normal stresses in the abutting geofoam (Figure 5-4). In addition, to improve the pressure cell installation over that which was used at the 3300 South Street instrumentation arrays, a precision slot was cut in the geofoam blocks using a computerized hotwire cutter to obtain an exact fit for the pressure cells and the pressure cells were inserted in these slots prior to installation of the geofoam blocks.

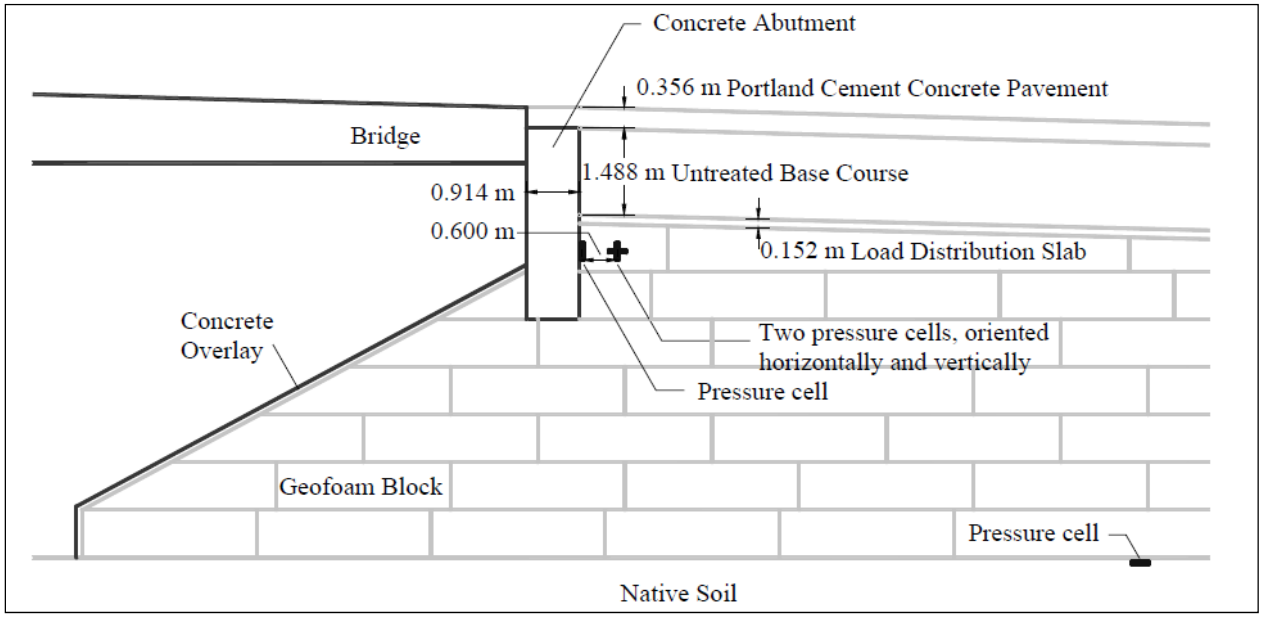

Figure 5-3 Geofoam Cross-Section (parallel to bridge) at the West End of the State Street Off Ramp.

At the State Street west instrumentation array (bottom to top), there is a one-half height (approximately 0.41 m) geofoam block layer, two full-height block layers and another one-half height block layer, resulting in a 2.46-m total geofoam height. At the middle instrumentation array, there are two layers of full height blocks of geofoam, making a 1.64-m total geofoam height. At the east instrumentation array, there is one full block layer of geofoam, producing a 0.82-m total geofoam height. All pressure cells for these three arrays were placed in the base sand, just below the lowest geofoam layer. No magnet extensometers were positioned in the geofoam at the State Street instrumentation arrays due to safety concern about reading the instrumentation when the ramp was opened to traffic.

At 100 South Street, near downtown Salt Lake City, UDOT and Syracuse University researchers installed instruments and collected data at two instrumentation arrays: the north array and the south array (Negussey and Studlein, 2003). These arrays are located in southbound I-15 where geofoam embankment was placed on the western side of I-15 where it intersects with 100 South Street. We chose to model the data from the south array because the instrumentation at this location is near the center of the embankment and more instrumentation was placed at this locale. The geofoam block at the south array consisted of (from bottom to top) one-half height block layer, eight full height block layers and one-half height block layer, making the total height of the geofoam embankment about 7.3 m. Magnet extensometer plates were installed underneath the first geofoam layer in the base sand and at every other block layer interface at approximately 2.5 m from the vertical face of the geofoam instrumentation array. Two pressure cells were embedded in the base sand at the south array. One pressure cell was placed 1.473 m from the face of the panel wall; the other was placed 2.692 m from the face of the same wall. The latter pressure cell malfunctioned soon after installation and will not be discussed further.

5.4 Data Interpretation

Many pressure cells located near the roadway surface showed a seasonal cycling of vertical stress, as shown in Figure 5-5. This behavior is attributed to thermal expansion and contraction of the geofoam, load distribution slab and/or Portland cement concrete pavement and the interaction of the load distribution slab and the tilt-up panel wall at their connection (Figure

5-3. Thermal loading was most pronounced for pressure cells placed at the top or above the geofoam embankment (Bartlett et al., 2001). The cycling was not as visible in pressure cell data located in the middle of the geofoam mass or in the base sand (Figure 5-3). For these evaluations, we chose to compare the average of the summer peak values with the *FLAC* results in order to estimate a representative maximum vertical stress that developed in the geofoam mass. Similarly, seasonal cycling was present in the magnet extensometer data. We chose to compare the average of the displacements measured by the magnet extensometers during summer months with the *FLAC* results.

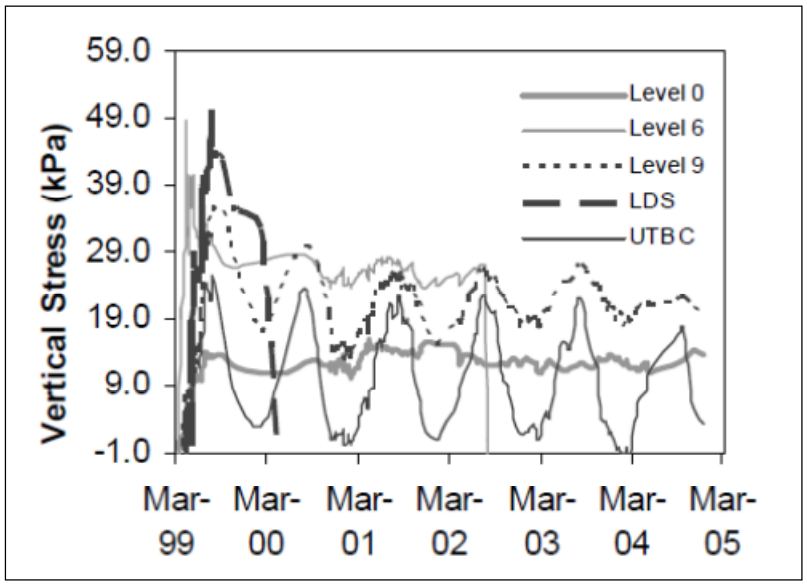

Figure 5-4 3300 South Street South Instrumentation Array Pressure Cell Data.

In a few cases, pressure cells located just above the load distribution slab recorded positive values for several months and then began to record negative values. If these pressure cells recorded positive values for a few seasonal cycles, then the average value in the summer is plotted in subsequent vertical stress figures. However, if a positive value was only recorded for one cycle or less, the data for the pressure cell were not used. This negative pressure cell behavior may be due to malfunctioning of the pressure cells, but it may also represent complex interactions occurring near the connection with the tilt-up panel wall (Figure 5-3), as evidenced by the pressure cell behavior and discussed in the following paragraph.

The load distribution slab has a somewhat rigid connection with the tilt-up panel wall, thus any expansion/contraction of the geofoam mass or overlying pavement section could transfer vertical loads to the wall and subsequently change the vertical pressure recorded in the cells placed just above and below the load distribution slab. In addition, the granular borrow and road base were compacted against the back of the panel wall. This can also cause vertical stress transfer due to the friction and horizontal stress that exists along this contact surface. Also, although not intended by the design, the top of the panel wall may interact with the cantilevered pavement slab. The design required a gap between the pavement slab and the top of the panel wall that is filled with an elastomeric material. This was done to minimize any interaction between the wall and the overlying pavement; however there probably is some interaction that is ongoing. Our *FLAC* models did not include these potential interactions at or near the connections and interfaces.

5.5 Material Properties

Material properties used in the *FLAC* modeling are given in Table 5-2. Type VIII geofoam, with a density of 18 kg/m^3 and a Poisson's ratio of 0.103, was used at all instrumentation array locations (Bartlett et al., 2001; Benchmark, 2003). Previous unconfined compression tests on 50-mm cube samples of Type VIII geofoam have produced compressive resistances between 97 and 111 kPa for 5 and 10% axial strain, respectively (Bartlett et al., 2000). In the *FLAC* models, we used a cohesion value (i.e., shear strength) approximately equal to 50% of the average unconfined compressive strength at an axial strain of 5%, (i.e., 50 kPa). (However, because the geofoam remained within the elastic range for all modeling, the selection of the cohesion value is unimportant for these evaluations.) In addition, direct shear tests have been performed to measure the interface friction between sand-geofoam and geofoam-geofoam contacts (Bartlett et al., 2000). Based on these tests, the interface friction angle between sand and geofoam is approximately 31° and the interface friction angle between geofoam and geofoam is approximately 42° (Bartlett et al., 2000).

Table 5-1 Material Properties for FLAC modeling

Material	ρ (kg/m^3)	ν	E (MPa)	K (MPa)	G (MPa)	φ (°)	c (MPa)
Preexisting soil Base sand	2160	0.350	100	111	37.0	35	0
Geofoam σ ≤ 15 kPa Geofoam σ > 15 kPa	18.00	0.103	1.70-2.70 10.0	0.714-1.13 4.20	0.771-1.22 4.53	35	0.025
LDS PCCP	2400	0.180	30000	15600	12700	25	25
UTBC	2240	0.35	100	111	37.0	35	0

Young's modulus for a mass of geofoam blocks is a function of the geofoam density, which depends on the type of geofoam. However, reported values for geofoam block modulus in the literature can be somewhat variable for the same type of geofoam due to sample size and edge effects. Researchers have measured moduli values of about 5 MPa from laboratory tests on small samples of Type VIII geofoam (Bartlett et al., 2000); but such tests may underestimate the true modulus of full-sized geofoam blocks due to crushing and damage of the edges of the samples. Recent testing on full-sized Type VIII geofoam block has yielded moduli values as high as 14 MPa (Elragi, 2000).

In addition, the use of Young's modulus to calculate the compression of the geofoam embankment is complicated by the curvature of the block. Vertical displacement upon initial loading is a combination of gap closure and seating of the slightly curved block (Bartlett et al., 2000; Negussey and Studlein, 2003). Block curvature develops during block cooling and is most noticeable along the longest dimension of the block. Trimming the block can minimize this curvature; however, the I-15 blocks, as manufactured, met the specified ± 0.5% dimensional and 5% flatness tolerances, hence trimming was not necessary. Block curvature was, however, accounted for during the placement of the geofoam blocks. Laborers sighted down the long dimension of each block to determine the direction of curvature and placed the blocks concave down to achieve a tighter block fit. Nonetheless, complete gap closure and seating between geofoam layers did not occur in the geofoam embankment until the final loads of the load distribution slab, base materials and pavement section had been placed atop the geofoam (Bartlett et al., 2001).

The curvature of the block and resulting gap closure upon loading produced extra complexity in our numerical modeling. The need for a modeling approach including gap closure behavior was recognized from the work of Negussey at al. (2001). These authors showed that the initial displacement behavior of a stack of geofoam blocks is non-linear. We chose to represent this non-linear behavior in *FLAC* using a simple bi-linear modulus that changes its value when a vertical stress of 15 kPa is reached (Figure 5-6). The lower modulus value was applied in the *FLAC* model for vertical normal stresses below 15 kPa and represents gap closure behavior. The higher modulus value was applied at vertical normal stresses above 15 kPa and represents true elastic compression of the geofoam. The 15 kPa break point was developed based on plots of the field performance data from the 100 South Street geofoam instrumentation array (Negussey et al., 2001).

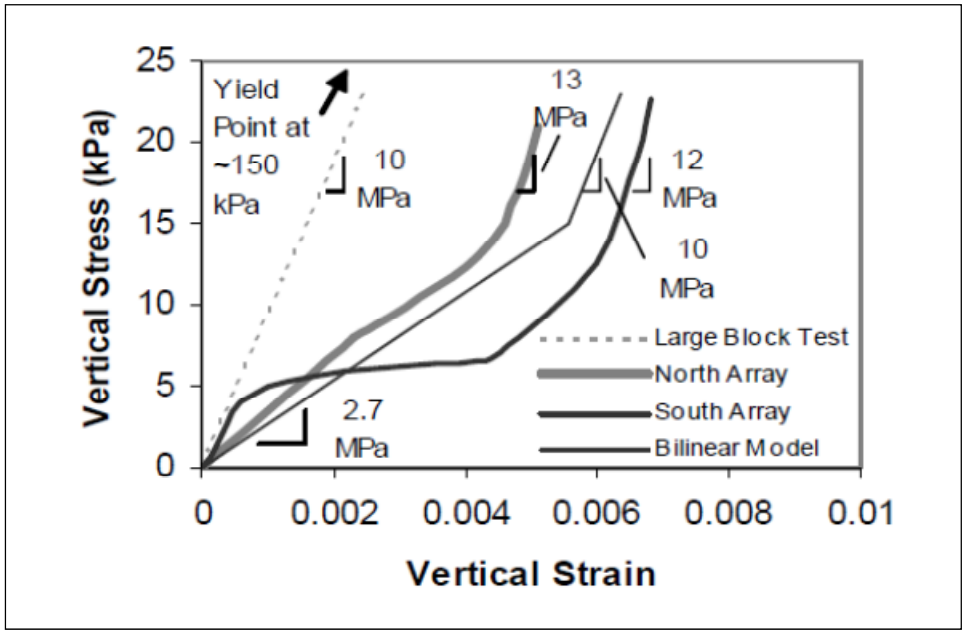

Figure 5-5 Stress-Strain Relationships from Field Data at 100 South Street, North and South Instrumentation Arrays, from Laboratory Test Data, and from the Bilinear Modulus used in Modeling. Adapted from Negussey et al. (2001) and Elragi (2000).

We used geofoam field performance data and analyses from the I-15 reconstruction at 100 South Street (Negussey et al., 2001) to develop the parameters for the low stress (i.e., gap closure) modulus for the bilinear model. Negussey et al. (2001) plotted vertical stress and strain from field measurements and suggested a low stress geofoam modulus of 2.3 to 2.7 MPa to

represent gap closure and seating. This data was developed by Negussey et al. from magnet-extensometer measurements of vertical displacement and pressure cell measurements taken at the 100 South Street instrument array locations. We tested *FLAC* models with low stress moduli of 1.7, 2.3 and 2.7 MPa to allow for some variation in this modulus. The bilinear model shown in Figure 5-6 is for a low stress modulus of 2.7 MPa.

We chose a high stress modulus of 10 MPa to represent elastic compression of the geofoam. This value is an average value consistent with recent large block laboratory tests (Elragi, 2000). The large block tests were performed on an unrestrained half-height block, compressed axially in a large loading frame at the University of Syracuse. This 10 MPa modulus was used in our modeling whenever the calculated vertical normal stress at a point in the *FLAC* model exceeded 15 kPa, as discussed later.

Typical properties were used to represent the various other materials in the numerical model. Properties for the load distribution slab and Portland cement concrete pavement were the suggested values for concrete properties in the *FLA*C manual (Itasca, 2005, "Structural Elements"). See Table 5-2 for the properties used for the base sand, underlying soil, pre-existing embankment, geofoam, load distribution slab (LDS), untreated base course (UTBC) and Portland cement concrete pavement (PCCP). The table includes mass density (ρ), Poisson's ratio (ν), Young's modulus (E), shear modulus (G), bulk modulus (K), friction angle (φ), and cohesion (c). It should be noted that a seating modulus of 1.7 to 2.7 MPa is listed in Table 5-2 for geofoam because the modeling considered and compared three low stress moduli (1.7, 2.3 and 2.7 MPa).

5.6 Modeling Approach

We chose to model the geofoam embankments in the finite difference program, *FLAC*. The explicit finite different approach, as implemented in *FLAC*, can reasonably approximate the measured stress distribution and vertical displacement in the geofoam mass for the static load case. *FLA*C also has capabilities for modeling the dynamic response and the potential for sliding between layers in a seismic event, which was modeled in a subsequent phase of the research (Bartlett and Lawton, 2008).

In order to replicate the stages of construction, the embankment cross-sections were built incrementally in *FLAC*. First, the particular geometry for the entire embankment was inputted using construction cross-section drawings at the instrumentation array locations. Then, the Portland cement concrete, untreated base course, load distribution slab, geofoam and backfill layers were given null properties in the *FLAC* model and the model was allowed to come to equilibrium. This step modeled the placement of and the resulting stresses and compression in the base sand due to its self-weight. Following self-weight compression of the base sand, gravity was "turned on" in the geofoam and adjacent backfill region. The entire geofoam mass was placed at once in the model. After placing the geofoam, *FLAC* again was allowed to come to static equilibrium. This represented the placement and resulting compression of the geofoam and backfill due to their self-weights. This step also produced additional displacement in the base sand from the placement of the geofoam and backfill. This additional displacement was added to the base sand displacements from the previous step. The stresses produced in this step resulted from the weights of the geofoam, backfill and base sand. Similarly, each subsequent layer in the model was incrementally added to the model and the model was allowed to come to static equilibrium.

To create numerical stability, we fixed the side boundaries of the *FLAC* models in the horizontal direction and fixed the bottom of the *FLAC* models in the vertical direction. The base of the model was set at 10 m below the first geofoam block layer. The horizontal extent of the model consisted of the face of the geofoam embankment on one side and the middle of the earthen embankment on the other. Interface nodes were used to connect the geofoam to the earthen embankment and foundation soil so as to allow the geofoam and soil to slide against each other. The two materials can deform independently and the use of interface nodes more realistically simulated the actual conditions. Each interface was given a normal stiffness as well as a shear stiffness. The stiffness of a given zone is $\max((K+1.33G)/\Delta z_{min})$, where K and G are the bulk and shear moduli respectively; and Δz_{min} is the smallest width of an adjoining zone in the normal direction (Itasca, 2005). Interfaces were also given an interface friction value (see Material Properties section) and a Mohr-Coulomb criterion was used for determining the initiation of sliding.

In order to implement the bilinear elastic model for the geofoam blocks, we wrote additional code in the *FLAC* command language, *FISH*, to check the vertical normal stress at the bottom of the geofoam mass and then to assign the appropriate modulus based on this check. When the vertical normal stress exceeded 15 kPa, the modulus changed from a relatively low value (e.g., 1.7-2.7 MPa) to a higher value of 10 MPa. As mentioned previously, the lower modulus, E_s, simulates the combined effects of gap closure and seating and the higher value of 10 MPa represents the true elastic modulus, E, of the geofoam mass. The FLAC code for the 3300 South, State Street and 100 South Arrays are found in Appendices 3, 4, and 5, respectively.

5.7 Results

We used *FLAC* and the bilinear model to analyze the stress distribution and the displacement of the geofoam embankments at 3300 South, State, and 100 South Streets. Our modeling process involved the comparison of the vertical stress distribution and differential displacements between layers predicted by the *FLAC* model with those measured by the pressure cells and magnet extensometers at the various instrumentation arrays.

Because of uncertainty in E_s, we analyzed and plotted *FLAC* results for low stress moduli of 1.7, 2.3, and 2.7 MPa and compared them against the measured results. The differential displacements between layers, presented in the plots hereafter, were measured shortly after the final dead loads (i.e., load distribution slab, untreated base course and pavement) were placed; thus, the plotted displacement data do not include any creep settlement.

We found that variations in E_s did not significantly change predictions of the vertical normal stress distribution; thus the vertical normal stress predictions are valid for E_s values between 1.7 to 2.7 MPa. This is simply because the final state of stress in the geofoam embankment is generally greater than 15 kPa; hence the *FLAC* model used the higher modulus to calculate the final state of stress. However, the variation of E_s values does affect the differential displacement predictions, because a significant amount of the displacement occurs at stress levels below 15 kPa.

5.7.1 3300 South Street Off Ramp Instrumentation Arrays

Figures 5-7 and 5-8 show the predicted results and measured data for the 3300 South Street south instrumentation array at a distance of 2.5 meters from the vertical geofoam face. As shown in Figure 5-7, an E_s value of 1.7 MPa yielded the best prediction of measured differential displacements. This graph also shows that the *FLAC* model predicts relatively uniform differential settlement (i.e., uniform strain) throughout the height of the geofoam, which is expected for a linear elastic material. However, the *FLAC* model somewhat under predicts the measured differential displacement between levels 6 and 8 and slightly over predicts the measured values between levels 8 and 9. The reason for the under prediction between levels 6 and 8 is unclear; however, the smaller measured and predicted differential displacements between levels 8 and 9 are attributed to the decrease in thickness of the geofoam block (i.e., one block as opposed to two). The under prediction betweens levels 6 and 8 and the slight over prediction between levels 8 and 9 are shown for all three values of E_s considered in the analysis (Figure 5-7).

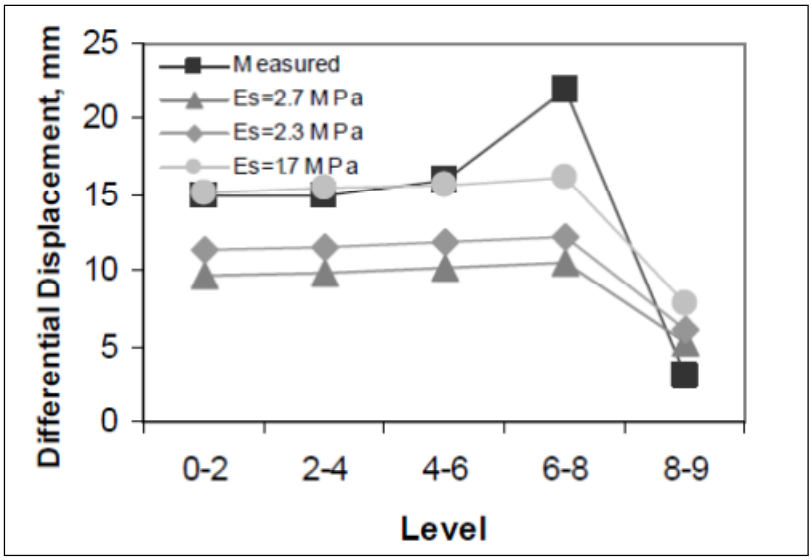

Figure 5-6 Predicted and Measured Differential Displacements between Geofoam Layers for the 3300 South Street South Instrumentation Array.

Figure 5-8 presents a comparison of the predicted and measured vertical stresses at the 3300 South Street south instrumentation array. In general, the *FLAC* model predicts a relatively uniform vertical stress of about 25 kPa in the geofoam embankment (levels 6 and 9) and about

13 kPa in the untreated base course (UTBC) layer just below the concrete pavement. The measured data are relatively similar at these elevations. A simple one-dimensional vertical stress calculation for the overburden stress of this embankment yields similar results for the vertical normal stress in the geofoam and at the base of the UTBC layer: a constant stress of about 27 kPa in the geofoam and 26 kPa just above the load distribution slab at the bottom of the UTBC layer. A vertical overburden stress of about 22 kPa is estimated in the UTBC by the one-dimensional computation; however, these simple calculations do not account for two-dimensional effects. We note that the pressure cell placed just above the load distribution slab (LDS) shows considerably higher measured stress than what was predicted by *FLAC* (Figure 5-8). This pressure cell measured positive vertical stresses of about 35 kPa for a few months and then began to record negative values. It appears that this pressure cell failed and we believe this datum should be disregarded.

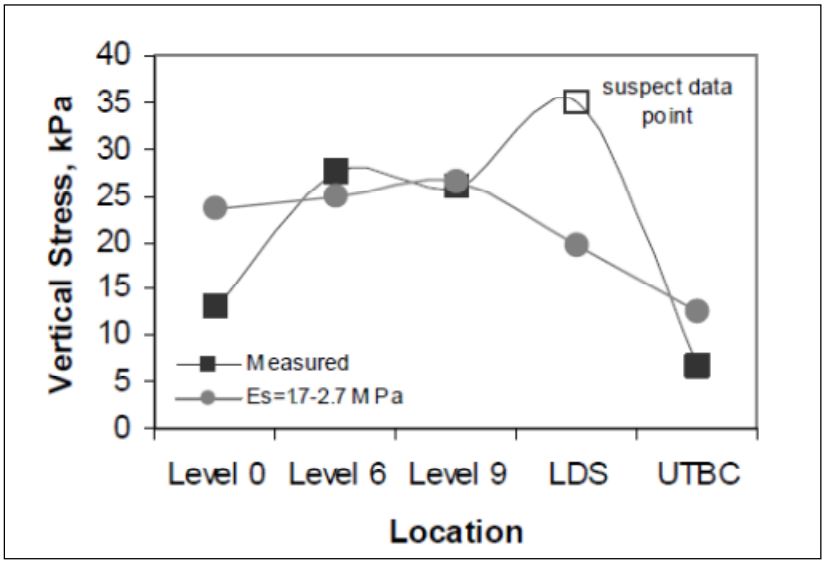

Figure 5-7 Predicted and Measured Vertical Stresses for the 3300 South Street South Instrumentation Array.

We also note that *FLAC* over predicted the measured vertical normal stress in the base sand (level 0) by about 100% (Figure 5-8). We observed a consistent over prediction trend when the FLAC results were compared with the measured vertical normal stress in the base sand. Elragi (2000), who also performed *FLAC* modeling of I-15 field data, obtained similar over-predictions. He hypothesized that the base sand and overlying geofoam block had partially lost

contact in some unexplained way. This led us to the conclusion that perhaps some other phenomenon, not accounted for in the *FLAC* model, has affected the measurement of vertical stress in the base sand. For example, it is possible that the curved contact surface of the untrimmed geofoam blocks are creating a partial arch which, in turn, is not allowing a uniform contact surface and equal distribution of vertical stress in the underlying sand.

Figure 5-9 shows the predicted and measured displacements at the 3300 South middle instrumentation array. This array is similar to the south array except that the geofoam embankment at this location is only 8 blocks high. As before, the *FLAC* model predicted relatively uniform differential settlement throughout the geofoam embankment. However, the field measurements are more variable, but not inconsistent with the *FLAC* model. Some of the variation in Figure 5-9 may be due to errors in reading the magnet extensometers, block and/or construction irregularities, such as curved block, or other complex interactions in the geofoam. It is difficult to judge which E_s value best matches the field measurements for this array, but 2.3 MPa appears to be a reasonable estimate of the average behavior.

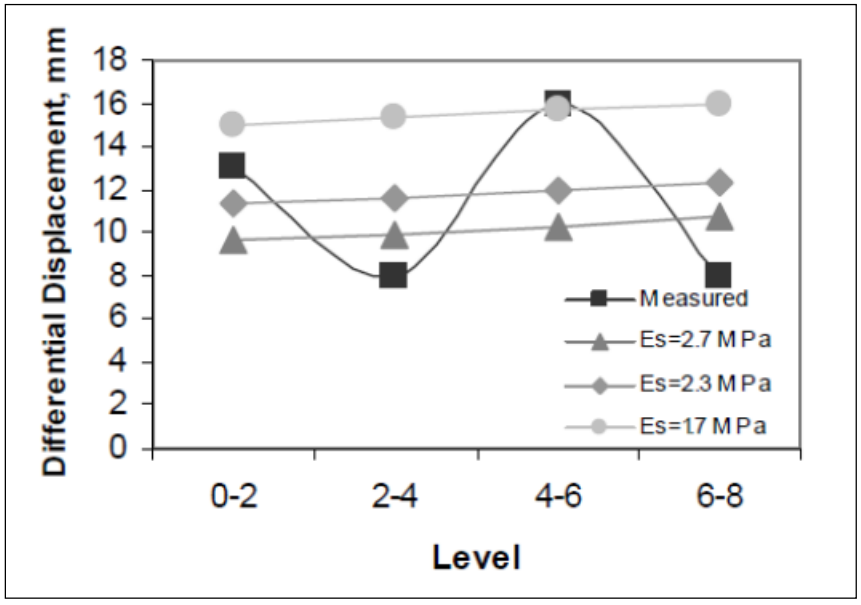

Figure 5-8 Predicted and Measured Differential Displacements between Geofoam Layers for the 3300 South Street Middle Instrumentation Array.

Figure 5-10 shows the measured and predicted vertical normal stresses at the 3300 South Street middle instrumentation array. The *FLAC* model predicts a rather uniform normal stress of 25 to 30 kPa in the geofoam (levels 5 and 8) and somewhat lesser values just above the LDS and just below the pavement in the UTBC. As previously discussed, the measured normal stress in the base sand (level 0) is significantly over predicted by the *FLAC* model. In addition, an unusually high normal stress of about 45 kPa was measured at level 5 by the pressure cell. Perhaps this may be attributed to a stress concentration caused by curvature or irregularities in the geofoam block shape.

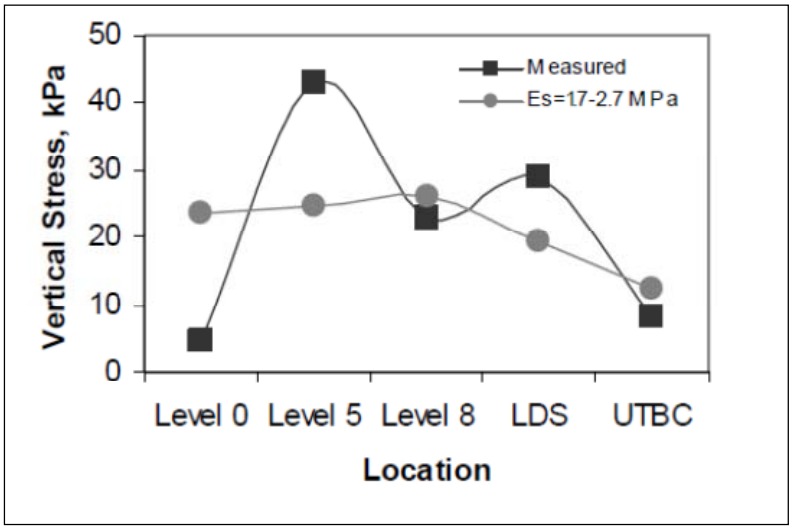

Figure 5-9 Predicted and Measured Vertical Stresses for the 3300 South Street Middle Instrumentation Array.

5.7.2 State Street Off Ramp Instrumentation Arrays

5-11 and 5-12 present stresses measured at the State Street off ramp instrumentation arrays. (No magnet extensometers were installed at this location.) Figure 5-11 shows the horizontal and vertical normal stress measured at and near the abutment face. The first data point, labeled "abutment horizontal," represents the measured and predicted horizontal stresses corresponding to the pressure cell that was cast flush with the concrete abutment face to measure horizontal stress. The points labeled "geofoam horizontal" and "geofoam vertical" represent the measured and predicted horizontal and vertical stresses from a vertically and a horizontally oriented pressure cell, respectively, inserted in the adjacent geofoam block (Figure 5-4). All

three pressure cells were installed at the same elevation. The pressure cell data in Figure 5-11 show that *FLAC* reasonably estimates the measured vertical stresses in the geofoam near the bridge abutment. However, the horizontal stresses recorded in the abutment face and in the adjacent geofoam block are somewhat overestimated and underestimated, respectively, by the *FLAC* model. The measured horizontal normal stress in the abutment face is 5 kPa and *FLAC* predicts 8.7 kPa; likewise the measured horizontal normal stress in the adjacent geofoam block is 12 kPa, compared to 7.9 kPa predicted by the *FLAC* model. These differences are most likely due to geofoam-structure interaction that is occurring in the abutment area. Nonetheless, both the measured data and the *FLAC* modeling show that the horizontal earth pressure is greater than what would be expected for at-rest conditions. These higher than expected normal stresses may be attributed to the lateral constraint and interaction at the abutment wall. (The at-rest earth pressure coefficient, K_o, is 0.11, based on the Poisson's ratio given in Table 5-2, and thus the horizontal stress should be about 2.6 kPa, if at-rest conditions were applicable.)

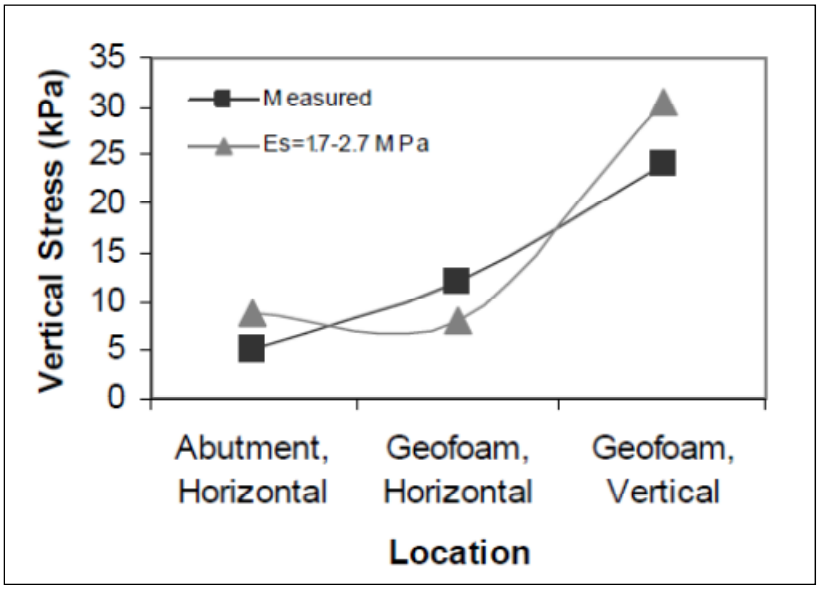

Figure 5-10 Predicted and Measured Horizontal and Vertical Stresses at and adjacent to the Abutment at the State Street Exit Ramp.

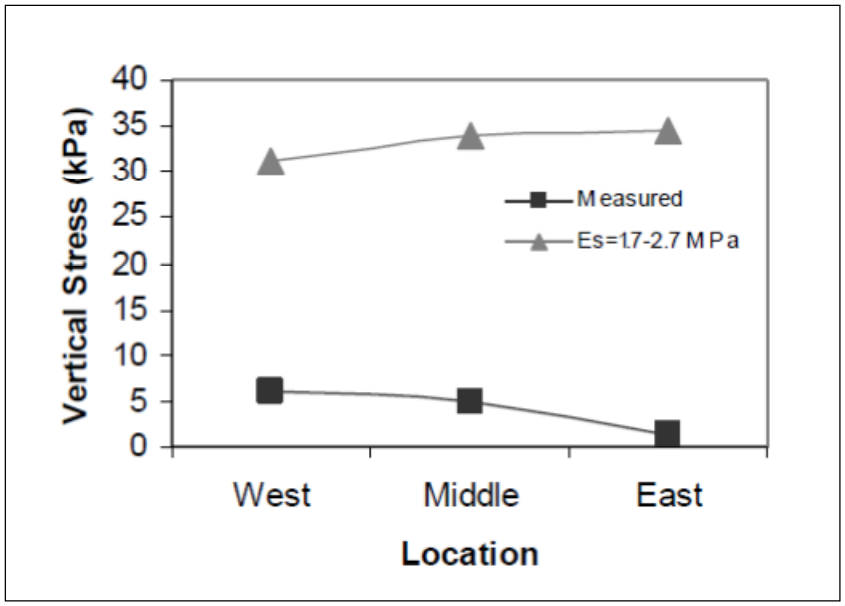

Figure 5-11 Predicted and Measured Vertical Stresses in the Base Sand for the State Street Exit Ramp.

Figure 5-12 shows the predicted and measured vertical normal stress in the base sand at the west, middle and south instrumentation arrays at State Street. (A one-dimensional overburden stress analysis yields a stress of about 26 kPa at all three arrays; FLAC predicts 30 to 35 kPa at these same locations.) However, as previously discussed (for the 3300 South Street), the *FLAC* model significantly over predicted the stresses measured in the base sand at these locations.

5.7.3 100 South Street Instrumentation Arrays

Figure 5-13 shows the predicted and measured differential settlement at 100 South Street, south instrumentation array. The *FLAC* model predicts relatively uniform differential displacement throughout the geofoam embankment. (Note that in this figure the geofoam thickness for the last two data points is less than the first three points. The data and *FLAC* differential settlement estimates for levels 7.5 and 8.5 are for only one layer of geofoam block, as opposed to two; the data and *FLAC* measurements for levels 8.5 and 9 are for a half block layer.) Although the measured differential displacements for the south array are somewhat variable, the *FLAC* model does reasonably predict the differential displacement pattern. In addition, an E_s value between 1.7 and 2.3 MPa appears to provide a reasonable match to the field measurements.

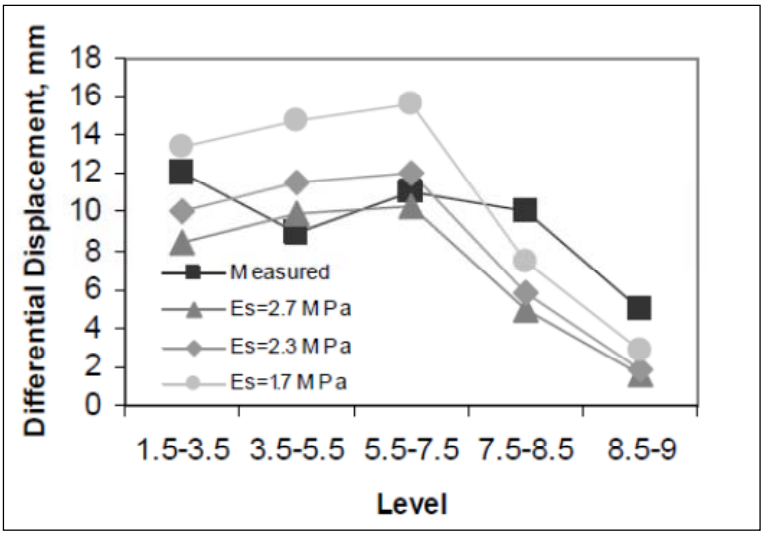

Figure 5-12 Predicted and Measured Differential Displacements between Geofoam Layers for the 100 South Street South Instrumentation Array.

The pressure cell data for the 100 South Street instrumentation arrays are not plotted because only one pressure cell provided useable data. This pressure cell was placed in the base sand and measured a vertical stress of about 33 kPa; the *FLAC* model predicted a vertical stress of 18 kPa. (A one-dimensional overburden stress analysis yields a vertical stress of about 27 kPa in the base sand for this embankment.) This pressure cell at this location is the only case in which the measured stress is higher than the estimated *FLAC* value. The installation of this pressure cell was not different than at previous arrays, thus potential installation issues do not easily explain this difference.

5.8 Conclusions

This section of the report presented construction field-monitoring data from three geofoam embankments for the I-15 Reconstruction Project in Salt Lake City, Utah and modeling results of these embankments using *FLAC*, a finite difference program. In general, *FLAC* produced reasonable estimates of the field measurements, both in terms of vertical and horizontal stress distribution and vertical displacement. We believe that numerical modeling provides valuable insight into the behavior and design of these complex, multilayered embankment systems.

We employed a simple bilinear elastic model for geofoam embankment stress-strain behavior to predict the stress distribution and vertical displacement of geofoam embankments. The validity of this model was verified by comparison of the numerical results to pressure cell and magnet extensometer measurements. In our bilinear model, we used a low stress elastic modulus ranging from 1.7 to 2.7 MPa to account for displacements occurring from gap closure and seating between the surfaces of the untrimmed geofoam blocks for vertical stresses below 15 KPa. We also found that an elastic modulus of 10 MPa reasonably reproduced the measured compression and vertical stress distribution found in Type VIII geofoam at higher stress levels (i.e., above 15 kPa). At these higher stress levels, elastic compression of the geofoam blocks dominates the displacement behavior of the geofoam embankment.

However, additional complexity not included in the numerical analyses was present in the field measurements. These complexities are attributed to thermal variations and loading created by wall/pavement/geofoam interaction, which were not explicitly considered in the modeling approach. Thus, some judgment was required in interpreting the field measurements and relating them to the numerical results. Most importantly, pressure cells placed near the top of the geofoam embankment and in the overlying base material near the concrete pavement surface showed strong seasonal stress fluctuations that are attributed to differential expansion and contraction of the embankment and pavement systems and their interaction with the adjacent panel wall via a relatively rigid connection. Also, the installation of the pressure cells in the basal bedding sand and the subsequent placement of overlying "arched" block appears to have created arching or a non-uniform contact surface that did not allow for complete vertical stress transfer to the underlying pressure cells.

In addition to stress and settlement distribution calculations, the bilinear *FLAC* model has application in determining the compressional, horizontal and contact stresses used in slope stability and seismic sliding calculations. The estimation of contact stresses at interfaces is particularly important for internal stability calculations for both static and dynamic cases. The results of this study and additional *FLAC* modeling was subsequently employed to evaluate the sliding stability of geofoam embankments subjected to strong ground motion resulting from major earthquakes (Bartlett and Lawton, 2009).

This page intentionally left blank

6.0 Long-Term Creep and Settlement

Instrumentation was installed at several locations to monitor the construction and postconstruction settlement performance of these technologies and embankments (Bartlett and Farnsworth, 2004). This section of the report will focus on the long term monitoring of three EPS embankment locales: (1) 100 South Street, (2) 3300 South Street and (3) State Street.

6.1 100 South Street Site

The I-15 Reconstruction at 100 South Street required raising and widening of the existing embankment to the limits of the right-of-way. The geofoam fills in both the north and southbound directions were placed over a 406-mm high-pressure natural gas line and other buried utilities (Figures 6-1 and 6-2). The southbound portion of this embankment employed approximately 3,400 m^3 of EPS 20, and the height of the embankment decreased southward to conform to the roadway elevation. The embankment height (not including the pavement thickness) decreased from 8.1 to 6.9 meters, corresponding to 10 to 8.5 layers of geofoam blocks, respectively (Figure 6-1). The geofoam embankment transitions to two-stage MSE walls on both the north and south sides. In this area, the top part of the existing embankment was sub excavated and replaced with scoria fill to raise the roadway grade within the utility corridor without causing primary consolidation in the underlying, compressible, foundation soils.

The instrumentation installed at this location consisted of: (1) basal vibrating wire (VW) total earth pressure cells placed in sand underneath the EPS, (2) horizontal inclinometers (one placed near the base and one near the top of embankment) and (3) two magnet extensometer placed within the geofoam fill (Figures 6-1 and 6-2) (Negussey and Stuedlein, 2003). The magnet plates for the extensometers were placed at EPS layers 0, 1.5, 3.5, 5.5, 7.5, 8.5 and 9.5 at the northern (i.e., left) location and at layers 0, 1.5, 3.5, 5.5, 7.5, 8.5, and 9 at the southern (i.e., right) location (Figure 6-1). All extensometer measurements were referenced to their respective base plate underlying the geofoam fill (and not the top of the riser pipe) hence, these data represent deformations of the geofoam fill with time and do not include any settlement of the foundation soils.

Figure 6-3 shows the construction and postconstruction strain time history of the southern location as calculated from the magnet extensometer observations. The basal layers (0 to 1.5 m) underwent 1.8 percent vertical strain by end of construction at approximately 300 days. The total strain of the EPS embankment (0 to 9 m) was about 1 percent at end of construction at this same location (Figure 6-3). Figure 6-4 shows the construction and postconstruction strain of the entire embankment (0 to 9 m). The vertical strain at the southern location is about 1.5 percent after 10 years of monitoring and is projected to be about 1.7 percent creep strain after 50 years.

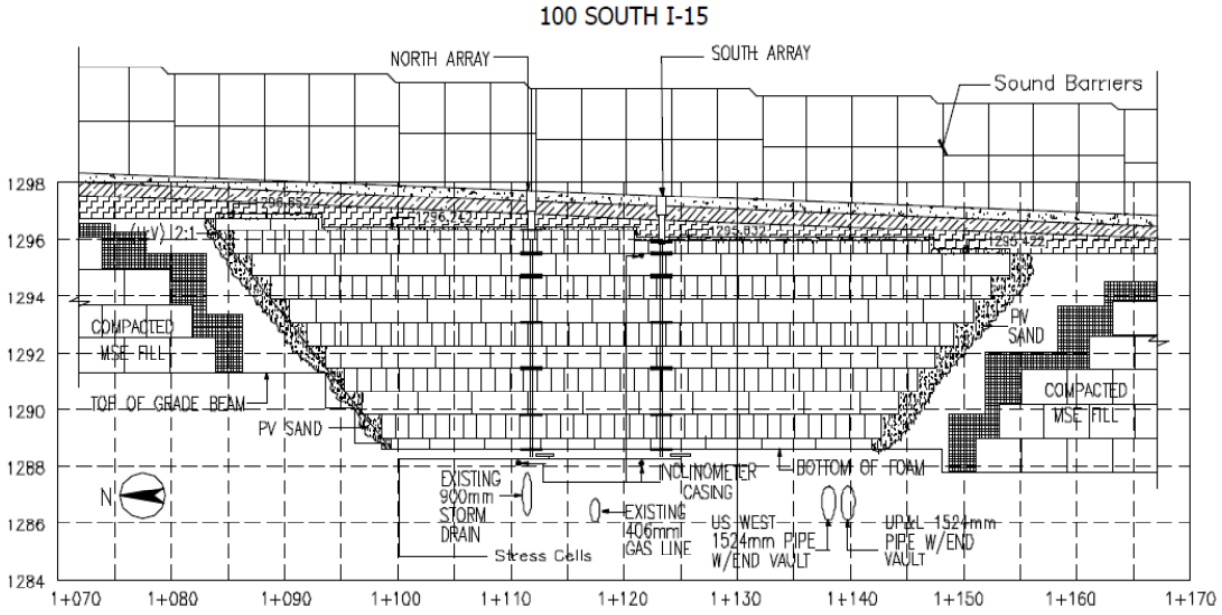

Figure 6-1 Profile View of the EPS Embankment and Instrumentation at 100 South Street, Salt Lake City, Utah, I-15 Reconstruction Project (Negussey and Stuedlein, 2003).

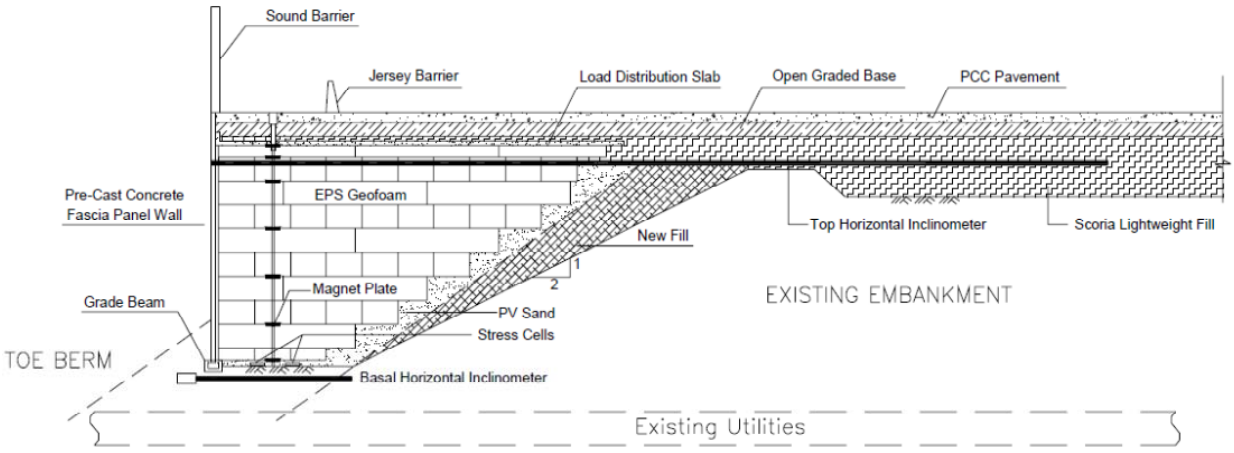

Figure 6-2 Cross Sectional View of the EPS Embankment and Instrumentation at 100 South Street, Salt Lake City, Utah, I-15 Reconstruction Project (Negussey and Stuedlein, 2003).

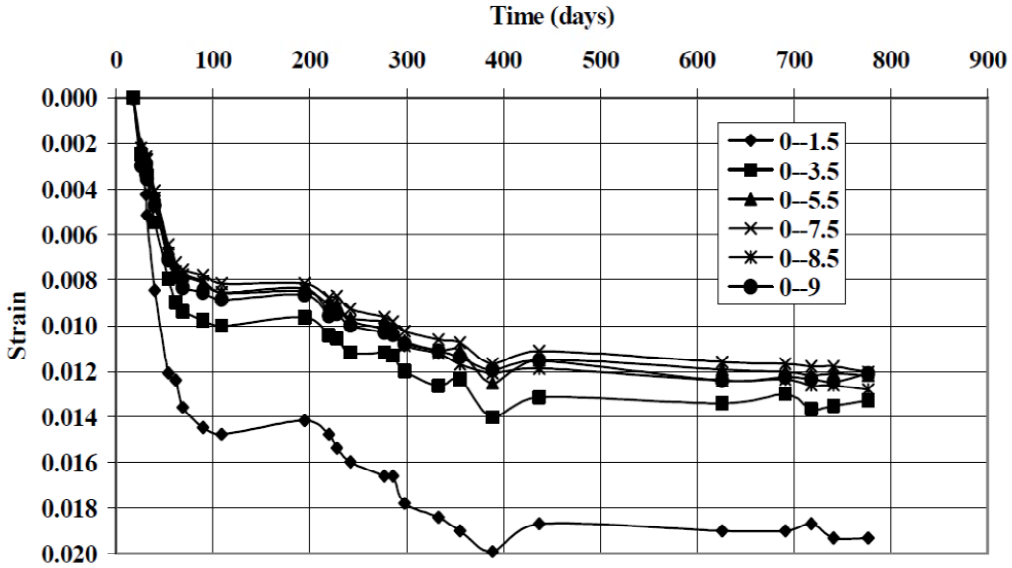

Figure 6-3 Construction and Post Construction Strain in EPS Measured in Southern Magnet Extensometer, 100 South Street Array, I-15 Reconstruction Project (Negussey and Stuedlein, 2003).

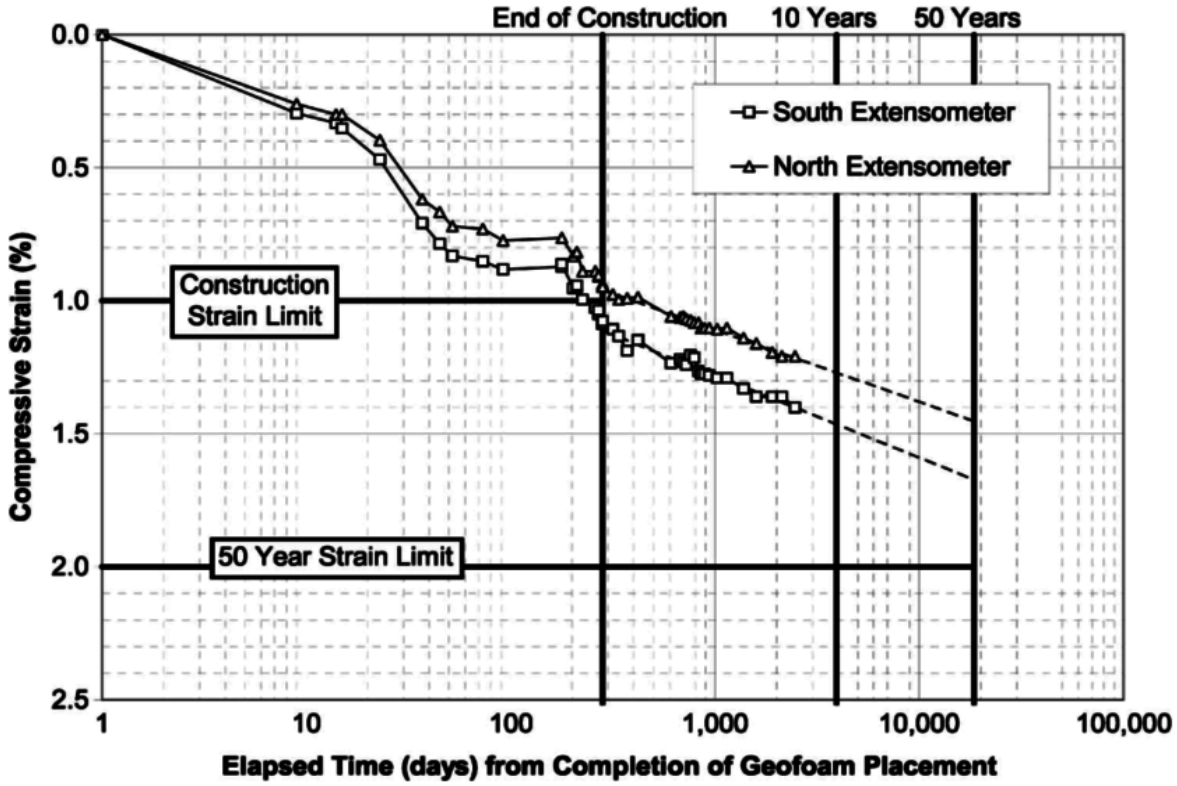

Figure 6-4 Construction and Post Construction Global Strain of Entire Thickness of EPS Embankment, 100 South Street Array, I-15 Reconstruction Project (Farnsworth et al., 2008).

The postconstruction settlement trend of Figure 6-4 is consistent with the limit 2 percent global strain in 50 years assumed in the I-15 design. Approximately 1 percent strain occurred during construction as materials were placed atop the EPS fill. The remaining strain is creep strain that has occurred postconstruction. Figure 6-3 shows that the lowest geofoam interval experienced more vertical strain when compared with the relatively uniform strain that occurred in the overlying layers. It should be noted that the foundation footing for the adjacent panel wall laterally restrains the lowest geofoam layer. As a result, the mean normal stress in the lower geofoam layers is probably somewhat higher than the corresponding states of stress in the overlying geofoam layers. This effect would produce more vertical strain and also suggests that the influence of confinement may need to be considered in future design evaluations, as appropriate.

The loading history and total stress observations from the VW pressure cells indicate that the measured internal vertical stress levels are in reasonable agreement with the design criterion (Figure 6-5). (The factored working stress design criterion of about 30 kPa for EPS 20 was selected during the design phase to limit the construction compression to 1 percent vertical strain at the end of construction period and to 2 percent compressional strain over a 50 year period.) Thus, we conclude that this design criterion has been validated given the strain measurements presented in Figure 6-4. However, we note that the 1 percent vertical strain measured during the construction period (Figure 6-4) does not entirely consist of elastic compression of the EPS block. Undoubtedly, some of this vertical strain has also resulted from small gap closure of the slightly curved block that occurred upon initial loading of the geofoam embankment. Complete seating and gap closure probably did not occur in the geofoam embankment until the final load was in place, which consisted of the combined weights of the load distribution slab (LDS), roadway base materials and pavement. Undoubtedly, a portion of the initial 1 percent strain during loading can be attributed to seating and gap closure (Negussey et al. 2001). This issue and the numerical modeling of these effects and the compressional behavior of the geofoam arrays are further discussed in Newman et al. (2010).

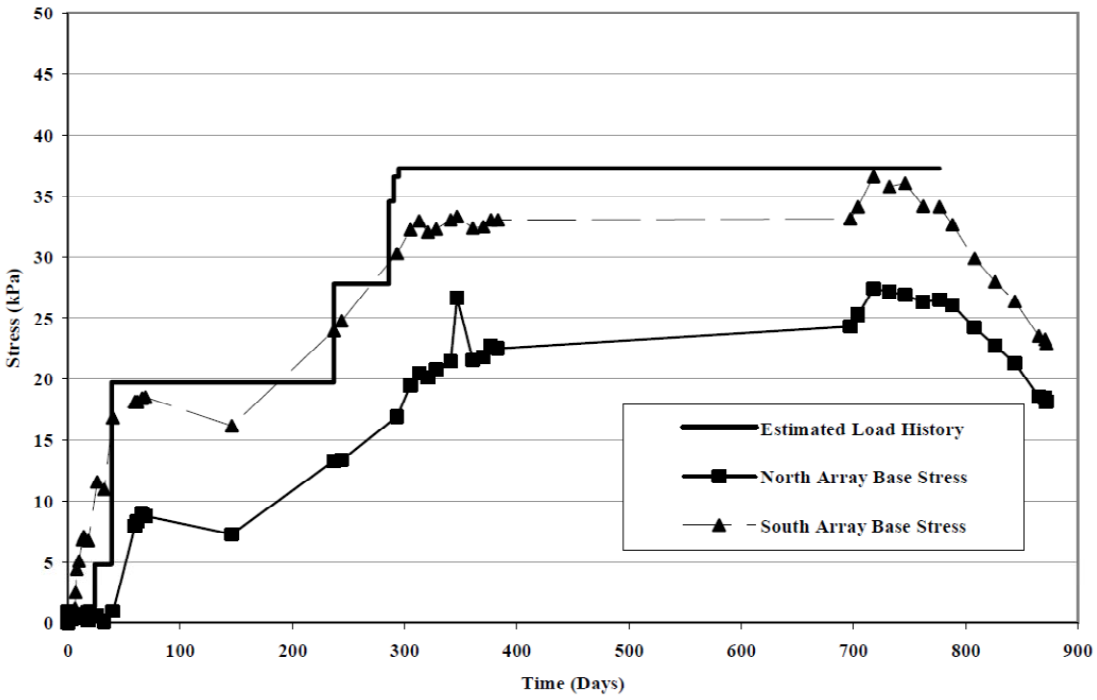

Figure 6-5 Loading History and Total Pressure Cell Measurements at the 100 South Street Array (Negussey and Stuedlein, 2003).

6.2 3300 South Street Site

The primary reason for use of geofoam at this site was the improvement of the global stability of a relatively high approach fill at a railroad crossing. Due to the height and extent of the embankment widening, design calculations suggested that the safety factor against shear failure in the foundation soils was lower than the required minimum value of 1.3 for short-term stability. Thus, if this embankment were to be constructed conventionally, it would require PV drain installation, basal geotextile reinforcement, staged embankment construction, surcharging, and a long construction hiatus to complete primary settlement before the abutments for the overpass bridge could be constructed. The planned construction sequencing and schedule for this bridge could not be accommodated using conventional construction, so EPS embankment was used to shorten the construction schedule and meet the required factor of safety.

The 3300 South Street geofoam array consisted of geotechnical instrumentation and high-precision digital level elevation surveys to measure the vertical compression and stresses that developed within the geofoam / foundation soil / pavement system. Two instrument arrays were installed at this site at mainline stationing 25+347 m, and stationing 25+315 m, respectively. At stationing 25+315, nine levels of geofoam were placed, making the total height of the geofoam approximately 7.3 m. Eight levels of geofoam were placed at stationing 25+347, making the total height of geofoam approximately 6.6 m. Figure 6-6 is a typical cross-section showing the instrument layout used at the 3300 South Street arrays.

Each array consisted of magnet extensometers, VW total pressure cells and survey points. Magnetic extensometers were used to monitor settlements of the foundation soil and deformations of the geofoam at various height intervals. Each extensometer stand-pipe was placed 2.4 m from the wall face and the 1.25-cm thick base plates were supported in the sand leveling course below the first layer of geofoam. Vibrating wire total pressure cells were installed in the base sand below the first level of geofoam block, approximately midway in the

geofoam fill, at the top of the geofoam fill, immediately above the load distribution slab and immediately below the concrete pavement (Figure 6-6).

Approximately 70 mm of construction related compression was measured within the geofoam mass during construction of the embankment at station 25+315 (Figure 6-7), which corresponds to about 1 percent global vertical strain within the entire EPS mass. Similar strains were measured at stationing 25+347 (Bartlett et al., 2001). The compression was a result of elastic compression of the geofoam, and seating and gap closure resulting from the placement of the load distribution slab, untreated base course and Portland cement concrete pavement. Unfortunately, the 1 percent vertical strain that occurred during load placement was sufficiently large to damage some of the fixed connections that secured the tilt-up panel wall to the load distribution slab (LDS). The damaged connections were subsequently repaired by drilling through the face of the panel wall at the elevation of the LDS and setting epoxy anchored dowels into the LDS.

These vertical stress measurements from the total pressure cells indicate that the stress through most of the geofoam upper part mass is about 25 to 30 kPa, which is approximately equal to the working stress design criterion of 30 kPa. The creep displacement has been about 20 mm, which corresponds to 0.27 percent over a two-year period and is consistent with the rate measured at 100 South Street for this same post construction period. Subsequent monitoring of the magnet extensometer at this location was terminated due to safety concerns as the interstate became operational.

The long-term consolidation settlement of the foundation soils underlying the 3300 South Street embankment is continuing (Figure 6-8). This data show about 40 mm of post construction foundation settlement has occurred in a 5.5-year post construction period. About 15 mm of this settlement occurred from the placement of the fill and pavement materials atop the EPS. The additional 25 mm of settlement occurred due to the placement of the toe berm, which was constructed at the base of the wall. The projected foundation settlement is about 50 mm in a 10-year post construction period. These data show that the usage of geofoam embankment at this location has met the I-15 Reconstruction performance goal of limiting the long-term settlement

to 75-mm or less in a 10-year post construction period (Farnsworth et al., 2008), despite the additional load produced by the toe berm.

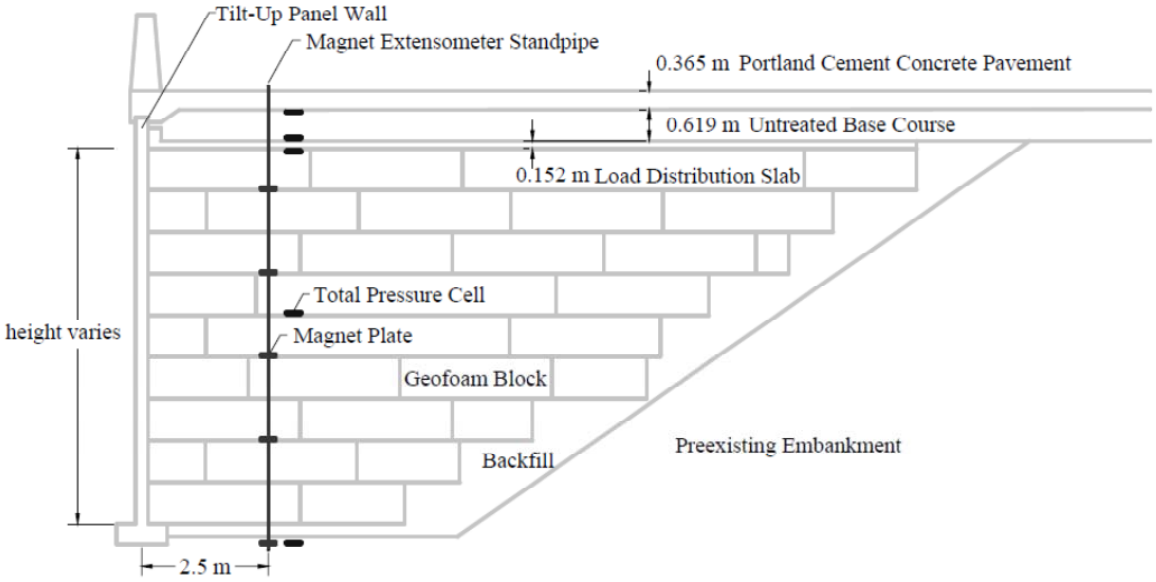

Figure 6-6 Typical Instrumentation Layout Used at the 3300 South Street Array (Newman et al. 2010).

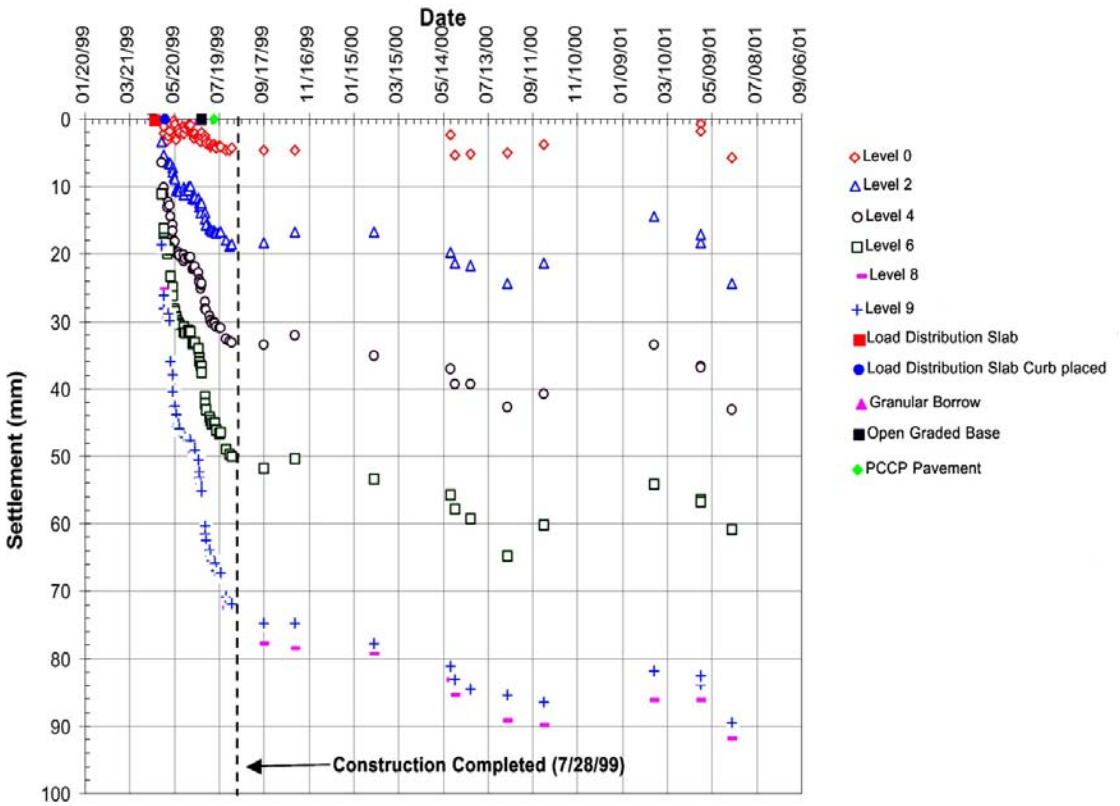

Figure 6-7 Vertical Displacement Versus Time for Geofoam Array at Station 25+347, 3300 South Street Array, I-15 Reconstruction Project (Bartlett et al., 2001).

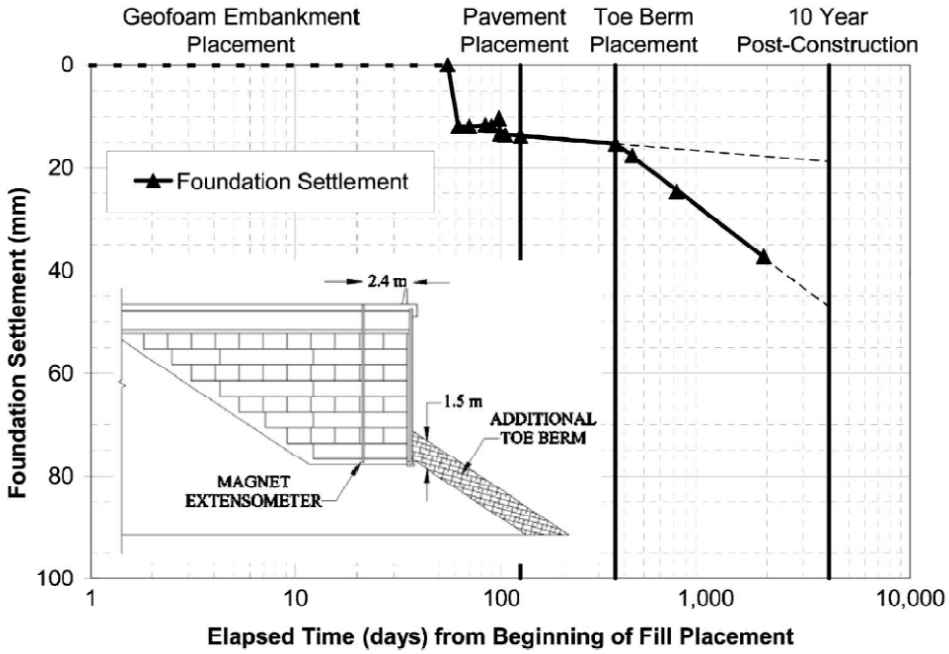

Figure 6-8 Foundation Settlement Versus Time for the Geofoam Embankment at 3300 South Street, I-15 Reconstruction Project (Farnsworth et al., 2008).

This page intentionally left blank

7.0 Numerical Modeling of Seismic Stability

7.1 Introduction

This section of the report evaluates the expected seismic performance of a typical freestanding geofoam embankment used in Utah by means of numerical modeling techniques incorporated in FLAC^{TM} (Fast Lagrangian Analysis of Continua) (Itasca, 2005). Comprehensive seismic design guidance for geofoam embankment has not been fully developed in the U.S., but Horvath (1995), Stark et al. (2002), Raid and Horvath (2004), and Kalinski and Pentapati (2006) give summaries of pseudostatic and numerical modeling approaches that may be applicable to the seismic design and evaluation of geofoam embankments for specific applications.

At high levels of strong motion, the dynamic response of geofoam embankment is relatively complex. Raid and Horvath (2004) have classified the rigid-body displacement and flexible deformation behaviors present in the geofoam mass as: (1) horizontal flexibility (lateral sway), (2) rigid-body translation (sliding) and (3) rigid-body rotation (rocking). This section presents a 2D evaluation approach to explore these behaviors and their impact on seismic stability using a representative set of acceleration time histories appropriate for western U.S. near-field earthquakes. This evaluation includes both the horizontal and vertical acceleration components of the candidate time histories in a fully coupled manner.

For the I-15 Reconstruction Project, the Utah Department of Transportation (UDOT) required that lightweight fill and geofoam embankment placed behind retaining walls be designed to a 500-year return period design basis event (500-yr DBE). Force-based pseudostatic techniques described in Horvath (1995) were used that in short consisted of: (1) calculating the fundamental period of the geofoam embankment, (2) determining the horizontal spectral acceleration for the 500-yr DBE at the fundamental period of the system, (3) calculating the inertial force acting on the centroid of the system as the mass times the spectral acceleration, and (4) using this inertial force in the subsequent stability analyses. The analyses performed by the design-build contractor showed that the geofoam embankment had adequate factors of safety against failure for the 500-yr DBE.

More recently, UDOT has adopted a larger DBE for embankments at bridge approaches. This standard requires that interstate bridges and their approach fills be capable of withstanding a 2500-yr DBE with minimal to no damage. For the Salt Lake Valley, the 2500-yr DBE is characteristically M7.0 to 7.5 earthquakes, that ruptures on the Salt Lake City segment of the Wasatch fault with an expected horizontal peak ground acceleration (PGA) of about 0.5 to 0.6 g throughout much of the central part of the Salt Lake Valley.

The horizontal and vertical acceleration time histories and their respective response spectra that were used in the evaluations are shown in Figures 7-1 and 7-2, respectively and Tables 7-1 and 7-2, respectively. These strong motion records were selected from the Pacific Earthquake Engineering Research (PEER) Center website and are unmodified. The acceleration records in Tables 7-1 and 7-2 were selected because their earthquake magnitude, source distance, and soil conditions are similar to those expected for the urban interstate corridor found in the central part of the Salt Lake Valley. These strong motion records were deconvolved to a depth equal to the base of the 2D numerical model (10 m below ground surface) using the 1D equivalent linear procedures described by Mejia and Dawson (2006). The steps and boundary conditions required to convolve the motion upward through the 2D model are described later.

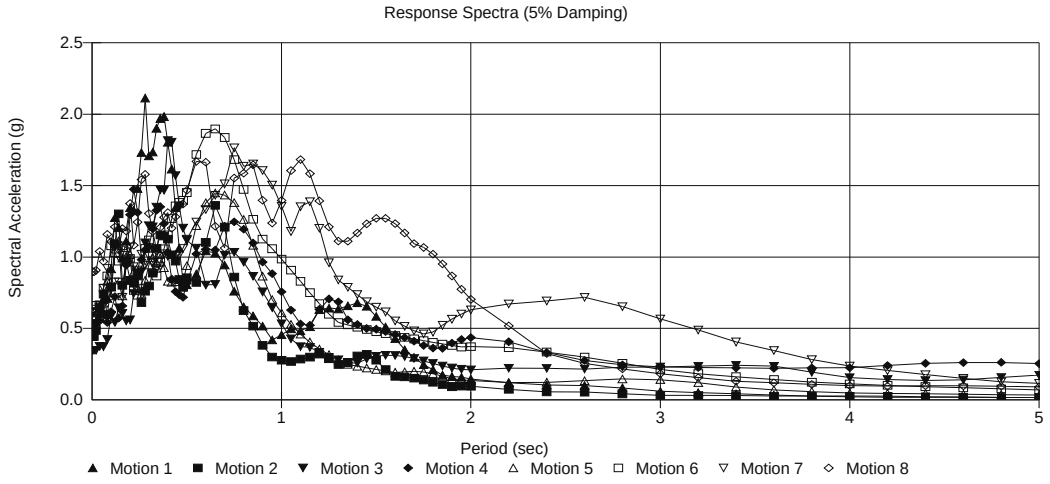

Figure 7-1 Five Percent Damped Horizontal Acceleration Response Spectra for the Evaluation Time Histories.

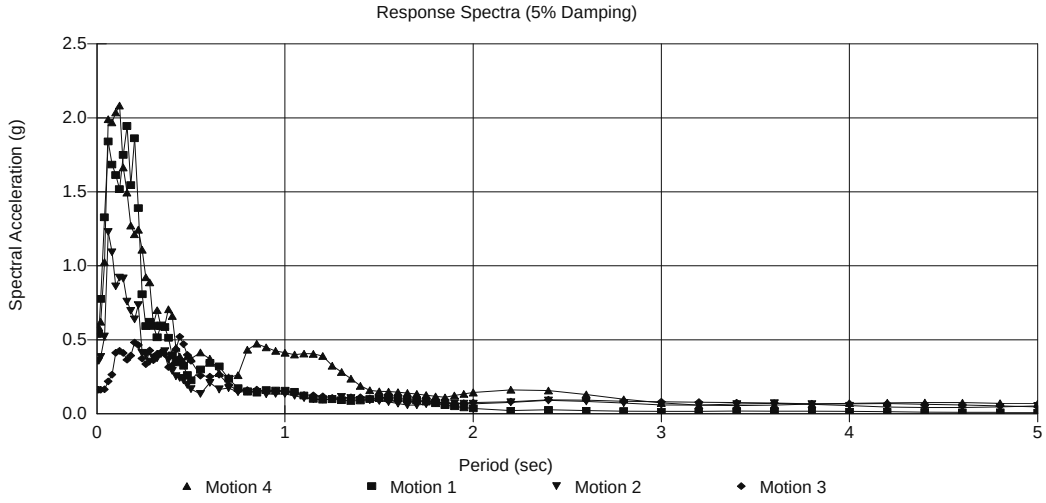

Figure 7-2 Five Percent Damped Vertical Acceleration Response Spectra for the Evaluation Time Histories.

Table 7-1 Horizontal Strong Motion Records Used in Evaluations.

Motion	Earthquake	M	R (km)	Component	PGA (g)
1	1989 Loma Prieta, CA	6.9	8.6	Capitola 000	0.52
2	1989 Loma Prieta, CA	6.9	8.6	Capitola 090	0.44
3	1999 Duzce, Turkey	7.1	8.2	Duzce 180	0.35
4	1999 Duzce, Turkey	7.1	8.2	Duzce 270	0.54
5	1992 Cape Mendocino, CA	7.1	9.5	Petrolia 000	0.59
6	1992 Cape Mendocino, CA	7.1	9.5	Petrolia 090	0.66
7	1994 Northridge, CA	6.7	6.2	Sylmar 052	0.61
8	1994 Northridge, CA	6.7	6.2	Sylmar 142	0.90

Table 7-2 Vertical Strong Motion Records Used in Evaluations.

Motion	Earthquake	M	R (km)	Component	PGA (g)
1	1989 Loma Prieta, CA	6.9	8.6	Capitola up	0.54
2	1999 Duzce, Turkey	7.1	8.2	Duzce up	0.36
3	1992 Cape Mendocino, CA	7.1	9.1	Petrolia up	0.16
4	1994 Northridge, CA	6.7	6.2	Sylmar up	0.59

7.2 Model Development and Properties

Figure 7-3 shows a typical freestanding geofoam embankment. At this location, the embankment is approximately 8 m high and 20 m wide and both sides are vertical (i.e., freestanding). The adjacent bridge is supported by piles and the approach slab and adjacent embankment are supported by geofoam. (The geomembrane draped over the geofoam in Figure 7-3 was removed and not used in the final construction because of concerns of the potential for sliding between the geofoam and geomembrane during a seismic event.) Instead, the load distribution slab was poured directly atop the uppermost geofoam layer.

Figure 7-4 is a cross-sectional view of a typical geofoam freestanding embankment. From bottom to top, it consists of bedding sand, geofoam block, reinforced concrete load distribution slab, road base (untreated base course), and unreinforced concrete pavement. A prefabricated tilt-up concrete panel wall protects the geofoam from damage and the wall is founded on an embedded slot footing. The panel wall is rigidly connected to the load distribution slab and a coping formed in the concrete pavement protects the panel top (Figure 7-4). An elastomeric material is placed between the coping and the panel top to limit the vertical and horizontal interaction at this point. In addition, the geofoam blocks do not contact against the back of the panel wall. Typically, a 0.2-m gap is left between the geofoam and the back of the wall to prevent interaction. However, continuous horizontal layers exist in the geofoam mass, which can allow for interlayer sliding if horizontal seismic forces are sufficient to initiate it. No such continuous vertical planes exist, because the blocks are staggered and the orientation is rotated 90 degrees on each successive layer (Figure 7-4). Lastly, the basal layer (layer 1) of geofoam is placed directly against the slot footing of the tilt-up panel wall and is constrained from horizontal movement.

Because most of the mass of the system is contained within the load distribution slab, road base, and pavement, the geofoam system is often modeled as an elastic single degree of freedom (SDOF) system with the a lumped rigid mass placed at the top and supported by a weightless rectangular geofoam embankment (Horvath, 1995). The combined weight of the load distribution slab, road base and pavement are represented in the lumped mass.
This approach in this report varies from this classic approach in the following important aspects: (1) two degrees of freedom (horizontal and vertical) movement are allowed, (2) nonlinear stress-strain relations are used for all materials, except for the lump mass, which was treated as an elastic material, (3) horizontal sliding is allowed between the geofoam layers by including interfaces nodes, and (4) both the horizontal and vertical components of the strong motion records were inputted into the model to explore their combined effects on the dynamic response and potential sliding.

We chose to model the geofoam embankment using an explicit finite difference program called *FLAC*^{TM} (Fast Lagrangian Analysis of Continua) (Itasca, 2005). The FLAC code

developed for the dynamic evaluations is presented in Appendix 6. The numerical approach, as implemented in *FLAC*, can reasonably approximate the measured pressure distribution and vertical deformation in the geofoam mass for the static load case, as previously discussed. *FLAC* also has the capability to model the 2D nonlinear dynamic response and the potential for interlayer sliding, which is the primary focus of this section of the report.

Figure 7-3 Typical Freestanding Geofoam Embankment at a Bridge Abutment.

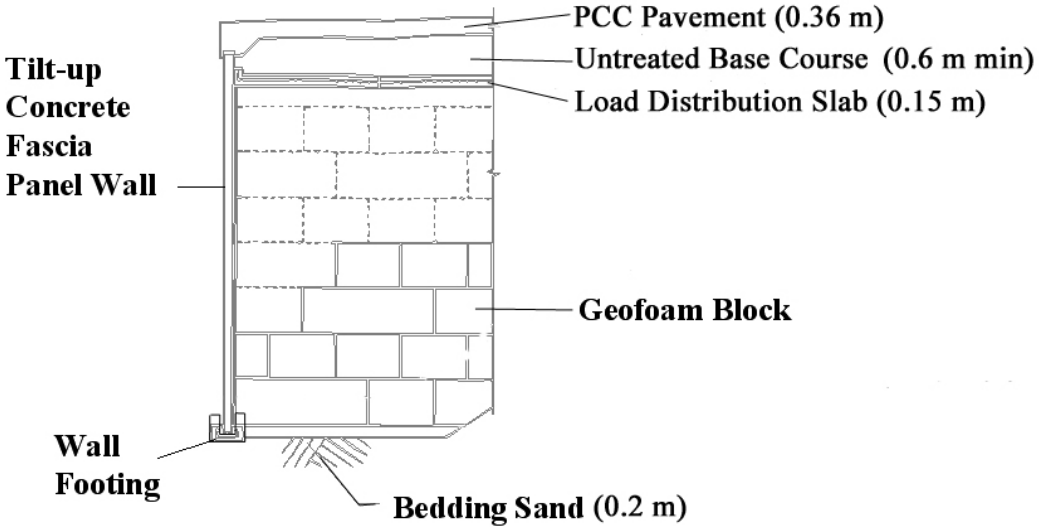

Figure 7-4 Typical Geofoam Cross-Section Used for the I-15 Reconstruction Project.

The geofoam elastic properties used in the *FLAC* model (Table 7-3) are from large block testing performed by Elragi (2000) and are considered to be representative of the geofoam commonly used on UDOT projects. The various other properties in this table are typical values and their selection, except for the foundation soil, do not affect the modeling greatly. The elastic properties for the foundation soil are representative of medium to medium-stiff clay, typical for the Salt Lake Valley.

FLAC's hysteretic damping option was used to model the nonlinear strain-dependent modulus and damping in the geofoam and foundation soil. The hysteretic damping option allows the nonlinear formulation in *FLAC* to use the same shear modulus degradation and damping curves developed for the equivalent linear method. Furthermore, the hysteretic damping option eliminates the need for large amounts of Rayleigh damping in the model, which greatly improves *FLAC's* computational speed. The hysteretic damping option can be used with either elastic or Mohr-Coulomb material properties. In the case of the former, nonlinear strain-dependent moduli and damping are calculated, but failure (yielding) does not occur; whereas in the latter case, yielding and plastic behavior are allowed. Because yielding is a form of energy dissipation (damping), for our sliding evaluations we chose to use the elastic properties shown in Table 7-3 with hysteretic damping for the geofoam and foundation soil, instead of applying Mohr-Coulomb

properties. This essentially means that the geofoam block will not be allowed to yield during sliding, which will in turn emphasize any potential sliding behavior.

Shear modulus degradation and damping curves appropriate for geofoam and the foundation soil were obtained from Athanasopoulos et al. (1999) and Sun et al. (1988), respectively. To implement the hysteretic damping option, *FLAC* offers various functions to fit the curvature of the shear modulus and damping curves. We selected the three-parameter sigmoidal model (sig3) (Itasca, 2005) to fit the shear modulus degradation curves (Figure 7-5). The sigmoidal model parameters used to obtain these curves are: $a = 1$, $b = -0.45$, and $x_0 = 0.3$ for geofoam and $a = 1.017$, $b = -0.587$, and $x_0 = -0.633$ for the foundation clay.

In addition to hysteretic damping, five percent Rayleigh damping was applied to the *FLAC* model at 200 Hz to eliminate some high frequency artificial numeric vibration that was occurring in the model. Because this damping was only applied to very high frequencies, it has no significant influence on the geofoam and foundation soil response.

We chose a 1 m by 1 m grid spacing for the model that consists of a 10-m thick clay foundation layer, 8-m high geofoam embankment, and 1-m thick lumped mass (Figure 7-6). The 0.2-m thick bedding sand layer was ignored. In addition, the lumped mass represents the combined masses of the load distribution slab, road base, and concrete pavement. The lumped mass was given elastic properties appropriate for concrete (Table 7-3), thus it essentially acts as a coherent system placed atop the geofoam, and because of its high stiffness, will essentially undergo no significant internal deformation.

For simplicity's sake, the panel wall was omitted from the *FLAC* model. Because a gap of 0.2 m is typically used between the geofoam face and the back of the panel wall, the wall does not restrain the geofoam in any manner. However, because the load distribution slab is connected to the panel wall and the load distribution slab interacts with the geofoam along their common contact surface (Figure 7-4), some amount of wall/geofoam interaction is expected. This interaction is omitted owing to the extra difficulty in including the wall in the dynamic analyses. Nonetheless, because the mass of the lump mass atop the geofoam embankment is

much greater than that of the panel wall, we believe that the FLAC model will capture the primary dynamic behavior of the system.

Interfacial nodes were used at interfaces 1 through 9 to allow sliding and separation in the model between the geofoam layers (Figure 7-6). Interface 1 is the foundation soil/geofoam contact surface, interfaces 2 through 8 are geofoam/geofoam contact surfaces (from bottom to top, respectively), and interface 9 is a geofoam/load distribution slab contact surface. FLAC requires Mohr-Coulomb properties and normal and shear stiffness at all interfaces. The required properties include: friction, cohesion, tensile strength, normal stiffness, and shear stiffness. However, we applied no cohesion, dilation, or tensile bond strengths at these interfaces. (The lack of tensile bond strength allows for separation between the geofoam layers.) Thus, sliding friction was used at the interfaces (Table 7-4). The friction angles in Table 7-4 were obtained from project-specific laboratory testing performed for the I-15 Reconstruction Project (Bartlett et al., 2000) and represent typical values for Type VIII geofoam. Frictional values for other projects may be somewhat different, depending on material, construction and environmental variables (Bartlett et al. 2000). In addition, these friction angles are intermediate values between the peak and residual friction angle. We also assumed that dilation due to sliding at the interfaces is negligible. In addition, the effects of gripper plates, which are commonly placed between geofoam layers during construction, are not considered a significant source of sliding resistance due to their relatively small size and were neglected in the analyses. Also the interface between the foundation soil and basal geofoam layer was "glued" so that slippage and sliding does not occur. This was done for two reasons: (1) sliding at this interface is constrained horizontally by the foundation of the panel wall (Figure 7-4), and (2) we wanted to ensure that full seismic forces are transferred to the geofoam embankment. Lastly, only sliding friction was used at interface 9 at the top of geofoam/bottom of lumped mass contact surface. In reality, this interface is more than a frictional contact, because the concrete slab is poured directly on the geofoam and some tensile and shear bonding undoubtedly occurs; this was neglected in our sliding evaluations.

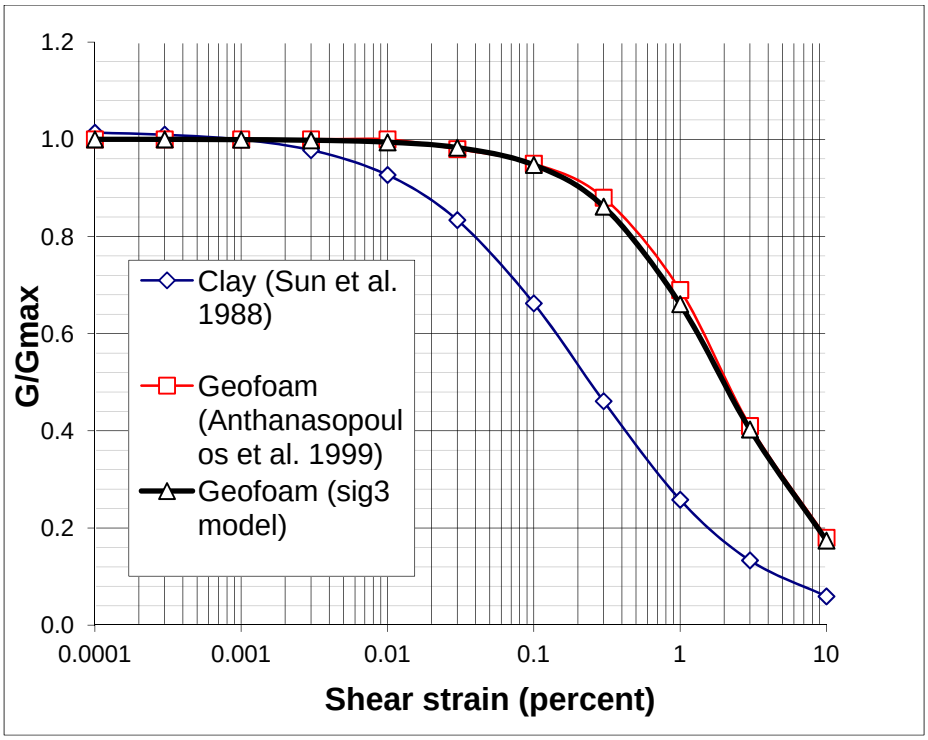

Figure 7-5 Modulus Degradation Curves Used in FLAC's Hysteretic Damping Option.

Table 7-3 Initial Elastic Properties for the FLAC model

Material Type	Layer No.	ρ (kg/m^3)[4]	E (MPa)[5]	ν[6]	K (MPa)[7]	G (MPa)[8]
Foundation Soil	1-10	1840	174	0.4	290.0	62.1
Geofoam	11-18	18	10	0.103	4.2	4.5
UTBC[1]	19	2241	570	0.35	633.3	211.1
LDS[2] & PCCP[3]	19	2401	30000	0.18	15625.0	12711.9

[1] Untreated base course, [2] Load distribution slab, [3] Portland concrete cement pavement, [4] Mass density, [5] Initial Young's modulus, [6] Poisson's ratio, [7] Bulk modulus, [8] Shear modulus

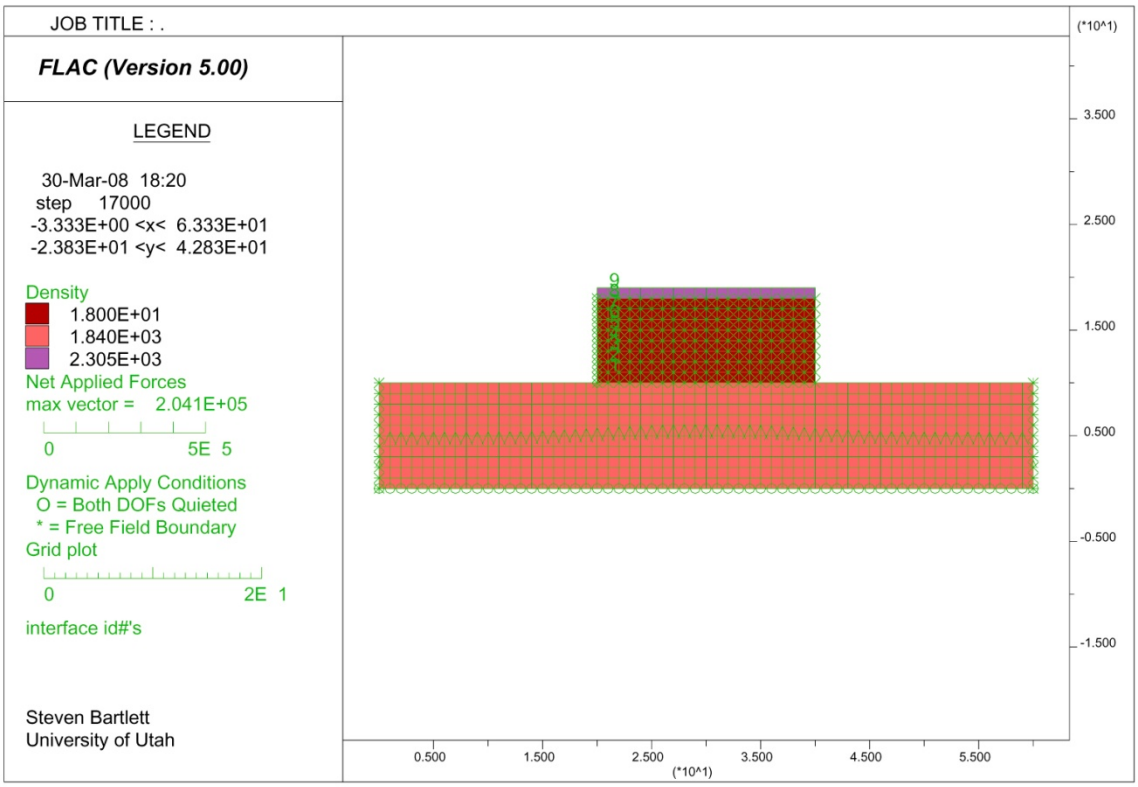

Figure 7-6 2D FLAC Model Used for Dynamic and Sliding Evaluations.

Table 7-4 Interfacial Properties Used for Sliding Evaluations in the FLAC Model.

Contact Surface	Interface number (bottom to top)	Normal and Shear Stiffness ($k_n = k_s$) (MPa)	Friction angle (degrees)
Geofoam-soil	1	102	31[1]
Geofoam-Geofoam	2-8	102	38
Geofoam-Lump Mass	9	102	38[2]

[1] A glued interface was used for interface 1 in FLAC because the geofoam is abutted against the panel wall footing and cannot slide. [2] Neglects any tensile or shear bonding that may develop between the top of geofoam and base of the load distribution slab.

Normal and shear stiffness at the interfaces are also required by *FLAC*. These are spring constants that represent the respective stiffness between two planes that are in contact with each other. Interfacial stiffness is often used in *FLAC* to represent the behavior of rock joints where

some elastic deformation in the joint is allowed before slippage occurs. However for geofoam block placed in layers, such elastic behavior before slippage occurs is probably small. Thus, for the case where only slippage and separation are considered at the interface (i.e., one geofoam subgrid is allowed to slide and/or open relative to another subgrid), the normal and shear stiffnesses used in the *FLAC* model are not important (Itasca, 2005). For this case, the *FLAC* user's manual recommends that the normal and shear interface stiffness (k_n and k_s, respectively) be set to ten times the stiffness of the neighboring zone:

$$k_n = k_s = 10\,[(K + 4/3G)/\Delta z_{min}]$$

where: Δz_{min} is the smallest width of an adjoining zone in the normal direction, which is 1 m for our model. However, if the material on one side of the interface is much stiffer than the other, then the above equation should be applied to the softer side, because the softer side dominates the deformability of the whole system. Thus, making the interfacial stiffness equal to ten times the soft side stiffness ensures that the interface has minimal influence on system compliance (Itasca, 2005). We followed these recommendations for all interfaces.

The final modeling issues to be addressed are the placement of the layers in the model, the applied boundary conditions, and how the strong motion is assigned to the base of the *FLAC* model. First, the *FLAC* model is constructed layer-by-layer and time stepped until force equilibrium is reached in the model. This is done by fixing the base of the model in the x and y coordinate directions and fixing the side of the model, where soil layers are present, in the x direction only. The geofoam is free standing, so no boundary condition is applied along its margins.

When static force equilibrium is reached, the model's boundary conditions are changed for the dynamic case. The bottom of the model is changed to a quiet (i.e., viscous) boundary in both the x and y directions and the sides of the soil model are changed to free-field boundaries (Figure 7-6). (The free-field boundary forces a 1D free-field boundary condition at the model's edge, which essentially treats the boundary as if it were placed at an infinite distance.) A compliant base is the preferred option for deep soil columns because downward propagating

waves are absorbed by the quiet boundary and are not reflected back into the model as would be the case for a rigid boundary (Mejia and Lawson, 2006). The quiet boundary requires a stress time history at the boundary; thus the velocity time history obtained at the base of the soil column from the deconvolution analysis was converted to a stress wave for the subsequent *FLAC* analyses. Itasca (2005) and Mejia and Lawson (2006) provide more information about this conversion and the steps required for deconvolution and convolution analyses. We followed these procedures and to verify the process, the surface acceleration time histories were obtained from *FLAC* at the top of the soil model and were compared with the original input acceleration time histories listed in Tables 7-1 and 7-2. This comparison showed that the free-field *FLAC* acceleration time histories were very similar, indicating that the deconvolution/convolution process had been performed correctly and ensuring that the proper level of accelerations were being input to the base of the geofoam embankment.

7.3 Sliding Evaluations

The potential for interlayer sliding in a geofoam embankment is often evaluated using pseudostatic techniques. In this approach, the inertial horizontal force at the fundamental period of the geofoam embankment is applied to the sliding calculation. It is calculated by multiplying the lumped mass of the system times the spectral acceleration at the embankment's fundamental period. The geofoam is treated as a single degree of freedom (SDOF) system and its fundamental period is calculated from Horvath (2004):

$$T_0 = 2\pi\{[(\sigma'_v H)/(Eg)[4(H/B)^2 + (12/5)(1+\nu)]\}^{0.5} \quad (7\text{-}1)$$

where: T_0 is the fundamental period, σ'_v is the vertical effective stress acting on the top of the geofoam from dead loads, H is the geofoam embankment height, E is the initial Young's modulus of the geofoam, g is the gravitational constant, B is the width of the geofoam embankment and ν is Poisson's ratio. When applied to the geofoam embankment shown in Figure 7-6 and the properties given in Table 7-3, the value T_0 is 0.52 s. As a check of the model, the embankment was constructed in *FLAC* on a rigid base and allowed to undergo free-vibration from a pulse load. This produced a T_0 value of 0.51 s, which is good agreement with the above

equation. A pseudostatic sliding calculation applied to our model and interface properties suggests that horizontal accelerations above 0.8 g should trigger sliding. The spectral values at T equals 0.5 s from Figure 7-1 vary from about 0.8 to 1.5 g; thus, interlayer sliding is expected to occur for most, if not all, of the input strong motion records used in our analyses.

The *FLAC* model was used to estimate the amount of sliding displacement in the geofoam embankment. To do this, the relative sliding displacement between successive layers of geofoam was calculated and summed as a function of time for all layer interfaces to calculate the total relative sliding displacement (TRSD) time history shown in Figure 7-7. The maximum TRSD values for each time history case are tabulated in Table 7-5.

The maximum TRSD values range from 0.01 m to greater than 1 m for the various cases listed in Table 7-5. TRSD values less than about 0.1 m are probably acceptable from an embankment performance standpoint; but larger values could have important consequences (i.e., potential damage to the panel wall, damage to approach slabs, etc). The strong motion record used for cases 4a and 4b produced unusually high amounts of sliding (1.3 m). This input horizontal displacement time history is compared with a more moderate sliding case (case 5) in Figure 7-8, top and bottom, respectively. The Duzce 270 record has a peak horizontal displacement of about 50 cm; whereas the Petrolia 000 record has a much smaller peak horizontal displacement of about 20 cm. This suggests that interlayer sliding is highly affected by the magnitude of the primary displacement pulses, their frequency and phasing.

We noted that TRSD values are usually higher when the vertical component of strong motion is included in the analysis. For example, some cases suggest that sliding displacement increases by a factor of 2 to 5; however, some cases produce essentially the same amount of sliding displacement (Table 7-5). This suggests that the magnitude of the vertical component of strong motion and its relation to horizontal displacement pulses in the horizontal record are important factors that affect sliding. The model also showed that relative sliding is greater near the base of the geofoam embankment and becomes successively less in upper layers (Figure 7-7). This trend was consistent for all models. No sliding was observed between the top of the

geofoam and base of the lumped mass, even though only a friction contact was used at this interface.

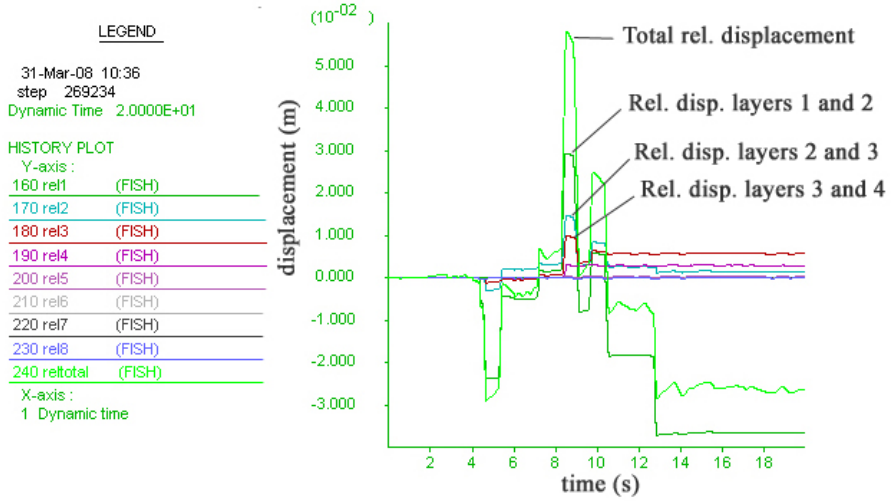

Figure 7-7 Relative Sliding Displacement Plot for Various Geofoam Layers for Case 1a.

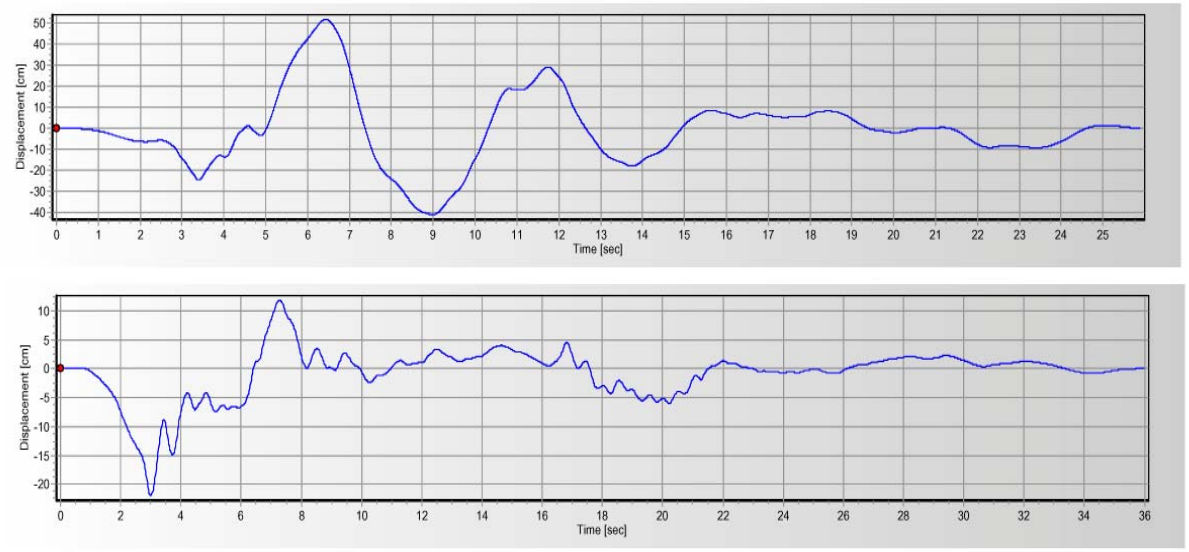

Figure 7-8 Comparison of Duzce 270 Input Displacement Time History (Case 4) (top) versus Petrolia 000 Input Displacement Time History (Case 5) (bottom).

Table 7-5 Summary of Relative Sliding Displacement for Various Cases.

Case	Horizontal Motion	Vertical Motion	Max. total relative sliding displacement (m)
1a	1	Not applied	0.06
1b	1	1	0.06
2a	2	Not applied	0.01
2b	2	1	0.05
3a	3	Not applied	0.06
3b	3	2	0.06
4a	4	Not applied	1.3
4b	4	2	1.3
5a	5	Not applied	0.005
5b	5	3	0.01
6a	6	Not applied	0.05
6b	6	3	0.06
7a	7	Not applied	0.5
7b	7	4	0.6
8a	8	Not applied	0.6
8b	8	4	0.5

Finally, we emphasize that the values reported in Table 7-5 are estimates from a numerical model that has not been calibrated with data from case histories or large-scale experiments; thus, some uncertainty exists in these sliding estimates. Because of this, we believe that it is important not to scrutinize solely the estimated displacements, but instead to see if their general magnitudes and trend suggest that a sliding stability threshold has been exceeded where the expected sliding may become unacceptably large. For example, three of the eight cases that included the vertical component of strong motion had TRSD values greater than 0.1 m (cases 4b, 7b and 8b). Because this represents 37.5 percent of the vertical + horizontal component cases, it

is probable that sliding displacement may be unacceptable for the particular geofoam configuration and DBE represented in our evaluations.

The potential for interlayer sliding in geofoam embankments can be easily addressed during construction. For large earthquakes, with significant nearby strong motion, we recommend that shear keys be constructed in the geofoam embankment to disrupt any continuous horizontal slide planes created by using current block placement practices. Shear keys are constructed by periodically installing half-height blocks in the geofoam mass that interrupt the horizontal planes (Figure 7-9). The strategic placement of shear keys will require the potential sliding surface to shear through a select number of geofoam blocks. Because of the relatively high shearing strength of the blocks, this pattern of placement will disrupt the failure surface and greatly improve the sliding resistance.

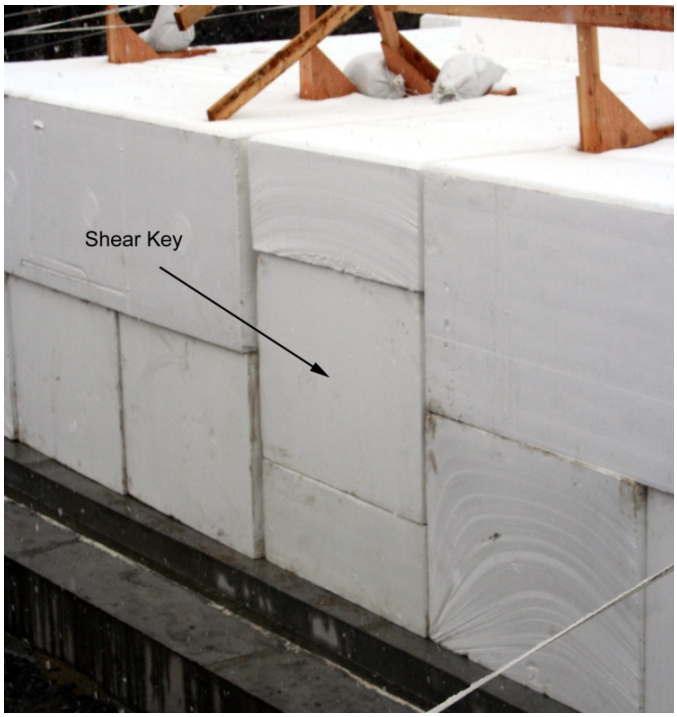

Figure 7-9 Shear Key Installed in Geofoam Embankment.

7.4 Example Shear Key Calculations

The potential for initiation of interlayer and basal sliding of a geofoam embankment can be evaluated using pseudo static techniques. This type of analysis is useful for evaluating the stability of simple systems when the embankment cross-section is a simple rectangle. In this approach, the inertial horizontal force acting on the geofoam embankment is applied at the centroid of the mass, which is usually at the top of the embankment. To calculate the appropriate acceleration, the geofoam is treated as a single degree of freedom (SDOF) oscillator (Horvath, 1995) and its fundamental period, T_0, is estimated using Equation 7-1 (Horvath, 2004). When this above equation is applied to an 8-m high by 20-m wide free-standing geofoam embankment using the properties given in Table 7-6, the value of T_0 is 0.52 s. The horizontal inertial force, F_h, produced by the earthquake is applied to the centroid of the lumped mass, which is approximately located at the top of the embankment near the mid-point of the pavement section:

$$F_h = S_a * m \qquad (7\text{-}2)$$

where: S_a is the spectral acceleration corresponding to T_0 obtained from the design basis earthquake acceleration response spectrum and m is the lumped mass of the system (combined mass of the pavement, road base and concrete load distribution slab). In the U.S., geofoam embankment is often considered to be a "retaining" structure/wall and as such, it is designed for a 5 percent damped S_a value that has a 10 percent probability of being exceeded in 50 years (i.e., average return period of 475 years) as specified by the American Association of Highway and Transportation Officials (AASHTO, 2010). An example 5 percent damped AASHTO spectrum for such an event is shown in Fig. 43.

Table 7-6 Properties for Sliding Calculations

Material Type	Layer No.	Thickness (m)	ρ [4] (kg/m^3)	E [5] (MPa)	ν [6]	K [7] (MPa)	G [8] (MPa)
Foundation Soil	1-10	varies	1840	174	0.4	290.0	62.1
Geofoam	11-18	8	18	10	0.103	4.2	4.5
UTBC[1]	19	0.610	2240	570	0.35	633	211
LDS[2] & PCCP[3]	19	0.508	2400	30000	0.18	15625	12712

[1] Untreated base course, [2] Load distribution slab, [3] Portland concrete cement pavement, [4] Mass density, [5] Initial Young's modulus, [6] Poisson's ratio, [7] Bulk modulus, [8] Shear modulus

In applying pseudo static techniques to interlayer and basal sliding evaluations, values of horizontal acceleration at various heights within the embankment are linearly interpolated, starting at the top of the EPS embankment and continuing to its base (NCHRP 529) (Table 7-7). The horizontal acceleration acting at the top interface of the embankment is the S_a value from the design spectrum at T=0.52s, which is of 0.848 g for the example case (Figure 7-10); the horizontal acceleration at the basal EPS/foundation soil interface is peak horizontal ground acceleration (PGA), which is 0.339 g for the example case and corresponds to the spectral acceleration at T=0 s (Figure 7-10).

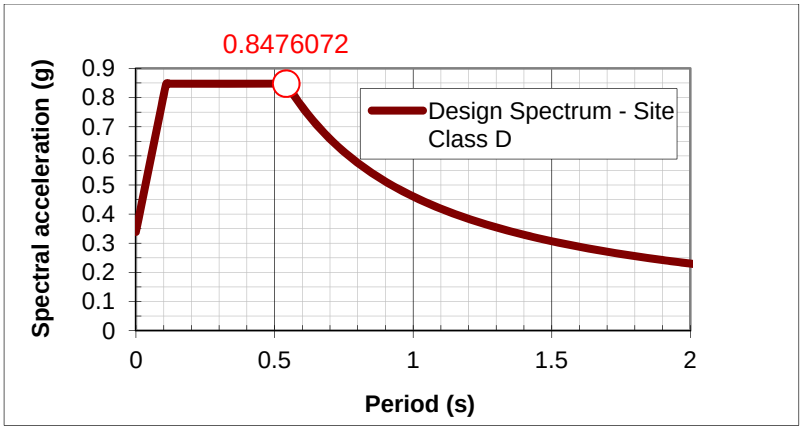

Figure 7-10 Five Percent Damped Acceleration Response Spectrum for Salt Lake Valley, Utah for Deep Soil Site (Site Class D).

Subsequently, force equals mass times acceleration is applied to the interpolated acceleration values at each interface elevation to estimate the inertial sliding force acting at that interface (Table 7-7). The frictional sliding resistance of the interface is calculated using the normal stress (i.e., vertical stress) acting at the interface multiplied by interface coefficient of friction and by the percentage of area available to resist sliding (expressed in decimal fraction). (The weight of the EPS is usually neglected in calculating the normal stress.) In this calculation, the coefficient of friction for geofoam-to-geofoam and geofoam-to-soil interfaces was estimated to be 0.8 and 0.6, respectively, based on direct shear testing from the I-15 Reconstruction Project (Bartlett et al. 2000). In addition, any potential bonding that develops between the EPS and the overlying concrete load distribution slab was ignored in this example at interface 9 (Table 7-7); but such a bond shear strength could be included if: (1) it can be reasonably obtained from experimental data, and (2) such a bond can be shown to persist throughout the design life of the embankment.

The recommended factor of safety against interlayer and basal sliding is 1.2 to 1.3, which may not be achieved at all interfaces relying on frictional resistance solely. For interfaces where unacceptably low safety factors are calculated, shear keys can be constructed during the placement of the geofoam block to reduce the potential for interlayer sliding. Such keys disrupt the development of horizontal sliding planes during earthquake shaking and are constructed by periodically placing half-height blocks in the geofoam mass followed by placing full-height block in the successive layer (Figure 7-9). The full-height block placed in the key acts as a barrier to sliding and the shear resistance of the block is mobilized to resist sliding. Therefore, the key greatly improves the factor of safety against interlayer sliding due to the relatively high shear strength of the EPS block (Table 7-7). The resisting force provided by the key is calculated by multiplying the shear strength of the block by the percentage of area occupied by the key (Table 7-7). We note that if a shear key is used at a particular interface, the area available for frictional contact must be reduced correspondingly when calculating the resisting sliding force (Table 7-7). Note also that shear keys were not required at interfaces 0 to 4, because the inertial forces in the embankment decrease at these lower elevations, increasing the factor of safety at lower elevations within the embankment.

Any sliding resistance provided by the fascia panel wall was omitted from the sliding calculations (Table 7-7). In the I-15 Reconstruction Project design, the fascia panel wall is not designed to resist horizontal seismic force imparted by the EPS backfill. Typically, a 0.2-m gap was left between the face of the geofoam block and the back of the wall to prevent interaction. However, this wall could be designed to resist horizontal inertial forces, if needed, for alternative situations.

Table 7-7 Example Interlayer Sliding Calculation

H =			8	m			
Block thickness =			0.81	m			
number of interfaces			9				
normal stress			25.36	kPa			
interface friction			0.8	(geofoam - geofoam)			
interface friction			0.6	(geofoam - soil)			
geofoam shear strength			23	psi (EPS19 used in shear key)			
geofoam shear strength			157.3	kPa			
interface #	Horiz. Accel. (g)	mass (kg/m^3)	inertial force (N/m^3)	resisting sliding force (N/m^3)	shear key coverage (%)	resisting force from key (N/m^3)	FS sliding (w / key)
9	0.848	2585	21497	19073	6	9439	1.33
8	0.791	2585	20064	19478	4	6293	1.28
7	0.735	2585	18631	19681	3	4720	1.31
6	0.678	2585	17198	19884	2	3146	1.34
5	0.622	2585	15765	20087	1	1573	1.37
4	0.565	2585	14332	20290	0	0	1.42
3	0.509	2585	12898	20290	0	0	1.57
2	0.452	2585	11465	20290	0	0	1.77
1	0.396	2585	10032	20290	0	0	2.02
0	0.339	2585	8599	15217	0	0	1.77

7.5 Horizontal Sway and Rocking

In addition to horizontal translation (i.e., sliding), Raid and Horvath (2004) discuss horizontal sway and rigid body rocking as fundamental free-standing geofoam embankment behaviors. Horizontal sway results from flexibility of the geofoam mass in the horizontal (x) direction, and rocking results from 2D rigid body rotation (Raid and Horvath, 2004).

In reality, the geofoam embankment is flexible when subjected to strong motion and will undergo both horizontal and vertical internal deformation as the mass attempts to sway and rock in response to the earthquake strong motion. Horizontal sway will primarily induce shear stresses and strains; whereas attempted rocking will mainly produce alternating tensile and

compressive stresses and their associated strains as the geofoam mass attempts to rock. If the rocking behavior is sufficiently large, then uplift may occur at the basal corners of the geofoam embankment.

The potential consequences of the above behaviors were explored using the developed *FLAC* model with the following modifications to the interfacial, material property, and loading conditions. First, we bonded all of the interfacial nodes within the geofoam mass (interfaces 2 through 9) to limit interface sliding, as if shear keys had been constructed in the mass. *FLAC* allows both tensile and shear bonds as interfacial properties. These values were set equal to the tensile and shearing strength of the geofoam (117.5 and 159 kPa, respectively), which are applicable to Type XIII geofoam (Benchmark Foam, 2003). A bonded interface also allows for a friction angle to be specified, so that when the bond is broken, friction can act along the interface. This value was set equal to 38 degrees (Table 7-4). Slippage along the interface was not allowed until the bond was broken. Second, a bonded interface condition was also specified at interface 9 (top of geofoam/bottom of lumped mass). The tensile bond at this location was also set equal to 117.5 kPa, which essentially means that the bond between the concrete and geofoam is strong enough that the geofoam will be ruptured in tension according to its tensile capacity before the bond is broken. In addition, a shear bonding of 70 kPa was used at this interface based on concrete/geofoam interface shear test data from Sheeley and Negussey (2000). A friction angle of 38 degrees was also assigned to this interface, which will only be used if the bond breaks. Third, the interface between the geofoam and the foundation soil (interface 1) was unglued, which will allow vertical separation (uplift). Any horizontal sliding displacement at this interface was limited by assigning a very high friction angle (89 degrees), which precluded horizontal sliding. Like the sliding model, this was done to constrain the basal geofoam horizontally, which models the actual horizontal restraint provided by the panel wall footing. However, uplift was still allowed at this interface to allow for any rocking/uplift behavior. Fourth, the Mohr-Coulomb model with hysteretic damping was applied to all geofoam layers to see if yielding is reached in the block during earthquake cycling. The geofoam was assigned tensile and shearing strengths of 117.5 kPa and 159 kPa, respectively (Benchmark Foam, 2003). Lastly, we only considered cases with both the vertical and horizontal components of strong motion.

Table 7-8 summarizes the maximum uplift at the embankment corners and general behavior for the horizontal sway and rocking case. The analyses suggest that some uplift occurs at the corners of the geofoam embankment that ranges from about 0.01 to 0.2 m. Horizontal sway and rocking modes can cause localized tensile yielding of the block that primarily occurs in the basal geofoam layers. However, in two cases, the tensile yielding propagated to higher levels in the embankment, causing the embankment to begin to decouple dynamically (Figure 7-11). Thus, we recommend that consideration be given to installing higher strength geofoam block (denser than Type VIII geofoam) in the basal layers of geofoam embankments to prevent this behavior. In addition, in a few cases, the interfacial bond between the top of the geofoam and the load distribution slab was broken during the modeling and the lumped mass above the geofoam began to slide atop the geofoam (Figure 7-11). Design considerations should be given to this contact surface to ensure that sufficient bond strength is available to prevent decoupling. In addition, placement of a geomembrane at this interface atop the geofoam embankment, as shown in Figure 7-3, is not recommended due to the relatively low angle of friction that realized at this contact surface. (Note that this geomembrane shown in Figure 7-3 was later removed prior to pouring the load distribution slab due to sliding concerns at this interface).

Table 7-8 Summary of Horizontal Sway and Rocking Results

Case	Max. uplift (left corner) (m)	Max. uplift (right corner) (m)	Local Yielding of Block	Bond broken between geofoam and LDS[1]
1b	0.06	0.05	No	No
2b	0.02	0.04	No	No
3b	0.2	0.2	Yes (some blocks in basal layer and 1 block under LDS)	Yes
4b	0.2	? rotation due to tensile yielding	Yes (some blocks in basal layers; tensile yielding developing)	Yes
5b	0.01	0.01	No	No
6b	0.03	0.03	No	No
7b	? rotation due to tensile yielding	0.2	Yes (some blocks in basal layers; tensile yielding developing)	Yes
8b	0.25	0.25	Yes (some blocks in basal layer)	No

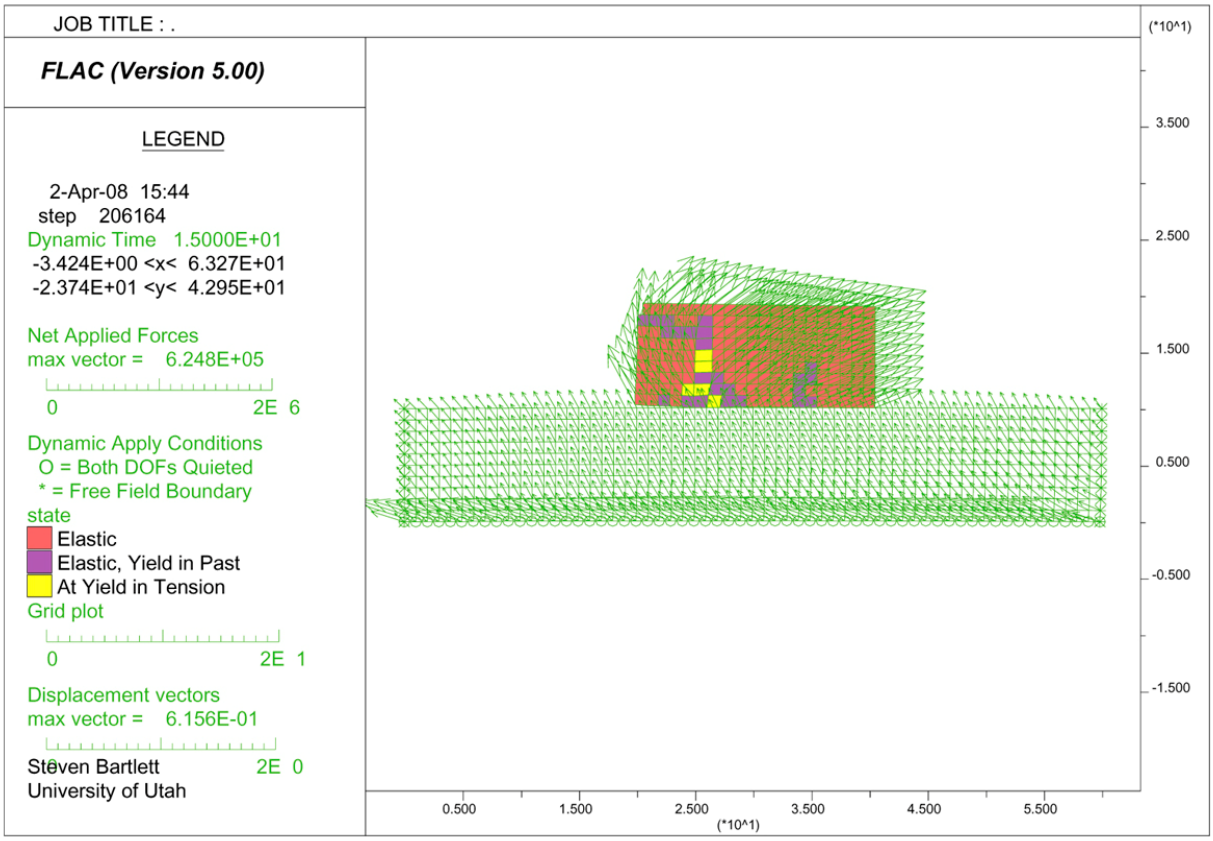

Figure 7-11 Upward Propagation of Tensile Yielding in the Geofoam Embankment and Decoupling of the Load Distribution Slab for case 7b.

7.6 Summary of Seismic Stability Evaluations

In general, the majority of the evaluated cases suggest that interlayer sliding is within tolerable limits (0.01 to 0.1 m); however, three input time histories produced interlayer sliding that was greater than 0.5 m, which is considered unacceptable from a performance standpoint. Because the model predicted a wide range of interlayer sliding displacement for the cases analyzed, this suggests that sliding is a highly nonlinear process and is strongly governed by the frequency content and long period displacement pulses present in the input time histories. The model also suggests that interlayer sliding displacement can, in some cases, increase when the vertical component of strong motion is included in the analysis. For cases where interlayer sliding is just initiating, the sliding displacement increases by a factor of 2 to 5 times when the vertical component of strong motion is added to the analyses. However, when the interlayer

sliding displacements are larger, the presence of the vertical component in the model is less important and the displacements remain the same or only slightly increase. Thus, we conclude that it is generally unconservative to ignore the vertical component of strong motion when estimating sliding displacement, but its inclusion is less important when the interlayer sliding displacement is well developed. All models showed that the interlayer sliding is generally concentrated in the basal layers and diminishes greatly in the higher layers. The potential for interlayer sliding displacement in geofoam embankments can be resolved by constructing shear keys within the geofoam mass to disrupt continuous horizontal layers that are being created by current construction practices.

The numerical model also suggests that internal deformation caused by rocking and sway can cause local tensile yielding of some blocks within the embankment, usually near the base. In some cases, this yielding can propagate upward and cause the embankment to begin to decouple dynamically. Consideration should be given to using blocks with higher strengths than Type VIII geofoam in the basal zones of geofoam embankments undergoing high levels of strong motion.

This page intentionally left blank

8.0 Finding and Recommendations

The I-15 Reconstruction Project provides a good case history illustrating the challenges of rapid construction of large embankments over soft soils in an urban setting. One of the key technologies employed was EPS geofoam, which was primarily used to prevent possible settlement damage to buried utilities that crossed or paralleled the new interstate alignment. Geofoam embankments had the best overall settlement performance of the technologies monitored (Farnsworth et al., 2008).

Field measurements show that elastic compression and gap closure of the EPS block produced about 1 percent vertical strain as the load distribution slab and overlying pavement materials were placed atop the EPS. In addition, the placement of these loads produced about 15 mm settlement in the foundation soils, as measured at the 3300 South Street site. Subsequently, the EPS embankment has undergone about 0.2 to 0.4 percent creep strain in a 10-year post construction period under a working stress level of about 20 to 35 kPa, as measured at two sites. In addition, the current creep trends and vertical stress measurements from the VW total pressure cells indicate that the design performance goals have been met. The measured internal vertical stress levels from the vibrating wire instruments are in reasonable agreement with the design limit of 30 kPa. This design criterion was selected to limit the construction compression of EPS Type VIII to about 1 percent vertical strain at the end of construction period and to about 2 percent compressional strain over a 50-year period. Subsequent long-term monitoring of the creep deformation shows that this 50-year criterion will be met with the maximum projected compressional strain of about 1.5 to 1.7 percent at the 3300 South and 100 South Street sites.

This report also reviews current design methods for calculating the allowable stress in EPS as put forth by various standards and guidance from Europe, U.S. and Japan. It recommends a method based on a combination of European Standards (EPS White Book, 2011) and NCHRP 529. Numerical methods based on multi-layered elastic solutions are also recommended for determining the vertical stress induced by live loads in EPS pavement systems that include a load distribution slab.

Numerical modeling was also done to determine the dead load in the EPS and the amount of vertical deformation resulting from such loads. The numerical modeling results were compared with the field performance measurements to validate the approach. For the dead loads, the resulting compression during construction is complex due to gap closure and block seating phenomena within the EPS embankment. In general, the numerical modeling produced reasonable estimates of the field measurements, both in terms of vertical and horizontal stress distribution and vertical displacement. Thus, we believe that numerical modeling provides valuable insight into the behavior and design of these complex, multilayered embankment systems.

This modeling was done using a simple bilinear elastic model for geofoam embankment stress-strain behavior to predict the stress distribution and vertical displacement of geofoam embankments. The validity of this model was verified by comparison of the numerical results to pressure cell and magnet extensometer measurements. In our bilinear model, we used a low stress elastic modulus ranging from 1.7 to 2.7 MPa to account for displacements occurring from gap closure and seating between the surfaces of the untrimmed geofoam blocks for vertical stresses below 15 KPa. We also found that an elastic modulus of 10 MPa reasonably reproduced the measured compression and vertical stress distribution found in Type VIII geofoam at higher stress levels (i.e., above 15 kPa). At these higher stress levels, elastic compression of the geofoam blocks dominates the displacement behavior of the geofoam embankment.

However, additional complexity not included in the numerical analyses was present in the field measurements. These complexities are attributed to thermal variations and loading created by wall/pavement/geofoam interaction, which were not explicitly considered in the modeling approach. Thus, some judgment was required in interpreting the field measurements and relating them to the numerical results. Most importantly, pressure cells placed near the top of the geofoam embankment and in the overlying base material near the concrete pavement surface showed strong seasonal stress fluctuations that are attributed to differential expansion and contraction of the embankment and pavement systems and their interaction with the adjacent panel wall via a relatively rigid connection. Also, the installation of the pressure cells in the basal bedding sand and the subsequent placement of overlying “arched” block appears to have

created arching or a non-uniform contact surface that did not allow for complete vertical stress transfer to the underlying pressure cells.

The assessment of the seismic stability of a typical EPS embankment similar to that used on the I-15 Reconstruction Project in Salt Lake City, Utah was performed using dynanmic, non-linear techniques. The evaluations suggest that interlayer sliding may be initiated in some cases and the amount of sliding displacements depends on the amplitude and long-period characteristics of the inputted strong motion. Therefore, shear keys or other structural/mechanical restraints are recommended for free-standing EPS embankment systems where the seismically-induced sliding displacement is potentially damaging to the geosystem.

This page intentionally left blank

9.0 REFERNECES

Anthanasopoulos, G. A., Pelekis, P. C. and Xenaki, V. C. (1999). "Dynamic Properties of EPS Geofoam: An Experimental Investigation," Geosynthetics International, Vol. 6, No. 3.

ASTM D 6817-07. Standard Specification for Rigid, Cellular Polystyrene Geofoam.

Bartlett, S., Negussey, D., Kimble, M., and Sheeley, M. (2000). "Use of Geofoam as Super-Lightweight Fill for I-15 Reconstruction." Transportation Research Board 79th Annual Meeting, Washington, D.C.

Bartlett, S.F., Farnsworth, C., Negussey, D., and Stuedlein, A.W. (2001). "Instrumentation and Long-Term Monitoring of Geofoam Embankments, I-15 Reconstruction Project, Salt Lake City, Utah." *Proceedings of the 3rd International EPS Geofoam Conference*, December 2001, Salt Lake City, Utah.

Bartlett, S.F. and Farnsworth, C.B. (2004). "Monitoring and Modeling of Innovative Foundation Treatment and Embankment Construction Used on the I-15 Reconstruction Project, Project Management Plan and Instrument Installation Report," UDOT Research Report No. UT-04.19, p. 202.

Bartlett, S. F. and Lawton E. C. (2008). "Evaluating the Seismic Stability and Performance of Freestanding Geofoam Embankment," 6th National Seismic Conference on Bridges and Highways, Charleston, S.C., July 27th –30th 2008, 17 p.

Bartlett, S. F., Negussey, D., Farnsworth, C. B., and Stuedlein, A., (2011). "Construction and Long-Term Performance of Transportation Infrastructure Constructed Using EPS Geofoam on Soft Soil Sites in Salt Lake Valley, Utah," EPS 2011 Geofoam Blocks in Construction Applications, Oslo Norway.

Benchmark Foam, Inc. (2003). "Physical Properties of EPS." April 4, 2004. <http://www.benchmarkfoam.com/benchmark/poly/properties.asp>

Burmister, D. M., 1943, "The Theory of Stresses and Displacements in Layered Systems and Applications to the Design of Airport Runways." Proceedings, Highway Research Board, Vol. 23 (1943), pp. 126–144.

Draft European Standard, 1998, European Committee for Standardization, Brussels.

Duškov, M., (1997). "EPS as a Light-Weight Sub-base Material in Pavement Structures" Ph. D. Thesis, Delft University of Technology, Delft, Netherlands.

Elragi, A. F. (2000). "Selected Engineering Properties and Applications of EPS Geofoam." PhD Dissertation. State University of New York College of Environmental Science and Forestry, Syracuse, NY.

Elragi, A. F., Negussey D., Kyanka, G. (2000). "Sample Size Effects on the Behavior of EPS Geofoam." Proceedings of the Soft Ground Technology Conference, ASCE Geotechnical Publication 112, the Netherlands, 2000.

EPS White Book, 2011, "EUMEPS Background Information on Standardization of EPS," Issued by EUMEPS in 2011, Version 31/03/11.

Farnsworth C. F., Bartlett S. F., Negussey, D. and Stuedlein A. (2008). "Construction and Post-Construction Settlement Performance of Innovative Embankment Systems, I-15 Reconstruction Project, Salt Lake City, Utah," Journal of Geotechnical and Geoenvironmental Engineering, ASCE (Vol. 134 pp. 289-301, March 2008).

Helwany, S., Dyer, J., Leidy, J., (1998). "Finite-Element Analyses of Flexible Pavements," Journal of Transportation Engineering, Vol. 124, No. 5, September/October 1998, pp. 491-499.

Horvath, J. S. (2004). "A Technical Note Regarding Calculating the Fundamental Period of an EPS-Block-Geofoam Embankment," Report No. CGT-2004-1, Manhattan College, School of Engineering, Center for Geotechnology, 10 p.

Horvath, J. S. (1995). Geofoam Geosynthetic, published by Horvath Engineering, P.C., Scarsdale, New York, U.S.A.

Krahn, John. (2004). "Stress and Deformation Modeling with SIGMA/W: An Engineering Methodology." GEO-SLOPE International, Ltd. Calgary, Alberta, Canada.

Itasca Consulting Group, Inc. (2005). "*FLAC*: Fast Lagrangian Analysis of Continua: User's Guide." Minneapolis, Minnesota.

Itasca Consulting Group, Inc. (2005). *FLAC*: Fast Lagrangian Analysis of Continua: Structural Elements, Version 5." Minneapolis, Minnesota.

Kalinski, M. E. and Pentapati, D. P. (2006). "Numerical Simulation of Dynamic Behavior of Geofoam Embankment," Transportation Research Record, No. 1975, pp. 89-95.

Mejia, L. H. and Dawson, E. H. (2006). "Earthquake Deconvolution in FLAC," 4th International FLAC Symposium in Numerical Modeling in Geomechanics, 2006 Itasca Consulting Group Inc., Minneapolis MN.

NCHRP 529, 2004, "Guideline and Recommended Standard for Geofoam Applications in Highway Embankments, NATIONAL COOPERATIVE HIGHWAY RESEARCH PROGRAM, 2004.

NCHRP Web Document No. 65, "Geofoam applications in the design and construction of highway embankments," Stark, T.D., Arellano, D, Horvath, J.S., Leshchinsky, D., NCHRP Project 24-11.

Negussey, D., Stuedlein, A. W., Bartlett, S. F., and Farnsworth, C. (2001). "Performance of Geofoam Embankment at 100 South, I-15 Reconstruction Project, Salt Lake City, Utah." *EPS Geofoam 2001, 3rd International Conference*, December 2001, Salt Lake City, Utah, p. 22.

Negussey, D. and Stuedlein, A. (2003). "Geofoam Fill Performance Monitoring." Utah Department of Transportaion Research Division Report No. UT-03.17. August 2003.

Newman, M. P., Bartlett S. F., Lawton, E. C., (2010). "Numerical Modeling of Geofoam Embankments," Journal of Geotechnical and Geoenvironmental Engineering, ASCE, February 2010, pp. 290-298.

Riad, H. L. and Horvath, J. S. (2004). "Analysis and Design of EPS-Geofoam Embankments for Seismic Design," ASCE Geo-Trans 2004, July 27-31, Los Angeles, California.

Sheeley M. and Negussey D. (2000). "An Investigation of Geofoam Interface Strength Behavior," Proceedings of the Soft Ground Technology Conference, ASCE Geotechnical Special Publication 112.

Stark, T. D., Arellano, D., Horvath, J. S. and Leshchinsky, D. (2002). *Guidelines for geofoam applications in embankment projects*, Final Rpt. - Natl. Coop. Hwy. Res. Prog. Proj. No. 24-11.

Sun, J. I., Golesorkhi, R. and Seed, H. B. (1988). "Dynamic Moduli and Damping Rations for Cohesive Soils," Earthquake Engineering Research Center, University of California, Berkeley, Report No. UCB/EERC-88/15, 42 p., 1988.

Tsukamoto, H., 2011, "History of R&D and Design Code for EDO-EPS Method in Japan, EPS 2011, Oslo, Norway.

This page intentionally left blank

APPENDIX 1 – FLAC Verification code

```
config axi
grid 20,30
gen 0,0 1.05,0 1.05,-1.05 0,-1.05 ratio 1.0 1.205
model elastic
prop density 29 bulk 1.67e6 shear 1.82e6 notnull i 1 30; EPS19
;
fix  x y i 31
fix  x i 1 20 j 32
history 999 unbalanced
;
apply syy -550e3 from 1,1 to 1,21
solve
```

This page intentionally left blank

APPENDIX 2 – FLAC Code for 55 kN (12.5 kip) Tire Load

```
; Vertical Stress Distribution
config axi
grid 30,20
gen 0,0 6.1,0 6.1,-3.04 0,-3.04 ratio 1.0 1.204
model elastic
prop density 2400 bulk 13021e6 shear 10593e6 notnull i 1 3 j 1 30; PCCP
prop density 2160 bulk 333e6 shear 154e6 notnull i 4 9 j 1 30; base
prop density 2400 bulk 13021e6 shear 10593e6 notnull i 10 j 1 30; LDS Concrete
prop density 18.4 bulk 1.67e6 shear 1.82e6 notnull i 11 30 j 1 30; EPS19
;
fix  x y i 31
fix  x i 1 30 j 32
history 999 unbalanced
;
;
;
apply syy -622e3 from 1,1 to 1,5
solve
;print syy line (0.015,0) (0.015,-3) 31
```

This page intentionally left blank

APPENDIX 3 – FLAC Code for 3300 South Array

```
0 header
1 code FLAC 5.0
1 source giic v2.0.393
1 date Tue Nov 16 16:53:02 GMT 2010
1 type giic-save
0 flac
1 config
2 axisym false
2 gwflow false
2 pstress false
2 cppudm false
2 ats false
2 creep false
2 dynamic false
2 thermal false
2 twophase false
2 extra 0
2 units 0
2 struct true
2 advanced false
2 water false
2 interface false
2 gravity true
2 excludereg false
2 solvefos false
2 record 2
0 plots
1 plot 2
2 display
3 viewport
4 autorange true
2 command plot pen history 1 line
2 name Level 0-
2 alias
2 count 1
2 item
3 name 1
3 line
1 plot 2
2 display
3 viewport
4 autorange true
2 command plot pen history 2 line
2 name Level 0
```

2 alias
2 count 1
2 item
3 name 2
3 line
1 plot 2
2 display
3 viewport
4 autorange true
2 command plot pen history 3 line
2 name Level 2
2 alias
2 count 1
2 item
3 name 3
3 line
1 plot 2
2 display
3 viewport
4 autorange true
2 command plot pen history 4 line
2 name Level 4
2 alias
2 count 1
2 item
3 name 4
3 line
1 plot 2
2 display
3 viewport
4 autorange true
2 command plot pen history 5 line
2 name Level 6
2 alias
2 count 1
2 item
3 name 5
3 line
1 plot 2
2 display
3 viewport
4 autorange true
2 command plot pen history 6 line
2 name Level 8
2 alias
2 count 1

2 item
3 name 6
3 line
1 plot 2
2 display
3 viewport
4 autorange true
2 command plot pen history 7 line
2 name 23406
2 alias
2 count 1
2 item
3 name 7
3 line
1 plot 2
2 display
3 viewport
4 xrange 10.0,45000.0
4 yrange -26757.441,0.0
2 command plot pen history 8 line
2 name 23405
2 alias
2 count 1
2 item
3 name 8
3 line
1 plot 2
2 display
3 viewport
4 autorange true
2 command plot pen history 9 line
2 name 23414
2 alias
2 count 1
2 item
3 name 9
3 line
1 plot 2
2 display
3 viewport
4 autorange true
2 command plot pen history 10 line
2 name 48833
2 alias
2 count 1
2 item

3 name 10
3 line
1 plot 2
2 display
3 viewport
4 autorange true
2 command plot pen history 11 line
2 name 48834
2 alias
2 count 1
2 item
3 name 11
3 line
1 plot 2
2 display
3 viewport
4 autorange true
2 command plot pen history 12 line
2 name unbal.
2 alias
2 count 1
2 item
3 name 12
3 line
1 plot 0
2 display
3 viewport
4 autorange true
2 command plot pen displacement attach iface
2 name disp. vector
2 count 3
2 item
3 name displacement
3 switch 3
2 item
3 name attach
3 switch 2
2 item
3 name iface
3 switch 11
1 plot 0
2 display
3 viewport
4 autorange true
2 command plot pen iface iface ydisp fill attach iface
2 name disp. contour

2 count 5
2 item
3 name iface
3 switch 11
2 item
3 name iface
3 switch 11
2 item
3 name ydisp
3 switch 5
3 mode 1
2 item
3 name attach
3 switch 2
2 item
3 name iface
3 switch 11
1 plot 0
2 display
3 viewport
4 autorange true
2 command plot pen syy fill attach iface
2 name stress contour
2 count 3
2 item
3 name syy
3 switch 5
3 mode 1
2 item
3 name attach
3 switch 2
2 item
3 name iface
3 switch 11
0 matlist
1 class User
1 material new1
2 model elastic
2 property
3 poisson_rat 0.25
1 class Geofoam
1 material Geofoam
2 model mohr
2 property
3 density 18.0
3 elastic_mod 4000000.0

3 poisson_rat 0.1
3 bulk_mod 1666670.0
3 shear_mod 1818180.0
0 CppModels
0 project tree
1 title 3300 South, Middle Array Incrementally and Bilinear Modulus
1 notes
1 tree
2 branch branch A
3 state
4 file 33middle.sav
4 batch
5 text ;E=2.7-10
5 text config
5 text grid 40,28
5 text m m i 1 29 j 1 14;mohr-coulomb model
5 text m m i 31 33 j 1 14
5 text m m i 38 40 j 1 14
5 text m m i 1 29 j 16 23
5 text m m i 31 39 j 16 23
5 text m m i 1 29 j 25 28
5 text m m i 31 39 j 25 28
5 text gen -2.5 -10 -2.5 0 0 0 0 -10 i 38 41 j 1 15
5 text gen -2.5 0 -2.5 6.608 0 6.608 0 0 i 37 40 j 16 24
5 text gen -2.5 6.608 -2.5 6.760 0 6.760 0 6.608 i 37 40 j 25 26
5 text gen same -2.5 7.370 0 7.370 same i 37 40 j 26 28
5 text gen same -2.5 7.726 0 7.726 same i 37 40 j 28 29
5 text ;
5 text gen -4.919 -10 -4.919 0 -2.5 0 -2.5 -10 i 31 34 j 1 15
5 text gen -4.919 0 -13.904 6.608 same -2.5 0 i 31 37 j 16 24
5 text gen -13.904 6.608 -13.904 6.760 same -2.5 6.608 i 31 37 j 25 26
5 text gen same -13.904 7.370 same same i 31 37 j 26 28
5 text gen same -13.904 7.726 same same i 31 37 j 28 29
5 text ;
5 text gen -39.7 -10 -39.7 0 -4.919 0 -4.919 -10 i 1 30 j 1 15
5 text gen -39.7 0 -39.7 6.608 -13.904 6.608 -4.919 0 i 1 30 j 16 24
5 text gen -39.7 6.608 -39.7 6.760 -13.904 6.760 -13.904 6.608 i 1 30 j 25 26
5 text gen same -39.7 7.370 -13.904 7.370 same i 1 30 j 26 28
5 text gen same -39.7 7.726 -13.904 7.726 same i 1 30 j 28 29
5 text ;
5 text attach Aside from 30,1 to 30,15 Bside from 31,1 to 31,15
5 text attach Aside from 34,1 to 34,15 Bside from 38,1 to 38,15
5 text attach Aside from 1,15 to 30,15 Bside from 1,16 to 30,16
5 text ;int 1 Aside from 31,15 to 34,15 Bside from 31,16 to 37,16
5 text ;int 2 Aside from 38,15 to 41,15 Bside from 37,16 to 40,16
5 text ;int 3 Aside from 30,16 to 30,24 Bside from 31,16 to 31,24

```
 5 text attach Aside from 30,25 to 30,29 Bside from 31,25 to 31,29
 5 text attach Aside from 1,24 to 30,24 Bside from 1,25 to 30,25
 5 text attach Aside from 31,24 to 40,24 Bside from 31,25 to 40,25
 5 text ;int 1 kn 5.53e7 ks 5.53e7 friction = 31 coh = 0 tbond=0 bslip on
 5 text ;int 2 kn 3.95e7 ks 3.95e7 friction = 31 coh = 0 tbond=0 bslip on
 5 text ;int 3 kn 5.53e7 ks 5.53e7 friction = 31 coh = 0 tbond=0 bslip on
 5 text gen line -39.7 6.760 0 6.760
 5 text gen line -39.7 7.370 0 7.370
 5 text ;
 5 text prop density=18.0 bulk=1.134E6 shear=1.224E6 cohesion=25.0E3 friction=31.0 reg i 32 j
17
 5 text prop density=2160.5 bulk=111.111E6 shear=37.037E6 cohesion=0.0 friction=35.0 reg i 2
j 17 ;backfill
 5 text prop density=2240.5 bulk=111.111E6 shear=37.037E6 cohesion=0.0 friction=35.0 reg i 2
j 25 ;utbc not lds
 5 text ;prop density=2400.5 bulk=15625E6 shear=12711.9E6 cohesion=25.0E6 friction=25.0
reg i 2 j 25 ;lds
 5 text prop density=2400.5 bulk=15625E6 shear=12711.9E6 cohesion=25.0E6 friction=25.0 reg
i 32 j 25 ;lds
 5 text prop density=2240.5 bulk=111.111E6 shear=37.037E6 cohesion=0.0 friction=35.0 reg i 2
j 26 ;utbc
 5 text prop density=2240.5 bulk=111.111E6 shear=37.037E6 cohesion=0.0 friction=35.0 reg i
32 j 26 ;utbc
 5 text prop density=2400.5 bulk=15625E6 shear=12711.9E6 cohesion=25.0E6 friction=25.0 reg
i 2 j 28 ;pccp
 5 text prop density=2400.5 bulk=15625E6 shear=12711.9E6 cohesion=25.0E6 friction=25.0 reg
i 32 j 28 ;pccp
 5 text prop density=2160.5 bulk=111.111E6 shear=37.037E6 cohesion=0.0 friction=35.0 reg i 2
j 2 ;bottom
 5 text prop density=2160.5 bulk=111.111E6 shear=37.037E6 cohesion=0.0 friction=35.0 reg i
32 j 2 ;bottom
 5 text prop density=2160.5 bulk=111.111E6 shear=37.037E6 cohesion=0.0 friction=35.0 reg i
39 j 2 ;bottom
 5 text ;
 5 text set grav=9.81
 5 text fix y j=1
 5 text fix x i=1
 5 text fix x i=41 j 1 15
 5 text fix x i=40 j 16 29
 5 text his 1 ydis i = 38 j = 15; level 0-
 5 text his 2 ydis i = 37 j = 16; level 0
 5 text his 3 ydis i = 37 j = 18; level 2
 5 text his 4 ydis i = 37 j = 20; level 4
 5 text his 5 ydis i = 37 j = 22; level 6
 5 text his 6 ydis i = 37 j = 24; level 8
 5 text his 7 syy i = 37 j = 16; 23406
```

```
 5 text his 8 syy i = 37 j = 20; 23405
 5 text his 9 syy i = 37 j = 23; 23414
 5 text his 10 syy i = 37 j = 26; 48833
 5 text his 11 syy i = 37 j = 27; 48834
 5 text his unbal
 5 text model null reg i 32 j 17
 5 text model null reg i 2 j 17
 5 text model null reg i 2 j 25
 5 text model null reg i 32 j 25
 5 text model null reg i 2 j 26
 5 text model null reg i 32 j 26
 5 text model null reg i 2 j 28
 5 text model null reg i 32 j 28
 5 text set large
 5 text step 2000
 5 text model mohr i 1 29 j 16 23
 5 text model mohr i 31 39 j 16 23
 5 text prop density=18.0 bulk=1.134E6 shear=1.224E6 cohesion=25.0E3 friction=31.0 reg i 32 j
17
 5 text prop density=2160.5 bulk=111.111E6 shear=37.037E6 cohesion=0.0 friction=35.0 reg i 2
j 17 ;backfill
 5 text int 1 Aside from 31,15 to 34,15 Bside from 31,16 to 37,16
 5 text int 2 Aside from 38,15 to 41,15 Bside from 37,16 to 40,16
 5 text int 3 Aside from 30,16 to 30,24 Bside from 31,16 to 31,24
 5 text int 1 kn 5.53e7 ks 5.53e7 friction = 31 coh = 0 tbond=0 bslip on
 5 text int 2 kn 3.95e7 ks 3.95e7 friction = 31 coh = 0 tbond=0 bslip on
 5 text int 3 kn 5.53e7 ks 5.53e7 friction = 31 coh = 0 tbond=0 bslip on
 5 text set large
 5 text def modulus
 5 text  loop n (1,numstep)
 5 text  if syy(37,16) > -15e3 then
 5 text   command
 5 text   prop density=18.0 bulk=1.134E6 shear=1.224E6 cohesion=25.0E3 friction=31.0 reg i 32
j 17
 5 text   int 1 kn 5.53e7 ks 5.53e7 friction = 31 coh = 0 tbond=0 bslip on
 5 text   int 2 kn 3.95e7 ks 3.95e7 friction = 31 coh = 0 tbond=0 bslip on
 5 text   int 3 kn 5.53e7 ks 5.53e7 friction = 31 coh = 0 tbond=0 bslip on
 5 text   step 25
 5 text   endcommand
 5 text  else
 5 text   command
 5 text   prop density=18.0 bulk=4.198E6 shear=4.533E6 cohesion=25.0E3 friction=31.0 reg i 32
j 17
 5 text   int 1 kn 2.05e8 ks 2.05e8 friction = 31 coh = 0 tbond=0 bslip on
 5 text   int 2 kn 1.46e8 ks 1.46e8 friction = 31 coh = 0 tbond=0 bslip on
 5 text   int 3 kn 2.05e8 ks 2.05e8 friction = 31 coh = 0 tbond=0 bslip on
```

```
 5 text   step 25
 5 text   endcommand
 5 text  endif
 5 text endloop
 5 text end
 5 text set numstep=160
 5 text modulus
 5 text model mohr i 1 29 j 25
 5 text model mohr i 31 39 j 25
 5 text prop density=2240.5 bulk=111.111E6 shear=37.037E6 cohesion=0.0 friction=35.0 reg i 2
j 25 ;utbc
 5 text ;prop density=2400.5 bulk=15625E6 shear=12711.9E6 cohesion=25.0E6 friction=25.0
reg i 2 j 25 ;lds
 5 text prop density=2400.5 bulk=15625E6 shear=12711.9E6 cohesion=25.0E6 friction=25.0 reg
i 32 j 25 ;lds
 5 text set numstep=520
 5 text modulus
 5 text model mohr i 1 29 j 26 27
 5 text model mohr i 31 39 j 26 27
 5 text prop density=2240.5 bulk=111.111E6 shear=37.037E6 cohesion=0.0 friction=35.0 reg i 2
j 26 ;utbc
 5 text prop density=2240.5 bulk=111.111E6 shear=37.037E6 cohesion=0.0 friction=35.0 reg i
32 j 26 ;utbc
 5 text set numstep=520
 5 text modulus
 5 text model mohr i 1 29 j 28
 5 text model mohr i 31 39 j 28
 5 text prop density=2400.5 bulk=15625E6 shear=12711.9E6 cohesion=25.0E6 friction=25.0 reg
i 2 j 28 ;pccp
 5 text prop density=2400.5 bulk=15625E6 shear=12711.9E6 cohesion=25.0E6 friction=25.0 reg
i 32 j 28 ;pccp
 5 text set numstep=520
 5 text modulus
 2 branch branch B
 3 state
 4 file 33middleb.sav
 4 batch
 5 text ;E=2.7-10
 5 text config
 5 text grid 40,28
 5 text m m i 1 29 j 1 14;mohr-coulomb model
 5 text m m i 31 33 j 1 14
 5 text m m i 38 40 j 1 14
 5 text m m i 1 29 j 16 23
 5 text m m i 31 39 j 16 23
 5 text m m i 1 29 j 25 28
```

```
 5 text m m i 31 39 j 25 28
 5 text gen -2.5 -10 -2.5 0 0 0 0 -10 i 38 41 j 1 15
 5 text gen -2.5 0 -2.5 6.608 0 6.608 0 0 i 37 40 j 16 24
 5 text gen -2.5 6.608 -2.5 6.760 0 6.760 0 6.608 i 37 40 j 25 26
 5 text gen same -2.5 7.370 0 7.370 same i 37 40 j 26 28
 5 text gen same -2.5 7.726 0 7.726 same i 37 40 j 28 29
 5 text ;
 5 text gen -4.919 -10 -4.919 0 -2.5 0 -2.5 -10 i 31 34 j 1 15
 5 text gen -4.919 0 -13.904 6.608 same -2.5 0 i 31 37 j 16 24
 5 text gen -13.904 6.608 -13.904 6.760 same -2.5 6.608 i 31 37 j 25 26
 5 text gen same -13.904 7.370 same same i 31 37 j 26 28
 5 text gen same -13.904 7.726 same same i 31 37 j 28 29
 5 text ;
 5 text gen -39.7 -10 -39.7 0 -4.919 0 -4.919 -10 i 1 30 j 1 15
 5 text gen -39.7 0 -39.7 6.608 -13.904 6.608 -4.919 0 i 1 30 j 16 24
 5 text gen -39.7 6.608 -39.7 6.760 -13.904 6.760 -13.904 6.608 i 1 30 j 25 26
 5 text gen same -39.7 7.370 -13.904 7.370 same i 1 30 j 26 28
 5 text gen same -39.7 7.726 -13.904 7.726 same i 1 30 j 28 29
 5 text ;
 5 text attach Aside from 30,1 to 30,15 Bside from 31,1 to 31,15
 5 text attach Aside from 34,1 to 34,15 Bside from 38,1 to 38,15
 5 text attach Aside from 1,15 to 30,15 Bside from 1,16 to 30,16
 5 text ;int 1 Aside from 31,15 to 34,15 Bside from 31,16 to 37,16
 5 text ;int 2 Aside from 38,15 to 41,15 Bside from 37,16 to 40,16
 5 text ;int 3 Aside from 30,16 to 30,24 Bside from 31,16 to 31,24
 5 text attach Aside from 30,25 to 30,29 Bside from 31,25 to 31,29
 5 text attach Aside from 1,24 to 30,24 Bside from 1,25 to 30,25
 5 text attach Aside from 31,24 to 40,24 Bside from 31,25 to 40,25
 5 text ;int 1 kn 4.65e7 ks 4.65e7 friction = 31 coh = 0 tbond=0 bslip on
 5 text ;int 2 kn 3.32e7 ks 3.32e7 friction = 31 coh = 0 tbond=0 bslip on
 5 text ;int 3 kn 4.65e7 ks 4.65e7 friction = 31 coh = 0 tbond=0 bslip on
 5 text gen line -39.7 6.760 0 6.760
 5 text gen line -39.7 7.370 0 7.370
 5 text ;
 5 text prop density=18.0 bulk=.953E6 shear=1.029E6 cohesion=25.0E3 friction=31.0 reg i 32 j
17
 5 text prop density=2160.5 bulk=111.111E6 shear=37.037E6 cohesion=0.0 friction=35.0 reg i 2
j 17 ;backfill
 5 text prop density=2240.5 bulk=111.111E6 shear=37.037E6 cohesion=0.0 friction=35.0 reg i 2
j 25 ;utbc not lds
 5 text ;prop density=2400.5 bulk=15625E6 shear=12711.9E6 cohesion=25.0E6 friction=25.0
reg i 2 j 25 ;lds
 5 text prop density=2400.5 bulk=15625E6 shear=12711.9E6 cohesion=25.0E6 friction=25.0 reg
i 32 j 25 ;lds
 5 text prop density=2240.5 bulk=111.111E6 shear=37.037E6 cohesion=0.0 friction=35.0 reg i 2
j 26 ;utbc
```

```
 5 text prop density=2240.5 bulk=111.111E6 shear=37.037E6 cohesion=0.0 friction=35.0 reg i
32 j 26 ;utbc
 5 text prop density=2400.5 bulk=15625E6 shear=12711.9E6 cohesion=25.0E6 friction=25.0 reg
i 2 j 28 ;pccp
 5 text prop density=2400.5 bulk=15625E6 shear=12711.9E6 cohesion=25.0E6 friction=25.0 reg
i 32 j 28 ;pccp
 5 text prop density=2160.5 bulk=111.111E6 shear=37.037E6 cohesion=0.0 friction=35.0 reg i 2
j 2 ;bottom
 5 text prop density=2160.5 bulk=111.111E6 shear=37.037E6 cohesion=0.0 friction=35.0 reg i
32 j 2 ;bottom
 5 text prop density=2160.5 bulk=111.111E6 shear=37.037E6 cohesion=0.0 friction=35.0 reg i
39 j 2 ;bottom
 5 text ;
 5 text set grav=9.81
 5 text fix y j=1
 5 text fix x i=1
 5 text fix x i=41 j 1 15
 5 text fix x i=40 j 16 29
 5 text his 1 ydis i = 38 j = 15; level 0-
 5 text his 2 ydis i = 37 j = 16; level 0
 5 text his 3 ydis i = 37 j = 18; level 2
 5 text his 4 ydis i = 37 j = 20; level 4
 5 text his 5 ydis i = 37 j = 22; level 6
 5 text his 6 ydis i = 37 j = 24; level 8
 5 text his 7 syy i = 37 j = 16; 23406
 5 text his 8 syy i = 37 j = 20; 23405
 5 text his 9 syy i = 37 j = 23; 23414
 5 text his 10 syy i = 37 j = 26; 48833
 5 text his 11 syy i = 37 j = 27; 48834
 5 text his unbal
 5 text model null reg i 32 j 17
 5 text model null reg i 2 j 17
 5 text model null reg i 2 j 25
 5 text model null reg i 32 j 25
 5 text model null reg i 2 j 26
 5 text model null reg i 32 j 26
 5 text model null reg i 2 j 28
 5 text model null reg i 32 j 28
 5 text set large
 5 text step 2000
 5 text model mohr i 1 29 j 16 23
 5 text model mohr i 31 39 j 16 23
 5 text prop density=18.0 bulk=.953E6 shear=1.029E6 cohesion=25.0E3 friction=31.0 reg i 32 j
17
 5 text prop density=2160.5 bulk=111.111E6 shear=37.037E6 cohesion=0.0 friction=35.0 reg i 2
j 17 ;backfill
```

```
 5 text int 1 Aside from 31,15 to 34,15 Bside from 31,16 to 37,16
 5 text int 2 Aside from 38,15 to 41,15 Bside from 37,16 to 40,16
 5 text int 3 Aside from 30,16 to 30,24 Bside from 31,16 to 31,24
 5 text int 1 kn 4.65e7 ks 4.65e7 friction = 31 coh = 0 tbond=0 bslip on
 5 text int 2 kn 3.32e7 ks 3.32e7 friction = 31 coh = 0 tbond=0 bslip on
 5 text int 3 kn 4.65e7 ks 4.65e7 friction = 31 coh = 0 tbond=0 bslip on
 5 text set large
 5 text def modulus
 5 text  loop n (1,numstep)
 5 text  if syy(37,16) > -15e3 then
 5 text   command
 5 text   prop density=18.0 bulk=.953E6 shear=1.029E6 cohesion=25.0E3 friction=31.0 reg i 32 j
17
 5 text   int 1 kn 4.65e7 ks 4.65e7 friction = 31 coh = 0 tbond=0 bslip on
 5 text   int 2 kn 3.32e7 ks 3.32e7 friction = 31 coh = 0 tbond=0 bslip on
 5 text   int 3 kn 4.65e7 ks 4.65e7 friction = 31 coh = 0 tbond=0 bslip on
 5 text   step 25
 5 text   endcommand
 5 text  else
 5 text   command
 5 text   prop density=18.0 bulk=4.198E6 shear=4.533E6 cohesion=25.0E3 friction=31.0 reg i 32
j 17
 5 text   int 1 kn 2.05e8 ks 2.05e8 friction = 31 coh = 0 tbond=0 bslip on
 5 text   int 2 kn 1.46e8 ks 1.46e8 friction = 31 coh = 0 tbond=0 bslip on
 5 text   int 3 kn 2.05e8 ks 2.05e8 friction = 31 coh = 0 tbond=0 bslip on
 5 text   step 25
 5 text   endcommand
 5 text  endif
 5 text endloop
 5 text end
 5 text set numstep=160
 5 text modulus
 5 text model mohr i 1 29 j 25
 5 text model mohr i 31 39 j 25
 5 text prop density=2240.5 bulk=111.111E6 shear=37.037E6 cohesion=0.0 friction=35.0 reg i 2
j 25 ;utbc not lds
 5 text ;prop density=2400.5 bulk=15625E6 shear=12711.9E6 cohesion=25.0E6 friction=25.0
reg i 2 j 25 ;lds
 5 text prop density=2400.5 bulk=15625E6 shear=12711.9E6 cohesion=25.0E6 friction=25.0 reg
i 32 j 25 ;lds
 5 text set numstep=520
 5 text modulus
 5 text model mohr i 1 29 j 26 27
 5 text model mohr i 31 39 j 26 27
 5 text prop density=2240.5 bulk=111.111E6 shear=37.037E6 cohesion=0.0 friction=35.0 reg i 2
j 26 ;utbc
```

```
 5 text prop density=2240.5 bulk=111.111E6 shear=37.037E6 cohesion=0.0 friction=35.0 reg i
32 j 26 ;utbc
 5 text set numstep=520
 5 text modulus
 5 text model mohr i 1 29 j 28
 5 text model mohr i 31 39 j 28
 5 text prop density=2400.5 bulk=15625E6 shear=12711.9E6 cohesion=25.0E6 friction=25.0 reg
i 2 j 28 ;pccp
 5 text prop density=2400.5 bulk=15625E6 shear=12711.9E6 cohesion=25.0E6 friction=25.0 reg
i 32 j 28 ;pccp
 5 text set numstep=520
 5 text modulus
 2 branch branch C
 3 state
 4 file 33middlec.sav
 4 batch
 5 text ;E=1.7-10
 5 text config
 5 text grid 40,28
 5 text m m i 1 29 j 1 14;mohr-coulomb model
 5 text m m i 31 33 j 1 14
 5 text m m i 38 40 j 1 14
 5 text m m i 1 29 j 16 23
 5 text m m i 31 39 j 16 23
 5 text m m i 1 29 j 25 28
 5 text m m i 31 39 j 25 28
 5 text gen -2.5 -10 -2.5 0 0 0 0 -10 i 38 41 j 1 15
 5 text gen -2.5 0 -2.5 6.608 0 6.608 0 0 i 37 40 j 16 24
 5 text gen -2.5 6.608 -2.5 6.760 0 6.760 0 6.608 i 37 40 j 25 26
 5 text gen same -2.5 7.370 0 7.370 same i 37 40 j 26 28
 5 text gen same -2.5 7.726 0 7.726 same i 37 40 j 28 29
 5 text ;
 5 text gen -4.919 -10 -4.919 0 -2.5 0 -2.5 -10 i 31 34 j 1 15
 5 text gen -4.919 0 -13.904 6.608 same -2.5 0 i 31 37 j 16 24
 5 text gen -13.904 6.608 -13.904 6.760 same -2.5 6.608 i 31 37 j 25 26
 5 text gen same -13.904 7.370 same same i 31 37 j 26 28
 5 text gen same -13.904 7.726 same same i 31 37 j 28 29
 5 text ;
 5 text gen -39.7 -10 -39.7 0 -4.919 0 -4.919 -10 i 1 30 j 1 15
 5 text gen -39.7 0 -39.7 6.608 -13.904 6.608 -4.919 0 i 1 30 j 16 24
 5 text gen -39.7 6.608 -39.7 6.760 -13.904 6.760 -13.904 6.608 i 1 30 j 25 26
 5 text gen same -39.7 7.370 -13.904 7.370 same i 1 30 j 26 28
 5 text gen same -39.7 7.726 -13.904 7.726 same i 1 30 j 28 29
 5 text ;
 5 text attach Aside from 30,1 to 30,15 Bside from 31,1 to 31,15
 5 text attach Aside from 34,1 to 34,15 Bside from 38,1 to 38,15
```

```
 5 text attach Aside from 1,15 to 30,15 Bside from 1,16 to 30,16
 5 text ;int 1 Aside from 31,15 to 34,15 Bside from 31,16 to 37,16
 5 text ;int 2 Aside from 38,15 to 41,15 Bside from 37,16 to 40,16
 5 text ;int 3 Aside from 30,16 to 30,24 Bside from 31,16 to 31,24
 5 text attach Aside from 30,25 to 30,29 Bside from 31,25 to 31,29
 5 text attach Aside from 1,24 to 30,24 Bside from 1,25 to 30,25
 5 text attach Aside from 31,24 to 40,24 Bside from 31,25 to 40,25
 5 text ;int 1 kn 3.48e7 ks 3.48e7 friction = 31 coh = 0 tbond=0 bslip on
 5 text ;int 2 kn 2.49e7 ks 2.49e7 friction = 31 coh = 0 tbond=0 bslip on
 5 text ;int 3 kn 3.48e7 ks 3.48e7 friction = 31 coh = 0 tbond=0 bslip on
 5 text gen line -39.7 6.760 0 6.760
 5 text gen line -39.7 7.370 0 7.370
 5 text ;
 5 text prop density=18.0 bulk=.714E6 shear=.771E6 cohesion=25.0E3 friction=31.0 reg i 32 j
17
 5 text prop density=2160.5 bulk=111.111E6 shear=37.037E6 cohesion=0.0 friction=35.0 reg i 2
j 17 ;backfill
 5 text prop density=2240.5 bulk=111.111E6 shear=37.037E6 cohesion=0.0 friction=35.0 reg i 2
j 25 ;utbc not lds
 5 text ;prop density=2400.5 bulk=15625E6 shear=12711.9E6 cohesion=25.0E6 friction=25.0
reg i 2 j 25 ;lds
 5 text prop density=2400.5 bulk=15625E6 shear=12711.9E6 cohesion=25.0E6 friction=25.0 reg
i 32 j 25 ;lds
 5 text prop density=2240.5 bulk=111.111E6 shear=37.037E6 cohesion=0.0 friction=35.0 reg i 2
j 26 ;utbc
 5 text prop density=2240.5 bulk=111.111E6 shear=37.037E6 cohesion=0.0 friction=35.0 reg i
32 j 26 ;utbc
 5 text prop density=2400.5 bulk=15625E6 shear=12711.9E6 cohesion=25.0E6 friction=25.0 reg
i 2 j 28 ;pccp
 5 text prop density=2400.5 bulk=15625E6 shear=12711.9E6 cohesion=25.0E6 friction=25.0 reg
i 32 j 28 ;pccp
 5 text prop density=2160.5 bulk=111.111E6 shear=37.037E6 cohesion=0.0 friction=35.0 reg i 2
j 2 ;bottom
 5 text prop density=2160.5 bulk=111.111E6 shear=37.037E6 cohesion=0.0 friction=35.0 reg i
32 j 2 ;bottom
 5 text prop density=2160.5 bulk=111.111E6 shear=37.037E6 cohesion=0.0 friction=35.0 reg i
39 j 2 ;bottom
 5 text ;
 5 text set grav=9.81
 5 text fix y j=1
 5 text fix x i=1
 5 text fix x i=41 j 1 15
 5 text fix x i=40 j 16 29
 5 text his 1 ydis i = 38 j = 15; level 0-
 5 text his 2 ydis i = 37 j = 16; level 0
 5 text his 3 ydis i = 37 j = 18; level 2
```

```
 5 text his 4 ydis i = 37 j = 20; level 4
 5 text his 5 ydis i = 37 j = 22; level 6
 5 text his 6 ydis i = 37 j = 24; level 8
 5 text his 7 syy i = 37 j = 16; 23406
 5 text his 8 syy i = 37 j = 20; 23405
 5 text his 9 syy i = 37 j = 23; 23414
 5 text his 10 syy i = 37 j = 26; 48833
 5 text his 11 syy i = 37 j = 27; 48834
 5 text his unbal
 5 text model null reg i 32 j 17
 5 text model null reg i 2 j 17
 5 text model null reg i 2 j 25
 5 text model null reg i 32 j 25
 5 text model null reg i 2 j 26
 5 text model null reg i 32 j 26
 5 text model null reg i 2 j 28
 5 text model null reg i 32 j 28
 5 text set large
 5 text step 2000
 5 text model mohr i 1 29 j 16 23
 5 text model mohr i 31 39 j 16 23
 5 text prop density=18.0 bulk=.714E6 shear=.771E6 cohesion=25.0E3 friction=31.0 reg i 32 j
17
 5 text prop density=2160.5 bulk=111.111E6 shear=37.037E6 cohesion=0.0 friction=35.0 reg i 2
j 17 ;backfill
 5 text int 1 Aside from 31,15 to 34,15 Bside from 31,16 to 37,16
 5 text int 2 Aside from 38,15 to 41,15 Bside from 37,16 to 40,16
 5 text int 3 Aside from 30,16 to 30,24 Bside from 31,16 to 31,24
 5 text int 1 kn 3.48e7 ks 3.48e7 friction = 31 coh = 0 tbond=0 bslip on
 5 text int 2 kn 2.49e7 ks 2.49e7 friction = 31 coh = 0 tbond=0 bslip on
 5 text int 3 kn 3.48e7 ks 3.48e7 friction = 31 coh = 0 tbond=0 bslip on
 5 text set large
 5 text def modulus
 5 text  loop n (1,numstep)
 5 text  if syy(37,16) > -15e3 then
 5 text   command
 5 text   prop density=18.0 bulk=.714E6 shear=.771E6 cohesion=25.0E3 friction=31.0 reg i 32 j
17
 5 text   int 1 kn 3.48e7 ks 3.48e7 friction = 31 coh = 0 tbond=0 bslip on
 5 text   int 2 kn 2.49e7 ks 2.49e7 friction = 31 coh = 0 tbond=0 bslip on
 5 text   int 3 kn 3.48e7 ks 3.48e7 friction = 31 coh = 0 tbond=0 bslip on
 5 text   step 25
 5 text   endcommand
 5 text  else
 5 text   command
```

```
 5 text   prop density=18.0 bulk=4.198E6 shear=4.533E6 cohesion=25.0E3 friction=31.0 reg i 32
j 17
 5 text   int 1 kn 2.05e8 ks 2.05e8 friction = 31 coh = 0 tbond=0 bslip on
 5 text   int 2 kn 1.46e8 ks 1.46e8 friction = 31 coh = 0 tbond=0 bslip on
 5 text   int 3 kn 2.05e8 ks 2.05e8 friction = 31 coh = 0 tbond=0 bslip on
 5 text   step 25
 5 text   endcommand
 5 text  endif
 5 text endloop
 5 text end
 5 text set numstep=160
 5 text modulus
 5 text model mohr i 1 29 j 25
 5 text model mohr i 31 39 j 25
 5 text prop density=2240.5 bulk=111.111E6 shear=37.037E6 cohesion=0.0 friction=35.0 reg i 2
j 25 ;utbc not lds
 5 text ;prop density=2400.5 bulk=15625E6 shear=12711.9E6 cohesion=25.0E6 friction=25.0
reg i 2 j 25 ;lds
 5 text prop density=2400.5 bulk=15625E6 shear=12711.9E6 cohesion=25.0E6 friction=25.0 reg
i 32 j 25 ;lds
 5 text set numstep=520
 5 text modulus
 5 text model mohr i 1 29 j 26 27
 5 text model mohr i 31 39 j 26 27
 5 text prop density=2240.5 bulk=111.111E6 shear=37.037E6 cohesion=0.0 friction=35.0 reg i 2
j 26 ;utbc
 5 text prop density=2240.5 bulk=111.111E6 shear=37.037E6 cohesion=0.0 friction=35.0 reg i
32 j 26 ;utbc
 5 text set numstep=520
 5 text modulus
 5 text model mohr i 1 29 j 28
 5 text model mohr i 31 39 j 28
 5 text prop density=2400.5 bulk=15625E6 shear=12711.9E6 cohesion=25.0E6 friction=25.0 reg
i 2 j 28 ;pccp
 5 text prop density=2400.5 bulk=15625E6 shear=12711.9E6 cohesion=25.0E6 friction=25.0 reg
i 32 j 28 ;pccp
 5 text set numstep=520
 5 text modulus
 0 eof
```

APPENDIX 4 – FLAC Code for State Street Array

```
0 header
1 code FLAC 5.0
1 source giic v2.0.369
1 date Sat Aug 26 08:34:06 MDT 2006
1 type giic-save
0 flac
1 config
2 axisym false
2 gwflow false
2 pstress false
2 cppudm false
2 ats false
2 creep false
2 dynamic false
2 thermal false
2 twophase false
2 extra 0
2 units 0
2 struct false
2 advanced false
2 water false
2 interface false
2 gravity true
2 excludereg false
2 solvefos false
2 record 2
0 plots
1 plot 2
2 display
3 viewport
4 autorange true
2 command plot pen history 1 line
2 name Level 0-
2 alias
2 count 1
2 item
3 name 1
3 line
1 plot 2
2 display
3 viewport
4 autorange true
2 command plot pen history 2 line
2 name Level 0
2 alias
```

2 count 1
2 item
3 name 2
3 line
1 plot 2
2 display
3 viewport
4 autorange true
2 command plot pen history 3 line
2 name Level 2
2 alias
2 count 1
2 item
3 name 3
3 line
1 plot 2
2 display
3 viewport
4 autorange true
2 command plot pen history 4 line
2 name Level 4
2 alias
2 count 1
2 item
3 name 4
3 line
1 plot 2
2 display
3 viewport
4 autorange true
2 command plot pen history 5 line
2 name Level 6
2 alias
2 count 1
2 item
3 name 5
3 line
1 plot 2
2 display
3 viewport
4 autorange true
2 command plot pen history 6 line
2 name 52203
2 alias
2 count 1
2 item

3 name 6
3 line
1 plot 2
2 display
3 viewport
4 autorange true
2 command plot pen history 7 line
2 name 52197
2 alias
2 count 1
2 item
3 name 7
3 line
1 plot 2
2 display
3 viewport
4 autorange true
2 command plot pen history 8 line
2 name 52201
2 alias
2 count 1
2 item
3 name 8
3 line
1 plot 2
2 display
3 viewport
4 autorange true
2 command plot pen history 9 line
2 name 52198
2 alias
2 count 1
2 item
3 name 9
3 line
1 plot 2
2 display
3 viewport
4 autorange true
2 command plot pen history 10 line
2 name 52200
2 alias
2 count 1
2 item
3 name 10
3 line

1 plot 2
2 display
3 viewport
4 autorange true
2 command plot pen history 11 line
2 name 52199
2 alias
2 count 1
2 item
3 name 11
3 line
1 plot 2
2 display
3 viewport
4 autorange true
2 command plot pen history 12 line
2 name unbal.
2 alias
2 count 1
2 item
3 name 12
3 line
1 plot 0
2 display
3 viewport
4 center 7.94335,2.2234573
4 radius 12.482412
4 orientation 0.0
2 command plot pen displacement attach iface
2 name disp. v
2 count 3
2 item
3 name displacement
3 switch 3
2 item
3 name attach
3 switch 2
2 item
3 name iface
3 switch 11
1 plot 0
2 display
3 viewport
4 autorange true
2 command plot pen ydisp fill attach iface
2 name disp

2 count 3
2 item
3 name ydisp
3 switch 5
3 mode 1
2 item
3 name attach
3 switch 2
2 item
3 name iface
3 switch 11
1 plot 0
2 display
3 viewport
4 autorange true
2 command plot pen syy fill attach iface
2 name stress
2 count 3
2 item
3 name syy
3 switch 5
3 mode 1
2 item
3 name attach
3 switch 2
2 item
3 name iface
3 switch 11
0 matlist
0 CppModels
0 project tree
1 title State Street Alignment Incrementally and Bilinear Modulus
1 notes
1 tree
2 branch branch A
3 state
4 file state.sav
4 batch
5 text ;2.7-10
5 text config
5 text grid 165,23
5 text m m i 1 9 j 1 9
5 text m m i 1 9 j 11 16
5 text m m i 11 12 j 1 9
5 text m m i 11 12 j 11 16
5 text m m i 11 12 j 18 23

```
5 text m m i 14 100 j 1 9
5 text m m i 14 100 j 11 23
5 text m m i 102 165 j 1 9
5 text m m i 102 165 j 15 23
5 text ;
5 text gen 0 -7 0 0 7.641 0 7.641 -7 i 1 10 j 1 10
5 text gen 0 0 0 .708 7.641 4.92 7.641 0 i 1 10 j 11 17
5 text gen 7.641 -7 7.641 0 8.541 0 8.541 -7 i 11 13 j 1 10
5 text gen 7.641 0 7.641 4.92 8.541 4.92 8.541 0 i 11 13 j 11 17
5 text gen 7.641 4.92 7.641 7.38 8.541 7.38 8.541 4.92 i 11 13 j 18 22
5 text gen same 7.641 7.736 8.541 7.736 same i 11 13 j 22 24
5 text ;
5 text gen 8.541 -7 8.541 0 105 .41 105 -7 i 14 101 j 1 10
5 text gen 8.541 0 8.541 5.74 105 2.87 105 .41 i 14 101 j 11 18
5 text gen same 8.541 5.892 105 3.022 same i 14 101 j 18 20
5 text gen same 8.541 7.38 105 4.741 same i 14 101 j 20 22
5 text gen same 8.541 7.736 105 5.097 same i 14 101 j 22 24
5 text ;
5 text gen 105 -7 105 .41 165 .82 165 -7 i 102 166 j 1 10
5 text gen 105 .41 105 2.87 165 1.64 165 .82 i 102 166 j 15 18
5 text gen same 105 3.022 165 1.792 same i 102 166 j 18 20
5 text gen same 105 4.741 165 2.914 same i 102 166 j 20 22
5 text gen same 105 5.097 165 3.270 same i 102 166 j 22 24
5 text ;
5 text attach Aside from 10,1 to 10,10 Bside from 11,1 to 11,10
5 text attach Aside from 10,11 to 10,17 Bside from 11,11 to 11,17
5 text attach Aside from 11,17 to 13,17 Bside from 11,18 to 13,18
5 text attach Aside from 13,1 to 13,10 Bside from 14,1 to 14,10
5 text attach Aside from 13,11 to 13,17 Bside from 14,11 to 14,17
5 text attach Aside from 13,18 to 13,19 Bside from 14,17 to 14,18
5 text attach Aside from 13,19 to 13,20 Bside from 14,18 to 14,20
5 text attach Aside from 13,20 to 13,24 Bside from 14,20 to 14,24
5 text int 1 Aside from 1,10 to 10,10 Bside from 1,11 to 10,11
5 text int 2 Aside from 11,10 to 13,10 Bside from 11,11 to 13,11
5 text int 3 Aside from 14,10 to 101,10 Bside from 14,11 to 101,11
5 text attach Aside from 101,1 to 101,10 Bside from 102,1 to 102,10
5 text int 4 Aside from 101,11 to 101,18 Bside from 102,15 to 102,18
5 text attach Aside from 101,18 to 101,24 Bside from 102,18 to 102,24
5 text int 5 Aside from 102,10 to 166,10 Bside from 102,15 to 166,15
5 text int 1 kn .395e8 ks .395e8 friction = 31 coh = 0 tbond=0 bslip on
5 text int 2 kn .553e8 ks .553e8 friction = 31 coh = 0 tbond=0 bslip on
5 text int 3 kn .553e8 ks .553e8 friction = 31 coh = 0 tbond=0 bslip on
5 text int 4 glue kn .553e8 ks .553e8
5 text int 5 kn .553e8 ks .553e8 friction = 31 coh = 0 tbond=0 bslip on
5 text ;
5 text gen line 8.541 5.74 105 2.87
```

```
 5 text gen line 105 2.87 166 1.64
 5 text gen line 8.541 5.892 105 3.022
 5 text gen line 105 3.022 166 1.792
 5 text gen line 7.641 7.38 8.541 7.38
 5 text gen line 8.541 7.38 105 4.741
 5 text gen line 105 4.741 166 2.914
 5 text ;
 5 text prop density=18.0 bulk=1.134E6 shear=1.224E6 cohesion=25.0E3 friction=31.0 reg i 2 j
12 ;geofoam
 5 text prop density=18.0 bulk=1.134E6 shear=1.224E6 cohesion=25.0E3 friction=31.0 reg i 12 j
12 ;geofoam
 5 text prop density=18.0 bulk=1.134E6 shear=1.224E6 cohesion=25.0E3 friction=31.0 reg i 16 j
12 ;geofoam
 5 text prop density=18.0 bulk=1.134E6 shear=1.224E6 cohesion=25.0E3 friction=31.0 reg i 110
j 17 ;geofoam
 5 text prop density=2400.5 bulk=15625E6 shear=12711.9E6 cohesion=25.0E6 friction=25.0 reg
i 12 j 19 ;abutment
 5 text prop density=2400.5 bulk=15625E6 shear=12711.9E6 cohesion=25.0E6 friction=25.0 reg
i 16 j 19 ;lds
 5 text prop density=2400.5 bulk=15625E6 shear=12711.9E6 cohesion=25.0E6 friction=25.0 reg
i 110 j 19 ;lds
 5 text prop density=2240.5 bulk=133.3333E6 shear=44.4444E6 cohesion=0.0 friction=35.0 reg
i 16 j 21 ;utbc
 5 text prop density=2240.5 bulk=133.3333E6 shear=44.4444E6 cohesion=0.0 friction=35.0 reg
i 110 j 21 ;utbc
 5 text prop density=2400.5 bulk=15625E6 shear=12711.9E6 cohesion=25.0E6 friction=25.0 reg
i 12 j 23 ;pccp
 5 text prop density=2400.5 bulk=15625E6 shear=12711.9E6 cohesion=25.0E6 friction=25.0 reg
i 16 j 23 ;pccp
 5 text prop density=2400.5 bulk=15625E6 shear=12711.9E6 cohesion=25.0E6 friction=25.0 reg
i 110 j 23 ;pccp
 5 text prop density=2160.5 bulk=133.3333E6 shear=44.4444E6 cohesion=0.0 friction=35.0 reg
i 2 j 2 ;bottom
 5 text prop density=2160.5 bulk=133.3333E6 shear=44.4444E6 cohesion=0.0 friction=35.0 reg
i 12 j 2 ;bottom
 5 text prop density=2160.5 bulk=133.3333E6 shear=44.4444E6 cohesion=0.0 friction=35.0 reg
i 16 j 2 ;bottom
 5 text prop density=2160.5 bulk=133.3333E6 shear=44.4444E6 cohesion=0.0 friction=35.0 reg
i 110 j 2 ;bottom
 5 text set grav=9.81
 5 text fix y j=1
 5 text fix x i=1
 5 text fix x i=11 j=18 24
 5 text fix x i=166
 5 text his ydis i = 15 j = 10; level0-
 5 text his ydis i = 15 j = 11; level 0
```

```
 5 text his ydis i = 15 j = 13; level 2
 5 text his ydis i = 15 j = 15; level 4
 5 text his ydis i = 15 j = 17; level 6
 5 text his sxx i = 12 j = 18; 52203
 5 text his sxx i = 14 j =17; 52197
 5 text his syy i = 14 j =17; 52201
 5 text his syy i = 120 j = 15; 52198
 5 text his syy i = 132 j = 15; 52200
 5 text his syy i = 154 j =15; 52199
 5 text his unbal
 5 text model null i 1 9 j 11 16
 5 text model null i 11 12 j 11 16
 5 text model null i 14 100 j 11 17
 5 text model null i 102 165 j 15 17
 5 text model null i 11 12 j 18 21
 5 text model null i 14 100 j 18 19
 5 text model null i 102 165 j 18 19
 5 text model null i 14 100 j 20 21
 5 text model null i 102 165 j 20 21
 5 text model null i 11 12 j 22 23
 5 text model null i 14 100 j 22 23
 5 text model null i 102 165 j 22 23
 5 text set large
 5 text step 2000
 5 text m m i 1 9 j 11 16
 5 text m m i 11 12 j 11 16
 5 text m m i 14 100 j 11 17
 5 text m m i 102 165 j 15 17
 5 text prop density=18.0 bulk=1.134E6 shear=1.224E6 cohesion=25.0E3 friction=31.0 reg i 2 j
12 ;geofoam
 5 text prop density=18.0 bulk=1.134E6 shear=1.224E6 cohesion=25.0E3 friction=31.0 reg i 12 j
12 ;geofoam
 5 text prop density=18.0 bulk=1.134E6 shear=1.224E6 cohesion=25.0E3 friction=31.0 reg i 16 j
12 ;geofoam
 5 text prop density=18.0 bulk=1.134E6 shear=1.224E6 cohesion=25.0E3 friction=31.0 reg i 110
j 17 ;geofoam
 5 text int 1 Aside from 1,10 to 10,10 Bside from 1,11 to 10,11
 5 text int 2 Aside from 11,10 to 13,10 Bside from 11,11 to 13,11
 5 text int 3 Aside from 14,10 to 101,10 Bside from 14,11 to 101,11
 5 text int 4 Aside from 101,11 to 101,18 Bside from 102,15 to 102,18
 5 text int 5 Aside from 102,10 to 166,10 Bside from 102,15 to 166,15
 5 text int 1 kn .553e8 ks .553e8 friction = 31 coh = 0 tbond=0 bslip on
 5 text int 2 kn .553e8 ks .553e8 friction = 31 coh = 0 tbond=0 bslip on
 5 text int 3 kn .553e8 ks .553e8 friction = 31 coh = 0 tbond=0 bslip on
 5 text int 4 glue kn .553e8 ks .553e8
 5 text int 5 kn .553e8 ks .553e8 friction = 31 coh = 0 tbond=0 bslip on
```

```
 5 text def modulus
 5 text  loop n (1,numstep)
 5 text  if syy(14,17) > -15e3 then
 5 text   command
 5 text   prop density=18.0 bulk=1.134E6 shear=1.224E6 cohesion=25.0E3 friction=31.0 reg i 2 j
12 ;geofoam
 5 text   prop density=18.0 bulk=1.134E6 shear=1.224E6 cohesion=25.0E3 friction=31.0 reg i 12
j 12 ;geofoam
 5 text   prop density=18.0 bulk=1.134E6 shear=1.224E6 cohesion=25.0E3 friction=31.0 reg i 16
j 12 ;geofoam
 5 text   prop density=18.0 bulk=1.134E6 shear=1.224E6 cohesion=25.0E3 friction=31.0 reg i
110 j 17 ;geofoam
 5 text   int 1 kn .553e8 ks .553e8 friction = 31 coh = 0 tbond=0 bslip on
 5 text   int 2 kn .553e8 ks .553e8 friction = 31 coh = 0 tbond=0 bslip on
 5 text   int 3 kn .553e8 ks .553e8 friction = 31 coh = 0 tbond=0 bslip on
 5 text   int 4 glue kn .553e8 ks .553e8
 5 text   int 5 kn .553e8 ks .553e8 friction = 31 coh = 0 tbond=0 bslip on
 5 text   step 25
 5 text   endcommand
 5 text  else
 5 text   command
 5 text   prop density=18.0 bulk=4.198E6 shear=4.533E6 cohesion=25.0E3 friction=31.0 reg i 2 j
12 ;geofoam
 5 text   prop density=18.0 bulk=4.198E6 shear=4.533E6 cohesion=25.0E3 friction=31.0 reg i 12
j 12 ;geofoam
 5 text   prop density=18.0 bulk=4.198E6 shear=4.533E6 cohesion=25.0E3 friction=31.0 reg i 16
j 12 ;geofoam
 5 text   prop density=18.0 bulk=4.198E6 shear=4.533E6 cohesion=25.0E3 friction=31.0 reg i
110 j 17 ;geofoam
 5 text   int 1 kn 2.05e8 ks 2.05e8 friction = 31 coh = 0 tbond=0 bslip on
 5 text   int 2 kn 2.05e8 ks 2.05e8 friction = 31 coh = 0 tbond=0 bslip on
 5 text   int 3 kn 2.05e8 ks 2.05e8 friction = 31 coh = 0 tbond=0 bslip on
 5 text   int 4 glue kn 2.05e8 ks 2.05e8
 5 text   int 5 kn 2.05e8 ks 2.05e8 friction = 31 coh = 0 tbond=0 bslip on
 5 text   step 25
 5 text   endcommand
 5 text  endif
 5 text  endloop
 5 text end
 5 text set numstep=300
 5 text modulus
 5 text m m i 11 12 j 18 21
 5 text m m i 14 100 j 18 19
 5 text m m i 102 165 j 18 19
 5 text prop density=2400.5 bulk=15625E6 shear=12711.9E6 cohesion=25.0E6 friction=25.0 reg
i 12 j 19 ;abutment
```

```
 5 text prop density=2400.5 bulk=15625E6 shear=12711.9E6 cohesion=25.0E6 friction=25.0 reg
i 16 j 19 ;lds
 5 text prop density=2400.5 bulk=15625E6 shear=12711.9E6 cohesion=25.0E6 friction=25.0 reg
i 110 j 19 ;lds
 5 text set numstep=600
 5 text modulus
 5 text m m i 14 100 j 20 21
 5 text m m i 102 165 j 20 21
 5 text prop density=2240.5 bulk=133.3333E6 shear=44.4444E6 cohesion=0.0 friction=35.0 reg
i 16 j 21 ;utbc
 5 text prop density=2240.5 bulk=133.3333E6 shear=44.4444E6 cohesion=0.0 friction=35.0 reg
i 110 j 21 ;utbc
 5 text set numstep=1200
 5 text modulus
 5 text m m i 11 12 j 22 23
 5 text m m i 14 100 j 22 23
 5 text m m i 102 165 j 22 23
 5 text prop density=2400.5 bulk=15625E6 shear=12711.9E6 cohesion=25.0E6 friction=25.0 reg
i 12 j 23 ;pccp
 5 text prop density=2400.5 bulk=15625E6 shear=12711.9E6 cohesion=25.0E6 friction=25.0 reg
i 16 j 23 ;pccp
 5 text prop density=2400.5 bulk=15625E6 shear=12711.9E6 cohesion=25.0E6 friction=25.0 reg
i 110 j 23 ;pccp
 5 text set numstep=800
 5 text modulus
 2 branch branch B
 3 state
 4 file stateb.sav
 4 batch
 5 text ;2.7-10
 5 text config
 5 text grid 50,23
 5 text m m i 1 9 j 1 9
 5 text m m i 1 9 j 11 16
 5 text m m i 11 12 j 1 9
 5 text m m i 11 12 j 11 16
 5 text m m i 11 12 j 18 23
 5 text m m i 14 50 j 1 9
 5 text m m i 14 50 j 11 23
 5 text ;
 5 text gen 0 -7 0 0 7.641 0 7.641 -7 i 1 10 j 1 10
 5 text gen 0 0 0 .708 7.641 4.92 7.641 0 i 1 10 j 11 17
 5 text gen 7.641 -7 7.641 0 8.541 0 8.541 -7 i 11 13 j 1 10
 5 text gen 7.641 0 7.641 4.92 8.541 4.92 8.541 0 i 11 13 j 11 17
 5 text gen 7.641 4.92 7.641 7.38 8.541 7.38 8.541 4.92 i 11 13 j 18 22
 5 text gen same 7.641 7.736 8.541 7.736 same i 11 13 j 22 24
```

```
 5 text ;
 5 text gen 8.541 -7 8.541 0 57 .41 57 -7 i 14 51 j 1 10
 5 text gen 8.541 0 8.541 5.74 57 2.87 57 .41 i 14 51 j 11 18
 5 text gen same 8.541 5.892 57 3.022 same i 14 51 j 18 20
 5 text gen same 8.541 7.38 57 4.741 same i 14 51 j 20 22
 5 text gen same 8.541 7.736 57 5.097 same i 14 51 j 22 24
 5 text ;
 5 text attach Aside from 10,1 to 10,10 Bside from 11,1 to 11,10
 5 text attach Aside from 10,11 to 10,17 Bside from 11,11 to 11,17
 5 text attach Aside from 11,17 to 13,17 Bside from 11,18 to 13,18
 5 text attach Aside from 13,1 to 13,10 Bside from 14,1 to 14,10
 5 text attach Aside from 13,11 to 13,17 Bside from 14,11 to 14,17
 5 text attach Aside from 13,18 to 13,19 Bside from 14,17 to 14,18
 5 text attach Aside from 13,19 to 13,20 Bside from 14,18 to 14,20
 5 text attach Aside from 13,20 to 13,24 Bside from 14,20 to 14,24
 5 text int 1 Aside from 1,10 to 10,10 Bside from 1,11 to 10,11
 5 text int 2 Aside from 11,10 to 13,10 Bside from 11,11 to 13,11
 5 text int 3 Aside from 14,10 to 51,10 Bside from 14,11 to 51,11
 5 text int 1 kn 5.53e7 ks 5.53e7 friction = 31 coh = 0 tbond=0 bslip on
 5 text int 2 kn 3.95e7 ks 3.95e7 friction = 31 coh = 0 tbond=0 bslip on
 5 text int 3 kn 5.53e7 ks 5.53e7 friction = 31 coh = 0 tbond=0 bslip on
 5 text ;
 5 text gen line 8.541 5.74 57 2.87
 5 text gen line 8.541 5.892 57 3.022
 5 text gen line 7.641 7.38 8.541 7.38
 5 text gen line 8.541 7.38 57 4.741
 5 text ;
 5 text prop density=18.0 bulk=1.134E6 shear=1.224E6 cohesion=25.0E3 friction=31.0 reg i 2 j
12 ;geofoam
 5 text prop density=18.0 bulk=1.134E6 shear=1.224E6 cohesion=25.0E3 friction=31.0 reg i 12 j
12 ;geofoam
 5 text prop density=18.0 bulk=1.134E6 shear=1.224E6 cohesion=25.0E3 friction=31.0 reg i 16 j
12 ;geofoam
 5 text prop density=2400.5 bulk=15625E6 shear=12711.9E6 cohesion=25.0E6 friction=25.0 reg
i 12 j 19 ;abutment
 5 text prop density=2400.5 bulk=15625E6 shear=12711.9E6 cohesion=25.0E6 friction=25.0 reg
i 16 j 19 ;lds
 5 text prop density=2240.5 bulk=111.11E6 shear=37.037E6 cohesion=0.0 friction=35.0 reg i 16
j 21 ;utbc
 5 text prop density=2400.5 bulk=15625E6 shear=12711.9E6 cohesion=25.0E6 friction=25.0 reg
i 12 j 23 ;pccp
 5 text prop density=2400.5 bulk=15625E6 shear=12711.9E6 cohesion=25.0E6 friction=25.0 reg
i 16 j 23 ;pccp
 5 text prop density=2160.5 bulk=111.11E6 shear=37.037E6 cohesion=0.0 friction=35.0 reg i 2 j
2 ;bottom
```

```
 5 text prop density=2160.5 bulk=111.11E6 shear=37.037E6 cohesion=0.0 friction=35.0 reg i 12
j 2 ;bottom
 5 text prop density=2160.5 bulk=111.11E6 shear=37.037E6 cohesion=0.0 friction=35.0 reg i 16
j 2 ;bottom
 5 text set grav=9.81
 5 text fix y j=1
 5 text fix x i=1
 5 text ;fix x i=11 j=18 24
 5 text fix x i=51
 5 text his ydis i = 15 j = 10; level0-
 5 text his ydis i = 15 j = 11; level 0
 5 text his ydis i = 15 j = 13; level 2
 5 text his ydis i = 15 j = 15; level 4
 5 text his ydis i = 15 j = 17; level 6
 5 text his sxx i = 12 j = 18; 52203
 5 text his sxx i = 14 j =17; 52197
 5 text his syy i = 14 j =17; 52201
 5 text his 12 unbal
 5 text model null i 1 9 j 11 16
 5 text model null i 11 12 j 11 16
 5 text model null i 14 50 j 11 17
 5 text model null i 11 12 j 18 21
 5 text model null i 14 50 j 18 19
 5 text model null i 14 50 j 20 21
 5 text model null i 11 12 j 22 23
 5 text model null i 14 50 j 22 23
 5 text set large
 5 text step 2000
 5 text m m i 1 9 j 11 16
 5 text m m i 11 12 j 11 16
 5 text m m i 14 50 j 11 17
 5 text prop density=18.0 bulk=1.134E6 shear=1.224E6 cohesion=25.0E3 friction=31.0 reg i 2 j
12 ;geofoam
 5 text prop density=18.0 bulk=1.134E6 shear=1.224E6 cohesion=25.0E3 friction=31.0 reg i 12 j
12 ;geofoam
 5 text prop density=18.0 bulk=1.134E6 shear=1.224E6 cohesion=25.0E3 friction=31.0 reg i 16 j
12 ;geofoam
 5 text int 1 Aside from 1,10 to 10,10 Bside from 1,11 to 10,11
 5 text int 2 Aside from 11,10 to 13,10 Bside from 11,11 to 13,11
 5 text int 3 Aside from 14,10 to 51,10 Bside from 14,11 to 51,11
 5 text int 1 kn 5.53e7 ks 5.53e7 friction = 31 coh = 0 tbond=0 bslip on
 5 text int 2 kn 3.95e7 ks 3.95e7 friction = 31 coh = 0 tbond=0 bslip on
 5 text int 3 kn 5.53e7 ks 5.53e7 friction = 31 coh = 0 tbond=0 bslip on
 5 text def modulus
 5 text  loop n (1,numstep)
 5 text  if syy(15,11) > -15e3 then
```

```
 5 text   command
 5 text   prop density=18.0 bulk=1.134E6 shear=1.224E6 cohesion=25.0E3 friction=31.0 reg i 32
j 17
 5 text   int 1 kn 5.53e7 ks 5.53e7 friction = 31 coh = 0 tbond=0 bslip on
 5 text   int 2 kn 3.95e7 ks 3.95e7 friction = 31 coh = 0 tbond=0 bslip on
 5 text   int 3 kn 5.53e7 ks 5.53e7 friction = 31 coh = 0 tbond=0 bslip on
 5 text   step 25
 5 text   endcommand
 5 text  else
 5 text   command
 5 text   prop density=18.0 bulk=4.198E6 shear=4.533E6 cohesion=25.0E3 friction=31.0 reg i 32
j 17
 5 text   int 1 kn 2.05e8 ks 2.05e8 friction = 31 coh = 0 tbond=0 bslip on
 5 text   int 2 kn 1.46e8 ks 1.46e8 friction = 31 coh = 0 tbond=0 bslip on
 5 text   int 3 kn 2.05e8 ks 2.05e8 friction = 31 coh = 0 tbond=0 bslip on
 5 text   step 25
 5 text   endcommand
 5 text  endif
 5 text endloop
 5 text end
 5 text set numstep=160
 5 text modulus
 5 text m m i 11 12 j 18 21
 5 text m m i 14 50 j 18 19
 5 text prop density=2400.5 bulk=15625E6 shear=12711.9E6 cohesion=25.0E6 friction=25.0 reg
i 12 j 19 ;abutment
 5 text prop density=2400.5 bulk=15625E6 shear=12711.9E6 cohesion=25.0E6 friction=25.0 reg
i 16 j 19 ;lds
 5 text set numstep=900
 5 text modulus
 5 text m m i 14 50 j 20 21
 5 text prop density=2240.5 bulk=111.11E6 shear=37.037E6 cohesion=0.0 friction=35.0 reg i 16
j 21 ;utbc
 5 text set numstep=900
 5 text modulus
 5 text m m i 11 12 j 22 23
 5 text m m i 14 50 j 22 23
 5 text prop density=2400.5 bulk=15625E6 shear=12711.9E6 cohesion=25.0E6 friction=25.0 reg
i 12 j 23 ;pccp
 5 text prop density=2400.5 bulk=15625E6 shear=12711.9E6 cohesion=25.0E6 friction=25.0 reg
i 16 j 23 ;pccp
 5 text set numstep=900
 5 text modulus
 0 eof
```

State Street East

0 header
1 code FLAC 5.0
1 source giic v2.0.369
1 date Sat Oct 07 09:25:26 MDT 2006
1 type giic-save
0 flac
1 config
2 axisym false
2 gwflow false
2 pstress false
2 cppudm false
2 ats false
2 creep false
2 dynamic false
2 thermal false
2 twophase false
2 extra 0
2 units 0
2 struct true
2 advanced false
2 water false
2 interface false
2 gravity true
2 excludereg false
2 solvefos false
2 record 2
0 plots
1 plot 2
2 display
3 viewport
4 autorange true
2 command plot pen history 1 line
2 name Level 0-
2 alias
2 count 1
2 item
3 name 1
3 line
1 plot 2
2 display
3 viewport
4 autorange true
2 command plot pen history 2 line
2 name Level 0

2 alias
2 count 1
2 item
3 name 2
3 line
1 plot 2
2 display
3 viewport
4 autorange true
2 command plot pen history 3 line
2 name Level 2
2 alias
2 count 1
2 item
3 name 3
3 line
1 plot 2
2 display
3 viewport
4 autorange true
2 command plot pen history 4 line
2 name 52199
2 alias
2 count 1
2 item
3 name 4
3 line
1 plot 2
2 display
3 viewport
4 autorange true
2 command plot pen history 5 line
2 name unbal
2 alias
2 count 1
2 item
3 name 5
3 line
1 plot 0
2 display
3 viewport
4 autorange true
2 command plot pen displacement attach iface
2 name disp. vector
2 count 3
2 item

3 name displacement
3 switch 3
2 item
3 name attach
3 switch 2
2 item
3 name iface
3 switch 11
1 plot 0
2 display
3 viewport
4 autorange true
2 command plot pen ydisp fill attach iface
2 name disp. contour
2 count 3
2 item
3 name ydisp
3 switch 5
3 mode 1
2 item
3 name attach
3 switch 2
2 item
3 name iface
3 switch 11
1 plot 0
2 display
3 viewport
4 autorange true
2 command plot pen syy fill attach iface
2 name stress
2 count 3
2 item
3 name syy
3 switch 5
3 mode 1
2 item
3 name attach
3 switch 2
2 item
3 name iface
3 switch 11
0 matlist
0 CppModels
0 project tree
1 title State Street East Array Incrementally and Bilinear Modulus

```
 1 notes
 1 tree
 2 state
 3 file stateeast.sav
 3 batch
 4 text config
 4 text grid 77,27
 4 text m m i 72 77 j 1 19
 4 text m m i 0 70 j 1 19
 4 text m m i 72 77 j 21 27
 4 text m m i 0 70 j 21 27
 4 text gen -.6 -10 -.6 0 0 0 0 -10 i 76 78 j 1 20
 4 text gen -.6 0 -.6 .82 0 .82 0 0 i 76 78 j 21 23
 4 text gen same -.6 .972 0 .972 same i 76 78 j 23 24
 4 text gen same -.6 2.318 0 2.318 same i 76 78 j 24 27
 4 text gen same -.6 2.674 0 2.674 same i 76 78 j 27 28
 4 text ;-----------------------------------------------
 4 text gen -2.494 -10 -2.494 0 same same i 72 76 j 1 20
 4 text gen -2.494 0 -2.494 .82 same same i 72 76 j 21 23
 4 text gen same -2.494 .972 same same i 72 76 j 23 24
 4 text gen same -2.494 2.318 same same i 72 76 j 24 27
 4 text gen same -2.494 2.674 same same i 72 76 j 27 28
 4 text ;-----------------------------------------------
 4 text gen -36.7 -10 -36.7 0 -2.494 0 -2.494 -10 i 0 71 j 1 20
 4 text gen -36.7 0 -36.7 .82 -2.494 .82 -2.494 0 0 i 0 71 j 21 23
 4 text gen same -36.7 .972 -2.494 .972 same i 0 71 j 23 24
 4 text gen same -36.7 2.318 -2.494 2.318 same i 0 71 j 24 27
 4 text gen same -36.7 2.674 -2.494 2.674 same i 0 71 j 27 28
 4 text ;-----------------------------------------------
 4 text attach Aside from 1,20 to 71,20 Bside from 1,21 to 71,21
 4 text int 1 Aside from 72,20 to 78,20 Bside from 72,21 to 78,21
 4 text attach Aside from 71,1 to 71,20 Bside from 72,1 to 72,20
 4 text int 2 Aside from 71,21 to 71,23 Bside from 72,21 to 72,23
 4 text attach Aside from 71,23 to 71,28 Bside from 72,23 to 72,28
 4 text int 1 kn 6.91e7 ks 6.91e7 friction = 31 coh = 0 tbond=0 bslip on
 4 text int 2 kn 6.91e7 ks 6.91e7 friction = 31 coh = 0 tbond=0 bslip on
 4 text gen line -36.7 .82 0 .82
 4 text gen line -36.7 .972 0 .972
 4 text gen line -36.7 2.318 0 2.318
 4 text prop density=18.0 bulk=1.134E6 shear=1.224E6 cohesion=25.0E3 friction=31.0 reg i 76 j
22 ;geofoam
 4 text prop density=2160.5 bulk=111.111E6 shear=37.037E6 cohesion=0.0 friction=35.0 reg i 2
j 22 ;backfill
 4 text prop density=2240.5 bulk=111.111E6 shear=37.037E6 cohesion=0.0 friction=35.0 reg i 2
j 23 ;utbc not lds
```

```
 4 text ;prop density=2400.5 bulk=15625E6 shear=12711.9E6 cohesion=25.0E6 friction=25.0
reg i 2 j 23 ;lds
 4 text prop density=2400.5 bulk=15625E6 shear=12711.9E6 cohesion=25.0E6 friction=25.0 reg
i 76 j 23 ;lds
 4 text prop density=2240.5 bulk=111.111E6 shear=37.037E6 cohesion=0.0 friction=35.0 reg i 2
j 24 ;utbc
 4 text prop density=2240.5 bulk=111.111E6 shear=37.037E6 cohesion=0.0 friction=35.0 reg i
76 j 24 ;utbc
 4 text prop density=2400.5 bulk=15625E6 shear=12711.9E6 cohesion=25.0E6 friction=25.0 reg
i 2 j 27 ;pccp
 4 text prop density=2400.5 bulk=15625E6 shear=12711.9E6 cohesion=25.0E6 friction=25.0 reg
i 76 j 27 ;pccp
 4 text prop density=2160.5 bulk=111.111E6 shear=37.037E6 cohesion=0.0 friction=35.0 reg i 2
j 2 ;bottom
 4 text prop density=2160.5 bulk=111.111E6 shear=37.037E6 cohesion=0.0 friction=35.0 reg i
76 j 2 ;bottom
 4 text set grav=9.81
 4 text fix y j=1
 4 text fix x i=1
 4 text fix x i=78
 4 text his ydis i = 76 j = 20 ; level 0-
 4 text his ydis i = 76 j = 21 ; level 0
 4 text his ydis i = 76 j = 23 ; level 1
 4 text his syy i = 76 j = 21 ; 52199
 4 text his unbal
 4 text model null i 72 77 j 21 22
 4 text model null i 0 70 j 21 22
 4 text model null i 72 77 j 23
 4 text model null i 0 70 j 23
 4 text model null i 72 77 j 24 26
 4 text model null i 0 70 j 24 26
 4 text model null i 72 77 j 27
 4 text model null i 0 70 j 27
 4 text set large
 4 text step 2000
 4 text model mohr i 72 77 j 21 22
 4 text model mohr i 0 70 j 21 22
 4 text prop density=18.0 bulk=1.134E6 shear=1.224E6 cohesion=25.0E3 friction=31.0 reg i 76 j
21 ;geofoam
 4 text prop density=2160.5 bulk=111.111E6 shear=37.037E6 cohesion=0.0 friction=35.0 reg i 2
j 21 ;backfill
 4 text int 1 Aside from 72,20 to 78,20 Bside from 72,21 to 78,21
 4 text int 2 Aside from 71,21 to 71,23 Bside from 72,21 to 72,23
 4 text int 1 kn 6.91e7 ks 6.91e7 friction = 31 coh = 0 tbond=0 bslip on
 4 text int 2 kn 6.91e7 ks 6.91e7 friction = 31 coh = 0 tbond=0 bslip on
 4 text set large
```

```
 4 text def modulus
 4 text  loop n (1,numstep)
 4 text  if syy(76,21) > -15e3 then
 4 text   command
 4 text   prop density=18.0 bulk=1.134E6 shear=1.224E6 cohesion=25.0E3 friction=31.0 reg i 76
j 21 ;geofoam
 4 text   int 1 kn 6.91e7 ks 6.91e7 friction = 31 coh = 0 tbond=0 bslip on
 4 text   int 2 kn 6.91e7 ks 6.91e7 friction = 31 coh = 0 tbond=0 bslip on
 4 text   step 25
 4 text   endcommand
 4 text  else
 4 text   command
 4 text   prop density=18.0 bulk=4.198E6 shear=4.533E6 cohesion=25.0E3 friction=31.0 reg i 76
j 21 ;geofoam
 4 text   int 1 kn 2.56e8 ks 2.56e8 friction = 31 coh = 0 tbond=0 bslip on
 4 text   int 2 kn 2.56e8 ks 2.56e8 friction = 31 coh = 0 tbond=0 bslip on
 4 text   step 25
 4 text   endcommand
 4 text  endif
 4 text endloop
 4 text end
 4 text set numstep=160
 4 text modulus
 4 text model mohr i 72 77 j 23
 4 text model mohr i 0 70 j 23
 4 text prop density=2240.5 bulk=111.111E6 shear=37.037E6 cohesion=0.0 friction=35.0 reg i 2
j 23 ;utbc not lds
 4 text ;prop density=2400.5 bulk=15625E6 shear=12711.9E6 cohesion=25.0E6 friction=25.0
reg i 2 j 23 ;lds
 4 text prop density=2400.5 bulk=15625E6 shear=12711.9E6 cohesion=25.0E6 friction=25.0 reg
i 76 j 23 ;lds
 4 text set numstep=160
 4 text modulus
 4 text model mohr i 72 77 j 24 26
 4 text model mohr i 0 70 j 24 26
 4 text prop density=2240.5 bulk=111.111E6 shear=37.037E6 cohesion=0.0 friction=35.0 reg i 2
j 24 ;utbc
 4 text prop density=2240.5 bulk=111.111E6 shear=37.037E6 cohesion=0.0 friction=35.0 reg i
76 j 24 ;utbc
 4 text set numstep=160
 4 text modulus
 4 text model mohr i 72 77 j 27
 4 text model mohr i 0 70 j 27
 4 text prop density=2400.5 bulk=15625E6 shear=12711.9E6 cohesion=25.0E6 friction=25.0 reg
i 2 j 27 ;pccp
```

```
 4 text prop density=2400.5 bulk=15625E6 shear=12711.9E6 cohesion=25.0E6 friction=25.0 reg
i 76 j 27 ;pccp
 4 text set numstep=160
 4 text modulus
 0 eof
```

APPENDIX 5 – FLAC Code for 100 South Street Array

```
0 header
1 code FLAC 5.0
1 source giic v2.0.369
1 date Thu Oct 12 19:46:15 MDT 2006
1 type giic-save
0 flac
1 config
2 axisym false
2 gwflow false
2 pstress false
2 cppudm false
2 ats false
2 creep false
2 dynamic false
2 thermal false
2 twophase false
2 extra 0
2 units 0
2 struct true
2 advanced false
2 water false
2 interface false
2 gravity true
2 excludereg false
2 solvefos false
2 record 2
0 plots
1 plot 2
2 display
3 viewport
4 autorange true
2 command plot pen history 1
2 name Level 0-
2 alias
2 count 1
2 item
3 name 1
1 plot 2
2 display
3 viewport
4 autorange true
2 command plot pen history 2 line
2 name Level 0
2 alias
2 count 1
```

2 item
3 name 2
3 line
1 plot 2
2 display
3 viewport
4 autorange true
2 command plot pen history 3 line
2 name Level 1.5
2 alias
2 count 1
2 item
3 name 3
3 line
1 plot 2
2 display
3 viewport
4 autorange true
2 command plot pen history 4 line
2 name Level 3.5
2 alias
2 count 1
2 item
3 name 4
3 line
1 plot 2
2 display
3 viewport
4 autorange true
2 command plot pen history 5 line
2 name Level 5.5
2 alias
2 count 1
2 item
3 name 5
3 line
1 plot 2
2 display
3 viewport
4 autorange true
2 command plot pen history 6
2 name Level 7.5
2 alias
2 count 1
2 item
3 name 6

1 plot 2
2 display
3 viewport
4 autorange true
2 command plot pen history 7 line
2 name Level 8.5
2 alias
2 count 1
2 item
3 name 7
3 line
1 plot 2
2 display
3 viewport
4 autorange true
2 command plot pen history 8 line
2 name Level 9
2 alias
2 count 1
2 item
3 name 8
3 line
1 plot 2
2 display
3 viewport
4 autorange true
2 command plot pen history 9 line
2 name 55540
2 alias
2 count 1
2 item
3 name 9
3 line
1 plot 2
2 display
3 viewport
4 autorange true
2 command plot pen history 10 line
2 name 55541
2 alias
2 count 1
2 item
3 name 10
3 line
1 plot 2
2 display

3 viewport
4 autorange true
2 command plot pen history 11 line
2 name unbal
2 alias
2 count 1
2 item
3 name 11
3 line
1 plot 0
2 display
3 viewport
4 autorange true
2 command plot pen displacement attach iface
2 name disp. vector
2 count 3
2 item
3 name displacement
3 switch 3
2 item
3 name attach
3 switch 2
2 item
3 name iface
3 switch 11
1 plot 0
2 display
3 viewport
4 autorange true
2 command plot pen ydisp fill attach iface
2 name disp. contour
2 count 3
2 item
3 name ydisp
3 switch 5
3 mode 1
2 item
3 name attach
3 switch 2
2 item
3 name iface
3 switch 11
1 plot 0
2 display
3 viewport
4 autorange true

2 command plot pen syy fill attach iface
2 name stress
2 count 3
2 item
3 name syy
3 switch 5
3 mode 1
2 item
3 name attach
3 switch 2
2 item
3 name iface
3 switch 11
0 matlist
0 CppModels
0 project tree
1 title 100 South, South Array Incrementally and Bilinear Modulus
1 notes
1 tree
2 branch branch A
3 state
4 file 100south.sav
4 batch
5 text ;E=2.7-10
5 text config
5 text grid 55,29
5 text m m i 1 4 j 1 14;mohr-coulomb model
5 text m m i 1 4 j 16 29
5 text m m i 10 11 j 1 14
5 text m m i 6 11 j 16 29
5 text m m i 13 55 j 1 14
5 text m m i 13 55 j 16 29
5 text gen 0 -12 0 0 1.473 0 1.473 -12 i 1 3 j 1 15
5 text gen 0 0 0 .41 1.473 .41 1.473 0 i 1 3 j 16 17
5 text gen same 0 6.97 1.473 6.97 same i 1 3 j 17 25
5 text gen same 0 7.38 1.473 7.38 same i 1 3 j 25 26
5 text gen same 0 7.532 1.473 7.532 same i 1 3 j 26 27
5 text gen same 0 8.142 1.473 8.142 same i 1 3 j 27 29
5 text gen same 0 8.498 1.473 8.498 same i 1 3 j 29 30
5 text ;
5 text gen same same 2.692 0 2.692 -12 i 3 5 j 1 15
5 text gen same same 2.692 .41 2.692 0 i 3 5 j 16 17
5 text gen same same 2.692 6.97 same i 3 5 j 17 25
5 text gen same same 2.692 7.38 same i 3 5 j 25 26
5 text gen same same 2.692 7.532 same i 3 5 j 26 27
5 text gen same same 2.692 8.142 same i 3 5 j 27 29

```
 5 text gen same same 2.692 8.498 same i 3 5 j 29 30
 5 text ;
 5 text gen 2.692 -12 2.692 0 3.792 0 3.792 -12 i 10 12 j 1 15
 5 text gen 2.692 0 2.692 .41 4.284 .41 3.792 0 i 6 12 j 16 17
 5 text gen same 2.692 6.97 12.148 6.97 same i 6 12 j 17 25
 5 text gen same 2.692 7.38 12.64 7.38 same i 6 12 j 25 26
 5 text gen same 2.692 7.532 12.64 7.532 same i 6 12 j 26 27
 5 text gen same 2.692 8.142 12.64 8.142 same i 6 12 j 27 29
 5 text gen same 2.692 8.498 12.64 8.498 same i 6 12 j 29 30
 5 text ;
 5 text gen 3.792 -12 3.792 0 45 0 45 -12  i 13 56 j 1 15
 5 text gen 3.792 0 4.284 .41 45 .41 45 0 i 13 56 j 16 17
 5 text gen same 12.148 6.97 45 6.97 same i 13 56 j 17 25
 5 text gen same 12.64 7.38 45 7.38 same i 13 56 j 25 26
 5 text gen same 12.64 7.532 45 7.532 same i 13 56 j 26 27
 5 text gen same 12.64 8.142 45 8.142 same i 13 56 j 27 29
 5 text gen same 12.64 8.498 45 8.498 same i 13 56 j 29 30
 5 text ;
 5 text int 1 Aside from 1,15 to 5,15 Bside from 1,16 to 5,16
 5 text int 2 Aside from 10,15 to 12,15 Bside from 6,16 to 12,16
 5 text attach Aside from 5,1 to 5,15 Bside from 10,1 to 10,15
 5 text attach Aside from 5,16 to 5,30 Bside from 6,16 to 6,30
 5 text attach Aside from 12,1 to 12,15 Bside from 13,1 to 13,15
 5 text int 3 Aside from 12,16 to 12,26 Bside from 13,16 to 13,26
 5 text attach Aside from 12,26 to 12,30 Bside from 13,26 to 13,30
 5 text attach Aside from 13,15 to 56,15 Bside from 13,16 to 56,16
 5 text int 1 kn 5.53e7 ks 5.53e7 friction = 31 coh = 0 tbond=0 bslip on
 5 text int 2 kn 3.95e7 ks 3.95e7 friction = 31 coh = 0 tbond=0 bslip on
 5 text int 3 kn 5.53e7 ks 5.53e7 friction = 31 coh = 0 tbond=0 bslip on
 5 text gen line 0 7.38 50 7.38
 5 text gen line 0 7.532 50 7.532
 5 text gen line 0 8.142 50 8.142
 5 text prop density=18.0 bulk=1.134E6 shear=1.224E6 cohesion=25.0E3 friction=31.0 reg i 1 j
18 ;geofoam
 5 text prop density=18.0 bulk=1.134E6 shear=1.224E6 cohesion=25.0E3 friction=31.0 reg i 10 j
18 ;geofoam
 5 text prop density=2160.5 bulk=111.111E6 shear=37.037E6 cohesion=0.0 friction=35.0 reg i
22 j 18 ;backfill
 5 text prop density=2400.5 bulk=15625E6 shear=12711.9E6 cohesion=25.0E6 friction=25.0 reg
i 2 j 26 ;lds
 5 text prop density=2400.5 bulk=15625E6 shear=12711.9E6 cohesion=25.0E6 friction=25.0 reg
i 10 j 26 ;lds
 5 text ;prop density=2400.5 bulk=15625E6 shear=12711.9E6 cohesion=25.0E6 friction=25.0
reg i 22 j 26 ;lds
 5 text prop density=2240.5 bulk=111.111E6 shear=37.037E6 cohesion=0.0 friction=35.0 reg i
22 j 26 ;utbc not lds
```

```
 5 text prop density=2240.5 bulk=111.111E6 shear=37.037E6 cohesion=0.0 friction=35.0 reg i 2
j 27 ;utbc
 5 text prop density=2240.5 bulk=111.111E6 shear=37.037E6 cohesion=0.0 friction=35.0 reg i
10 j 27 ;utbc
 5 text prop density=2240.5 bulk=111.111E6 shear=37.037E6 cohesion=0.0 friction=35.0 reg i
22 j 27 ;utbc
 5 text prop density=2400.5 bulk=15625E6 shear=12711.9E6 cohesion=25.0E6 friction=25.0 reg
i 2 j 29 ;pccp
 5 text prop density=2400.5 bulk=15625E6 shear=12711.9E6 cohesion=25.0E6 friction=25.0 reg
i 10 j 29 ;pccp
 5 text prop density=2400.5 bulk=15625E6 shear=12711.9E6 cohesion=25.0E6 friction=25.0 reg
i 22 j 29 ;pccp
 5 text prop density=2160.5 bulk=111.111E6 shear=37.037E6 cohesion=0.0 friction=35.0 reg i 2
j 2 ;bottom
 5 text prop density=2160.5 bulk=111.111E6 shear=37.037E6 cohesion=0.0 friction=35.0 reg i
10 j 2 ;bottom
 5 text prop density=2160.5 bulk=111.111E6 shear=37.037E6 cohesion=0.0 friction=35.0 reg i
22 j 2 ;bottom
 5 text set grav=9.81
 5 text fix y j=1
 5 text fix x i=1
 5 text fix x i =56
 5 text his ydis i = 5 j = 15; level 0-
 5 text his ydis i = 5 j = 16; level 0
 5 text his ydis i = 5 j = 18; level 1.5
 5 text his ydis i = 5 j = 20; level 3.5
 5 text his ydis i = 5 j = 22; level 5.5
 5 text his ydis i = 5 j = 24; level 7.5
 5 text his ydis i = 5 j = 25; level 8.5
 5 text his ydis i = 5 j = 26; level 9
 5 text his syy i = 3 j = 16; 55540
 5 text his syy i = 6 j = 16; 55541
 5 text his unbal
 5 text model null i 1 4 j 16 25
 5 text model null i 6 11 j 16 25
 5 text model null i 13 55 j 16 25
 5 text model null i 1 4 j 26
 5 text model null i 6 11 j 26
 5 text model null i 13 55 j 26
 5 text model null i 1 4 j 27 28
 5 text model null i 6 11  j 27 28
 5 text model null i 13 55 j 27 28
 5 text model null i 1 4 j 29
 5 text model null i 6 11  j 29
 5 text model null i 13 55 j 29
 5 text set large
```

```
 5 text step 2000
 5 text model mohr i 1 4 j 16 25
 5 text model mohr i 6 11 j 16 25
 5 text model mohr i 13 55 j 16 25
 5 text prop density=18.0 bulk=1.134E6 shear=1.224E6 cohesion=25.0E3 friction=31.0 reg i 2 j
18 ;geofoam
 5 text prop density=18.0 bulk=1.134E6 shear=1.224E6 cohesion=25.0E3 friction=31.0 reg i 10 j
18 ;geofoam
 5 text prop density=2160.5 bulk=111.111E6 shear=37.037E6 cohesion=0.0 friction=35.0 reg i
22 j 18 ;backfill
 5 text int 1 Aside from 1,15 to 5,15 Bside from 1,16 to 5,16
 5 text int 2 Aside from 10,15 to 12,15 Bside from 6,16 to 12,16
 5 text int 3 Aside from 12,16 to 12,26 Bside from 13,16 to 13,26
 5 text int 1 kn 5.53e7 ks 5.53e7 friction = 31 coh = 0 tbond=0 bslip on
 5 text int 2 kn 3.95e7 ks 3.95e7 friction = 31 coh = 0 tbond=0 bslip on
 5 text int 3 kn 5.53e7 ks 5.53e7 friction = 31 coh = 0 tbond=0 bslip on
 5 text set large
 5 text def modulus
 5 text  loop n (1,numstep)
 5 text  if syy(3,16) > -15e3 then
 5 text   command
 5 text prop density=18.0 bulk=1.134E6 shear=1.224E6 cohesion=25.0E3 friction=31.0 reg i 2 j
18 ;geofoam
 5 text prop density=18.0 bulk=1.134E6 shear=1.224E6 cohesion=25.0E3 friction=31.0 reg i 10 j
18 ;geofoam
 5 text   int 1 kn 5.53e7 ks 5.53e7 friction = 31 coh = 0 tbond=0 bslip on
 5 text   int 2 kn 3.95e7 ks 3.95e7 friction = 31 coh = 0 tbond=0 bslip on
 5 text   int 3 kn 5.53e7 ks 5.53e7 friction = 31 coh = 0 tbond=0 bslip on
 5 text   step 25
 5 text   endcommand
 5 text  else
 5 text   command
 5 text   prop density=18.0 bulk=4.198E6 shear=4.533E6 cohesion=25.0E3 friction=31.0 reg i 2 j
18
 5 text   prop density=18.0 bulk=4.198E6 shear=4.533E6 cohesion=25.0E3 friction=31.0 reg i 10
j 18
 5 text   int 1 kn 2.05e8 ks 2.05e8 friction = 31 coh = 0 tbond=0 bslip on
 5 text   int 2 kn 1.46e8 ks 1.46e8 friction = 31 coh = 0 tbond=0 bslip on
 5 text   int 3 kn 2.05e8 ks 2.05e8 friction = 31 coh = 0 tbond=0 bslip on
 5 text   step 25
 5 text   endcommand
 5 text  endif
 5 text endloop
 5 text end
 5 text set numstep=160
 5 text modulus
```

```
 5 text model mohr i 1 4 j 26
 5 text model mohr i 6 11  j 26
 5 text model mohr i 13 55 j 26
 5 text prop density=2400.5 bulk=15625E6 shear=12711.9E6 cohesion=25.0E6 friction=25.0 reg
i 2 j 26 ;lds
 5 text prop density=2400.5 bulk=15625E6 shear=12711.9E6 cohesion=25.0E6 friction=25.0 reg
i 10 j 26 ;lds
 5 text ;prop density=2400.5 bulk=15625E6 shear=12711.9E6 cohesion=25.0E6 friction=25.0
reg i 22 j 26 ;lds
 5 text prop density=2240.5 bulk=111.111E6 shear=37.037E6 cohesion=0.0 friction=35.0 reg i
22 j 26 ;utbc not lds
 5 text set numstep=160
 5 text modulus
 5 text model mohr i 1 4 j 27 28
 5 text model mohr i 6 11  j 27 28
 5 text model mohr i 13 55 j 27 28
 5 text prop density=2240.5 bulk=111.111E6 shear=37.037E6 cohesion=0.0 friction=35.0 reg i 2
j 27 ;utbc
 5 text prop density=2240.5 bulk=111.111E6 shear=37.037E6 cohesion=0.0 friction=35.0 reg i
10 j 27 ;utbc
 5 text prop density=2240.5 bulk=111.111E6 shear=37.037E6 cohesion=0.0 friction=35.0 reg i
22 j 27 ;utbc
 5 text set numstep=160
 5 text modulus
 5 text model mohr i 1 4 j 29
 5 text model mohr i 6 11  j 29
 5 text model mohr i 13 55 j 29
 5 text prop density=2400.5 bulk=15625E6 shear=12711.9E6 cohesion=25.0E6 friction=25.0 reg
i 2 j 29 ;pccp
 5 text prop density=2400.5 bulk=15625E6 shear=12711.9E6 cohesion=25.0E6 friction=25.0 reg
i 10 j 29 ;pccp
 5 text prop density=2400.5 bulk=15625E6 shear=12711.9E6 cohesion=25.0E6 friction=25.0 reg
i 22 j 29 ;pccp
 5 text set numstep=250
 5 text modulus
 2 branch branch B
 3 state
 4 file 100southb.sav
 4 batch
 5 text ;E=2.3-10
 5 text config
 5 text grid 55,29
 5 text m m i 1 4 j 1 14;mohr-coulomb model
 5 text m m i 1 4 j 16 29
 5 text m m i 10 11 j 1 14
 5 text m m i 6 11 j 16 29
```

```
5 text m m i 13 55 j 1 14
5 text m m i 13 55 j 16 29
5 text gen 0 -12 0 0 1.473 0 1.473 -12 i 1 3 j 1 15
5 text gen 0 0 0 .41 1.473 .41 1.473 0 i 1 3 j 16 17
5 text gen same 0 6.97 1.473 6.97 same i 1 3 j 17 25
5 text gen same 0 7.38 1.473 7.38 same i 1 3 j 25 26
5 text gen same 0 7.532 1.473 7.532 same i 1 3 j 26 27
5 text gen same 0 8.142 1.473 8.142 same i 1 3 j 27 29
5 text gen same 0 8.498 1.473 8.498 same i 1 3 j 29 30
5 text ;
5 text gen same same 2.692 0 2.692 -12 i 3 5 j 1 15
5 text gen same same 2.692 .41 2.692 0 i 3 5 j 16 17
5 text gen same same 2.692 6.97 same i 3 5 j 17 25
5 text gen same same 2.692 7.38 same i 3 5 j 25 26
5 text gen same same 2.692 7.532 same i 3 5 j 26 27
5 text gen same same 2.692 8.142 same i 3 5 j 27 29
5 text gen same same 2.692 8.498 same i 3 5 j 29 30
5 text ;
5 text gen 2.692 -12 2.692 0 3.792 0 3.792 -12 i 10 12 j 1 15
5 text gen 2.692 0 2.692 .41 4.284 .41 3.792 0 i 6 12 j 16 17
5 text gen same 2.692 6.97 12.148 6.97 same i 6 12 j 17 25
5 text gen same 2.692 7.38 12.64 7.38 same i 6 12 j 25 26
5 text gen same 2.692 7.532 12.64 7.532 same i 6 12 j 26 27
5 text gen same 2.692 8.142 12.64 8.142 same i 6 12 j 27 29
5 text gen same 2.692 8.498 12.64 8.498 same i 6 12 j 29 30
5 text ;
5 text gen 3.792 -12 3.792 0 45 0 45 -12  i 13 56 j 1 15
5 text gen 3.792 0 4.284 .41 45 .41 45 0 i 13 56 j 16 17
5 text gen same 12.148 6.97 45 6.97 same i 13 56 j 17 25
5 text gen same 12.64 7.38 45 7.38 same i 13 56 j 25 26
5 text gen same 12.64 7.532 45 7.532 same i 13 56 j 26 27
5 text gen same 12.64 8.142 45 8.142 same i 13 56 j 27 29
5 text gen same 12.64 8.498 45 8.498 same i 13 56 j 29 30
5 text ;
5 text int 1 Aside from 1,15 to 5,15 Bside from 1,16 to 5,16
5 text int 2 Aside from 10,15 to 12,15 Bside from 6,16 to 12,16
5 text attach Aside from 5,1 to 5,15 Bside from 10,1 to 10,15
5 text attach Aside from 5,16 to 5,30 Bside from 6,16 to 6,30
5 text attach Aside from 12,1 to 12,15 Bside from 13,1 to 13,15
5 text int 3 Aside from 12,16 to 12,26 Bside from 13,16 to 13,26
5 text attach Aside from 12,26 to 12,30 Bside from 13,26 to 13,30
5 text attach Aside from 13,15 to 56,15 Bside from 13,16 to 56,16
5 text int 1 kn 4.65e7 ks 4.65e7 friction = 31 coh = 0 tbond=0 bslip on
5 text int 2 kn 3.32e7 ks 3.32e7 friction = 31 coh = 0 tbond=0 bslip on
5 text int 3 kn 4.65e7 ks 4.65e7 friction = 31 coh = 0 tbond=0 bslip on
5 text gen line 0 7.38 50 7.38
```

```
 5 text gen line 0 7.532 50 7.532
 5 text gen line 0 8.142 50 8.142
 5 text prop density=18.0 bulk=.953E6 shear=1.029E6 cohesion=25.0E3  friction=31.0 reg i 1 j
18 ;geofoam
 5 text prop density=18.0 bulk=.953E6 shear=1.029E6 cohesion=25.0E3  friction=31.0 reg i 10 j
18 ;geofoam
 5 text prop density=2160.5 bulk=111.11E6 shear=37.037E6 cohesion=0.0 friction=35.0 reg i 22
j 18 ;backfill
 5 text prop density=2400.5 bulk=15625E6 shear=12711.9E6 cohesion=25.0E6 friction=25.0 reg
i 2 j 26 ;lds
 5 text prop density=2400.5 bulk=15625E6 shear=12711.9E6 cohesion=25.0E6 friction=25.0 reg
i 10 j 26 ;lds
 5 text ;prop density=2400.5 bulk=15625E6 shear=12711.9E6 cohesion=25.0E6 friction=25.0
reg i 22 j 26 ;lds
 5 text prop density=2240.5 bulk=111.11E6 shear=37.037E6 cohesion=0.0 friction=35.0 reg i 22
j 26 ;utbc not lds
 5 text prop density=2240.5 bulk=111.11E6 shear=37.037E6 cohesion=0.0 friction=35.0 reg i 2 j
27 ;utbc
 5 text prop density=2240.5 bulk=111.11E6 shear=37.037E6 cohesion=0.0 friction=35.0 reg i 10
j 27 ;utbc
 5 text prop density=2240.5 bulk=111.11E6 shear=37.037E6 cohesion=0.0 friction=35.0 reg i 22
j 27 ;utbc
 5 text prop density=2400.5 bulk=15625E6 shear=12711.9E6 cohesion=25.0E6 friction=25.0 reg
i 2 j 29 ;pccp
 5 text prop density=2400.5 bulk=15625E6 shear=12711.9E6 cohesion=25.0E6 friction=25.0 reg
i 10 j 29 ;pccp
 5 text prop density=2400.5 bulk=15625E6 shear=12711.9E6 cohesion=25.0E6 friction=25.0 reg
i 22 j 29 ;pccp
 5 text prop density=2160.5 bulk=111.11E6 shear=37.037E6 cohesion=0.0 friction=35.0 reg i 2 j
2 ;bottom
 5 text prop density=2160.5 bulk=111.11E6 shear=37.037E6 cohesion=0.0 friction=35.0 reg i 10
j 2 ;bottom
 5 text prop density=2160.5 bulk=111.11E6 shear=37.037E6 cohesion=0.0 friction=35.0 reg i 22
j 2 ;bottom
 5 text set grav=9.81
 5 text fix y j=1
 5 text fix x i=1
 5 text fix x i =56
 5 text his ydis i = 5 j = 15; level 0-
 5 text his ydis i = 5 j = 16; level 0
 5 text his ydis i = 5 j = 18; level 1.5
 5 text his ydis i = 5 j = 20; level 3.5
 5 text his ydis i = 5 j = 22; level 5.5
 5 text his ydis i = 5 j = 24; level 7.5
 5 text his ydis i = 5 j = 25; level 8.5
 5 text his ydis i = 5 j = 26; level 9
```

```
 5 text his syy i = 3 j = 16; 55540
 5 text his syy i = 6 j = 16; 55541
 5 text his unbal
 5 text model null i 1 4 j 16 25
 5 text model null i 6 11 j 16 25
 5 text model null i 13 55 j 16 25
 5 text model null i 1 4 j 26
 5 text model null i 6 11 j 26
 5 text model null i 13 55 j 26
 5 text model null i 1 4 j 27 28
 5 text model null i 6 11  j 27 28
 5 text model null i 13 55 j 27 28
 5 text model null i 1 4 j 29
 5 text model null i 6 11  j 29
 5 text model null i 13 55 j 29
 5 text set large
 5 text step 2000
 5 text model mohr i 1 4 j 16 25
 5 text model mohr i 6 11 j 16 25
 5 text model mohr i 13 55 j 16 25
 5 text prop density=18.0 bulk=.953E6 shear=1.029E6 cohesion=25.0E3  friction=31.0 reg i 2 j
18 ;geofoam
 5 text prop density=18.0 bulk=.953E6 shear=1.029E6 cohesion=25.0E3  friction=31.0 reg i 10 j
18 ;geofoam
 5 text prop density=2160.5 bulk=111.111E6 shear=37.037E6 cohesion=0.0 friction=35.0 reg i
22 j 18 ;backfill
 5 text int 1 Aside from 1,15 to 5,15 Bside from 1,16 to 5,16
 5 text int 2 Aside from 10,15 to 12,15 Bside from 6,16 to 12,16
 5 text int 3 Aside from 12,16 to 12,26 Bside from 13,16 to 13,26
 5 text int 1 kn 4.65e7 ks 4.65e7 friction = 31 coh = 0 tbond=0 bslip on
 5 text int 2 kn 3.32e7 ks 3.32e7 friction = 31 coh = 0 tbond=0 bslip on
 5 text int 3 kn 4.65e7 ks 4.65e7 friction = 31 coh = 0 tbond=0 bslip on
 5 text set large
 5 text def modulus
 5 text  loop n (1,numstep)
 5 text  if syy(3,16) > -15e3 then
 5 text   command
 5 text   prop density=18.0 bulk=.953E6 shear=1.029E6 cohesion=25.0E3  friction=31.0 reg i 2 j
18 ;geofoam
 5 text   prop density=18.0 bulk=.953E6 shear=1.029E6 cohesion=25.0E3  friction=31.0 reg i 10
j 18 ;geofoam
 5 text   int 1 kn 4.65e7 ks 4.65e7 friction = 31 coh = 0 tbond=0 bslip on
 5 text   int 2 kn 3.32e7 ks 3.32e7 friction = 31 coh = 0 tbond=0 bslip on
 5 text   int 3 kn 4.65e7 ks 4.65e7 friction = 31 coh = 0 tbond=0 bslip on
 5 text   step 25
 5 text   endcommand
```

```
 5 text  else
 5 text   command
 5 text   prop density=18.0 bulk=4.198E6 shear=4.533E6 cohesion=25.0E3 friction=31.0 reg i 2 j
18
 5 text   prop density=18.0 bulk=4.198E6 shear=4.533E6 cohesion=25.0E3 friction=31.0 reg i 10
j 18
 5 text   int 1 kn 2.05e8 ks 2.05e8 friction = 31 coh = 0 tbond=0 bslip on
 5 text   int 2 kn 1.46e8 ks 1.46e8 friction = 31 coh = 0 tbond=0 bslip on
 5 text   int 3 kn 2.05e8 ks 2.05e8 friction = 31 coh = 0 tbond=0 bslip on
 5 text   step 25
 5 text   endcommand
 5 text  endif
 5 text endloop
 5 text end
 5 text set numstep=160
 5 text modulus
 5 text model mohr i 1 4 j 26
 5 text model mohr i 6 11  j 26
 5 text model mohr i 13 55 j 26
 5 text prop density=2400.5 bulk=15625E6 shear=12711.9E6 cohesion=25.0E6 friction=25.0 reg
i 2 j 26 ;lds
 5 text prop density=2400.5 bulk=15625E6 shear=12711.9E6 cohesion=25.0E6 friction=25.0 reg
i 10 j 26 ;lds
 5 text ;prop density=2400.5 bulk=15625E6 shear=12711.9E6 cohesion=25.0E6 friction=25.0
reg i 22 j 26 ;lds
 5 text prop density=2240.5 bulk=111.11E6 shear=37.037E6 cohesion=0.0 friction=35.0 reg i 22
j 26 ;utbc not lds
 5 text set numstep=160
 5 text modulus
 5 text model mohr i 1 4 j 27 28
 5 text model mohr i 6 11  j 27 28
 5 text model mohr i 13 55 j 27 28
 5 text prop density=2240.5 bulk=111.11E6 shear=37.037E6 cohesion=0.0 friction=35.0 reg i 2 j
27 ;utbc
 5 text prop density=2240.5 bulk=111.11E6 shear=37.037E6 cohesion=0.0 friction=35.0 reg i 10
j 27 ;utbc
 5 text prop density=2240.5 bulk=111.11E6 shear=37.037E6 cohesion=0.0 friction=35.0 reg i 22
j 27 ;utbc
 5 text set numstep=160
 5 text modulus
 5 text model mohr i 1 4 j 29
 5 text model mohr i 6 11  j 29
 5 text model mohr i 13 55 j 29
 5 text prop density=2400.5 bulk=15625E6 shear=12711.9E6 cohesion=25.0E6 friction=25.0 reg
i 2 j 29 ;pccp
```

```
 5 text prop density=2400.5 bulk=15625E6 shear=12711.9E6 cohesion=25.0E6 friction=25.0 reg
i 10 j 29 ;pccp
 5 text prop density=2400.5 bulk=15625E6 shear=12711.9E6 cohesion=25.0E6 friction=25.0 reg
i 22 j 29 ;pccp
 5 text set numstep=250
 5 text modulus
 2 branch branch C
 3 state
 4 file 100southc.sav
 4 batch
 5 text ;E=1.7-10
 5 text config
 5 text grid 55,29
 5 text m m i 1 4 j 1 14;mohr-coulomb model
 5 text m m i 1 4 j 16 29
 5 text m m i 10 11 j 1 14
 5 text m m i 6 11 j 16 29
 5 text m m i 13 55 j 1 14
 5 text m m i 13 55 j 16 29
 5 text gen 0 -12 0 0 1.473 0 1.473 -12 i 1 3 j 1 15
 5 text gen 0 0 0 .41 1.473 .41 1.473 0 i 1 3 j 16 17
 5 text gen same 0 6.97 1.473 6.97 same i 1 3 j 17 25
 5 text gen same 0 7.38 1.473 7.38 same i 1 3 j 25 26
 5 text gen same 0 7.532 1.473 7.532 same i 1 3 j 26 27
 5 text gen same 0 8.142 1.473 8.142 same i 1 3 j 27 29
 5 text gen same 0 8.498 1.473 8.498 same i 1 3 j 29 30
 5 text ;
 5 text gen same same 2.692 0 2.692 -12 i 3 5 j 1 15
 5 text gen same same 2.692 .41 2.692 0 i 3 5 j 16 17
 5 text gen same same 2.692 6.97 same i 3 5 j 17 25
 5 text gen same same 2.692 7.38 same i 3 5 j 25 26
 5 text gen same same 2.692 7.532 same i 3 5 j 26 27
 5 text gen same same 2.692 8.142 same i 3 5 j 27 29
 5 text gen same same 2.692 8.498 same i 3 5 j 29 30
 5 text ;
 5 text gen 2.692 -12 2.692 0 3.792 0 3.792 -12 i 10 12 j 1 15
 5 text gen 2.692 0 2.692 .41 4.284 .41 3.792 0 i 6 12 j 16 17
 5 text gen same 2.692 6.97 12.148 6.97 same i 6 12 j 17 25
 5 text gen same 2.692 7.38 12.64 7.38 same i 6 12 j 25 26
 5 text gen same 2.692 7.532 12.64 7.532 same i 6 12 j 26 27
 5 text gen same 2.692 8.142 12.64 8.142 same i 6 12 j 27 29
 5 text gen same 2.692 8.498 12.64 8.498 same i 6 12 j 29 30
 5 text ;
 5 text gen 3.792 -12 3.792 0 45 0 45 -12  i 13 56 j 1 15
 5 text gen 3.792 0 4.284 .41 45 .41 45 0 i 13 56 j 16 17
 5 text gen same 12.148 6.97 45 6.97 same i 13 56 j 17 25
```

```
 5 text gen same 12.64 7.38 45 7.38 same i 13 56 j 25 26
 5 text gen same 12.64 7.532 45 7.532 same i 13 56 j 26 27
 5 text gen same 12.64 8.142 45 8.142 same i 13 56 j 27 29
 5 text gen same 12.64 8.498 45 8.498 same i 13 56 j 29 30
 5 text ;
 5 text int 1 Aside from 1,15 to 5,15 Bside from 1,16 to 5,16
 5 text int 2 Aside from 10,15 to 12,15 Bside from 6,16 to 12,16
 5 text attach Aside from 5,1 to 5,15 Bside from 10,1 to 10,15
 5 text attach Aside from 5,16 to 5,30 Bside from 6,16 to 6,30
 5 text attach Aside from 12,1 to 12,15 Bside from 13,1 to 13,15
 5 text int 3 Aside from 12,16 to 12,26 Bside from 13,16 to 13,26
 5 text attach Aside from 12,26 to 12,30 Bside from 13,26 to 13,30
 5 text attach Aside from 13,15 to 56,15 Bside from 13,16 to 56,16
 5 text int 1 kn 3.48e7 ks 3.48e7 friction = 31 coh = 0 tbond=0 bslip on
 5 text int 2 kn 2.49e7 ks 2.49e7 friction = 31 coh = 0 tbond=0 bslip on
 5 text int 3 kn 3.48e7 ks 3.48e7 friction = 31 coh = 0 tbond=0 bslip on
 5 text gen line 0 7.38 50 7.38
 5 text gen line 0 7.532 50 7.532
 5 text gen line 0 8.142 50 8.142
 5 text prop density=18.0 bulk=.714E6 shear=.771E6 cohesion=25.0E3  friction=31.0 reg i 1 j 18
;geofoam
 5 text prop density=18.0 bulk=.714E6 shear=.771E6 cohesion=25.0E3  friction=31.0 reg i 10 j
18 ;geofoam
 5 text prop density=2160.5 bulk=111.11E6 shear=37.037E6 cohesion=0.0 friction=35.0 reg i 22
j 18 ;backfill
 5 text prop density=2400.5 bulk=15625E6 shear=12711.9E6 cohesion=25.0E6 friction=25.0 reg
i 2 j 26 ;lds
 5 text prop density=2400.5 bulk=15625E6 shear=12711.9E6 cohesion=25.0E6 friction=25.0 reg
i 10 j 26 ;lds
 5 text ;prop density=2400.5 bulk=15625E6 shear=12711.9E6 cohesion=25.0E6 friction=25.0
reg i 22 j 26 ;lds
 5 text prop density=2240.5 bulk=111.11E6 shear=37.037E6 cohesion=0.0 friction=35.0 reg i 22
j 26 ;utbc not lds
 5 text prop density=2240.5 bulk=111.11E6 shear=37.037E6 cohesion=0.0 friction=35.0 reg i 2 j
27 ;utbc
 5 text prop density=2240.5 bulk=111.11E6 shear=37.037E6 cohesion=0.0 friction=35.0 reg i 10
j 27 ;utbc
 5 text prop density=2240.5 bulk=111.11E6 shear=37.037E6 cohesion=0.0 friction=35.0 reg i 22
j 27 ;utbc
 5 text prop density=2400.5 bulk=15625E6 shear=12711.9E6 cohesion=25.0E6 friction=25.0 reg
i 2 j 29 ;pccp
 5 text prop density=2400.5 bulk=15625E6 shear=12711.9E6 cohesion=25.0E6 friction=25.0 reg
i 10 j 29 ;pccp
 5 text prop density=2400.5 bulk=15625E6 shear=12711.9E6 cohesion=25.0E6 friction=25.0 reg
i 22 j 29 ;pccp
```

```
 5 text prop density=2160.5 bulk=111.11E6 shear=37.037E6 cohesion=0.0 friction=35.0 reg i 2 j
2 ;bottom
 5 text prop density=2160.5 bulk=111.11E6 shear=37.037E6 cohesion=0.0 friction=35.0 reg i 10
j 2 ;bottom
 5 text prop density=2160.5 bulk=111.11E6 shear=37.037E6 cohesion=0.0 friction=35.0 reg i 22
j 2 ;bottom
 5 text set grav=9.81
 5 text fix y j=1
 5 text fix x i=1
 5 text fix x i =56
 5 text his ydis i = 5 j = 15; level 0-
 5 text his ydis i = 5 j = 16; level 0
 5 text his ydis i = 5 j = 18; level 1.5
 5 text his ydis i = 5 j = 20; level 3.5
 5 text his ydis i = 5 j = 22; level 5.5
 5 text his ydis i = 5 j = 24; level 7.5
 5 text his ydis i = 5 j = 25; level 8.5
 5 text his ydis i = 5 j = 26; level 9
 5 text his syy i = 3 j = 16; 55540
 5 text his syy i = 6 j = 16; 55541
 5 text his unbal
 5 text model null i 1 4 j 16 25
 5 text model null i 6 11 j 16 25
 5 text model null i 13 55 j 16 25
 5 text model null i 1 4 j 26
 5 text model null i 6 11 j 26
 5 text model null i 13 55 j 26
 5 text model null i 1 4 j 27 28
 5 text model null i 6 11  j 27 28
 5 text model null i 13 55 j 27 28
 5 text model null i 1 4 j 29
 5 text model null i 6 11  j 29
 5 text model null i 13 55 j 29
 5 text set large
 5 text step 2000
 5 text model mohr i 1 4 j 16 25
 5 text model mohr i 6 11 j 16 25
 5 text model mohr i 13 55 j 16 25
 5 text prop density=18.0 bulk=.714E6 shear=.771E6 cohesion=25.0E3  friction=31.0 reg i 2 j 18
;geofoam
 5 text prop density=18.0 bulk=.714E6 shear=.771E6 cohesion=25.0E3  friction=31.0 reg i 10 j
18 ;geofoam
 5 text prop density=2160.5 bulk=111.11E6 shear=37.037E6 cohesion=0.0 friction=35.0 reg i 22
j 18 ;backfill
 5 text int 1 Aside from 1,15 to 5,15 Bside from 1,16 to 5,16
 5 text int 2 Aside from 10,15 to 12,15 Bside from 6,16 to 12,16
```

```
 5 text int 3 Aside from 12,16 to 12,26 Bside from 13,16 to 13,26
 5 text int 1 kn 3.48e7 ks 3.48e7 friction = 31 coh = 0 tbond=0 bslip on
 5 text int 2 kn 2.49e7 ks 2.49e7 friction = 31 coh = 0 tbond=0 bslip on
 5 text int 3 kn 3.48e7 ks 3.48e7 friction = 31 coh = 0 tbond=0 bslip on
 5 text set large
 5 text def modulus
 5 text  loop n (1,numstep)
 5 text  if syy(3,16) > -15e3 then
 5 text   command
 5 text   prop density=18.0 bulk=.714E6 shear=.771E6 cohesion=25.0E3  friction=31.0 reg i 2 j
18 ;geofoam
 5 text   prop density=18.0 bulk=.714E6 shear=.771E6 cohesion=25.0E3  friction=31.0 reg i 10 j
18 ;geofoam
 5 text   int 1 kn 3.48e7 ks 3.48e7 friction = 31 coh = 0 tbond=0 bslip on
 5 text   int 2 kn 2.49e7 ks 2.49e7 friction = 31 coh = 0 tbond=0 bslip on
 5 text   int 3 kn 3.48e7 ks 3.48e7 friction = 31 coh = 0 tbond=0 bslip on
 5 text   step 25
 5 text   endcommand
 5 text  else
 5 text   command
 5 text   prop density=18.0 bulk=4.198E6 shear=4.533E6 cohesion=25.0E3 friction=31.0 reg i 2 j
18
 5 text   prop density=18.0 bulk=4.198E6 shear=4.533E6 cohesion=25.0E3 friction=31.0 reg i 10
j 18
 5 text   int 1 kn 2.05e8 ks 2.05e8 friction = 31 coh = 0 tbond=0 bslip on
 5 text   int 2 kn 1.46e8 ks 1.46e8 friction = 31 coh = 0 tbond=0 bslip on
 5 text   int 3 kn 2.05e8 ks 2.05e8 friction = 31 coh = 0 tbond=0 bslip on
 5 text   step 25
 5 text   endcommand
 5 text  endif
 5 text endloop
 5 text end
 5 text set numstep=160
 5 text modulus
 5 text model mohr i 1 4 j 26
 5 text model mohr i 6 11  j 26
 5 text model mohr i 13 55 j 26
 5 text prop density=2400.5 bulk=15625E6 shear=12711.9E6 cohesion=25.0E6 friction=25.0 reg
i 2 j 26 ;lds
 5 text prop density=2400.5 bulk=15625E6 shear=12711.9E6 cohesion=25.0E6 friction=25.0 reg
i 10 j 26 ;lds
 5 text ;prop density=2400.5 bulk=15625E6 shear=12711.9E6 cohesion=25.0E6 friction=25.0
reg i 22 j 26 ;lds
 5 text prop density=2240.5 bulk=111.11E6 shear=37.037E6 cohesion=0.0 friction=35.0 reg i 22
j 26 ;utbc not lds
 5 text set numstep=160
```

```
 5 text modulus
 5 text model mohr i 1 4 j 27 28
 5 text model mohr i 6 11  j 27 28
 5 text model mohr i 13 55 j 27 28
 5 text prop density=2240.5 bulk=111.11E6 shear=37.037E6 cohesion=0.0 friction=35.0 reg i 2 j
27 ;utbc
 5 text prop density=2240.5 bulk=111.11E6 shear=37.037E6 cohesion=0.0 friction=35.0 reg i 10
j 27 ;utbc
 5 text prop density=2240.5 bulk=111.11E6 shear=37.037E6 cohesion=0.0 friction=35.0 reg i 22
j 27 ;utbc
 5 text set numstep=160
 5 text modulus
 5 text model mohr i 1 4 j 29
 5 text model mohr i 6 11  j 29
 5 text model mohr i 13 55 j 29
 5 text prop density=2400.5 bulk=15625E6 shear=12711.9E6 cohesion=25.0E6 friction=25.0 reg
i 2 j 29 ;pccp
 5 text prop density=2400.5 bulk=15625E6 shear=12711.9E6 cohesion=25.0E6 friction=25.0 reg
i 10 j 29 ;pccp
 5 text prop density=2400.5 bulk=15625E6 shear=12711.9E6 cohesion=25.0E6 friction=25.0 reg
i 22 j 29 ;pccp
 5 text set numstep=250
 5 text modulus
 0 eof
```

APPENDIX 6 – FLAC Dynamic Model

```
; sliding evalution
0 header
1 code FLAC 5.0
1 source giic v2.0.393
1 date Mon Mar 31 14:17:38 MST 2008
1 type giic-save
0 flac
1 config
2 axisym false
2 gwflow false
2 pstress false
2 cppudm false
2 ats false
2 creep false
2 dynamic true
2 thermal false
2 twophase false
2 extra 5
2 units 0
2 struct false
2 advanced false
2 water false
2 interface false
2 gravity true
2 excludereg false
2 solvefos false
2 record 2
0 plots
1 plot 2
2 display
3 viewport
4 autorange true
2 command plot pen history 20
2 name unbal
2 alias
2 title
2 count 1
2 item
3 name 20
1 plot 0
2 display
3 viewport
4 center 30.366581,9.300506
4 radius 18.56324
4 orientation 0.0
```

2 command plot pen apply xdisp fill displacement
2 name vectors
2 title
2 count 3
2 item
3 name apply
3 switch 3
2 item
3 name xdisp
3 switch 5
3 mode 1
2 item
3 name displacement
3 switch 3
1 plot 2
2 display
3 viewport
4 autorange true
2 command plot pen history 2 vs 1
2 name h wave
2 alias
2 title
2 versus 1
2 count 1
2 item
3 name 2
1 plot 2
2 display
3 viewport
4 autorange true
2 command plot pen history 4 line vs 1
2 name x disp bot
2 alias
2 title
2 versus 1
2 count 1
2 item
3 name 4
3 line
1 plot 2
2 display
3 viewport
4 autorange true
2 command plot pen history 6 line vs 1
2 name x disp geofoam bot
2 alias

2 title
2 versus 1
2 count 1
2 item
3 name 6
3 line
1 plot 2
2 display
3 viewport
4 autorange true
2 command plot pen history 8 line vs 1
2 name x disp geofoam top
2 alias
2 versus 1
2 count 1
2 item
3 name 8
3 line
1 plot 2
2 display
3 viewport
4 autorange true
2 command plot pen history 16 vs 1
2 name x acc ff
2 alias
2 versus 1
2 count 1
2 item
3 name 16
1 plot 2
2 display
3 viewport
4 autorange true
2 command plot pen history 10 line 11 vs 1
2 name x acc geofoam top
2 alias
2 versus 1
2 count 2
2 item
3 name 10
3 line
2 item
3 name 11
1 plot 2
2 display
3 viewport

4 autorange true
2 command plot pen history 11 line vs 1
2 name x acc geofoam base
2 alias
2 versus 1
2 count 1
2 item
3 name 11
3 line
1 plot 2
2 display
3 viewport
4 autorange true
2 command plot pen history 15 line vs 1
2 name v wave
2 alias
2 versus 1
2 count 1
2 item
3 name 15
3 line
1 plot 2
2 display
3 viewport
4 autorange true
2 command plot pen history 12 line vs 1
2 name y acc base
2 alias
2 versus 1
2 count 1
2 item
3 name 12
3 line
1 plot 2
2 display
3 viewport
4 autorange true
2 command plot pen history 13 line vs 1
2 name y acc geofoam top
2 alias
2 versus 1
2 count 1
2 item
3 name 13
3 line
1 plot 2

2 display
3 viewport
4 autorange true
2 command plot pen history 14 line vs 1
2 name y acc geofoam base
2 alias
2 versus 1
2 count 1
2 item
3 name 14
3 line
1 plot 2
2 display
3 viewport
4 autorange true
2 command plot pen history 11 line 14 line vs 1
2 name x & y accel geofoam base
2 alias
2 versus 1
2 count 2
2 item
3 name 11
3 line
2 item
3 name 14
3 line
1 plot 2
2 display
3 viewport
4 autorange true
2 command plot pen history 160 line 170 line 180 line 190 line 200 line 210 line 220 line 230 line 240 line vs 1
2 name reldisp1
2 alias
2 versus 1
2 count 9
2 item
3 name 160
3 line
2 item
3 name 170
3 line
2 item
3 name 180
3 line
2 item

3 name 190
3 line
2 item
3 name 200
3 line
2 item
3 name 210
3 line
2 item
3 name 220
3 line
2 item
3 name 230
3 line
2 item
3 name 240
3 line
1 plot 2
2 display
3 viewport
4 autorange true
2 command plot pen history 17 line vs 1
2 name y acc ff
2 alias
2 versus 1
2 count 1
2 item
3 name 17
3 line
0 matlist
0 CppModels
0 project tree
1 title Capitola_000 Record
1 notes
1 tree
2 state
3 file static1up
3 batch
4 text ;8 m high by 20 m wide geofoam embankment
4 text ;1 m concrete atop
4 text ;
4 text config dynamic extra 5
4 text ;
4 text ;
4 text ; GENERATION OF GRID
4 text ;

```
4 text grid 60 33
4 text model elastic j 1 11
4 text model elastic i 21 40 j 12
4 text model elastic i 21 40 j 14
4 text model elastic i 21 40 j 16
4 text model elastic i 21 40 j 18
4 text model elastic i 21 40 j 20
4 text model elastic i 21 40 j 22
4 text model elastic i 21 40 j 24
4 text model elastic i 21 40 j 26
4 text model elastic i 21 40 j 28
4 text model elastic i 21 40 j 30
4 text model elastic i 21 40 j 32
4 text ;
4 text ; NULLS OUT PARTS OF MODEL TO CREATE INTERFACES
4 text ;
4 text model null i 1 20 j 11 33
4 text model null i 41 60 j 11 33
4 text model null i 21 41 j 11
4 text model null i 21 41 j 12 33
4 text ;
4 text gen 0 0 0 10 60 10 60 0 j 1 11
4 text ;
4 text ; PROPERTIES FOR FOUNDATION SOIL
4 text prop bulk 290e6 shear 62.1e6 den 1840 i 1 60 j 1 9 ;foundation properties
4 text prop bulk 290e6 shear 62.1e6 den 1840 i 1 60 j 10 ;foundation properties
4 text ;
4 text ; GRAVITY ON FOR STATIC FORCES
4 text set grav 9.81
4 text ;
4 text ; BOUNDARY CONDITIONS FOR STATIC CASE
4 text ; fix right side of soil box
4 text fix x i 1 j 1 21
4 text ; fix left side of soil box
4 text fix x i 61 j 1 21
4 text ;fix base
4 text fix y j 1
4 text ; STATIC LOADING
4 text set dyn off
4 text his 20 unbal
4 text ;
4 text ; PLACES FOUNDATION SOIL
4 text ;
4 text step 2000
4 text ;
4 text ; MAPS ELEMENTS TO GRID POINTS FOR EMBANKMENT
```

```
 4 text ;
 4 text ; ADDS IN GEOFOAM
 4 text model elastic i 21 40 j 12
 4 text model elastic i 21 40 j 14
 4 text model elastic i 21 40 j 16
 4 text model elastic i 21 40 j 18
 4 text model elastic i 21 40 j 20
 4 text model elastic i 21 40 j 22
 4 text model elastic i 21 40 j 24
 4 text model elastic i 21 40 j 26
 4 text ;
 4 text ;
 4 text gen 20 10 20 11 40 11 40 10 i 21 41 j 12 13
 4 text gen 20 11 20 12 40 12 40 11 i 21 41 j 14 15
 4 text gen 20 12 20 13 40 13 40 12 i 21 41 j 16 17
 4 text gen 20 13 20 14 40 14 40 13 i 21 41 j 18 19
 4 text gen 20 14 20 15 40 15 40 14 i 21 41 j 20 21
 4 text gen 20 15 20 16 40 16 40 15 i 21 41 j 22 23
 4 text gen 20 16 20 17 40 17 40 16 i 21 41 j 24 25
 4 text gen 20 17 20 18 40 18 40 17 i 21 41 j 26 27
 4 text ;
 4 text ; CREATES INTERFACES FOR SLIDE PLANES
 4 text ;
 4 text int 1 Aside from 21,11 to 41,11 Bside from 21,12 to 41,12
 4 text int 2 Aside from 21,13 to 41,13 Bside from 21,14 to 41,14
 4 text int 3 Aside from 21,15 to 41,15 Bside from 21,16 to 41,16
 4 text int 4 Aside from 21,17 to 41,17 Bside from 21,18 to 41,18
 4 text int 5 Aside from 21,19 to 41,19 Bside from 21,20 to 41,20
 4 text int 6 Aside from 21,21 to 41,21 Bside from 21,22 to 41,22
 4 text int 7 Aside from 21,23 to 41,23 Bside from 21,24 to 41,24
 4 text int 8 Aside from 21,25 to 41,25 Bside from 21,26 to 41,26
 4 text ;
 4 text ; INTERFACE PROPERTIES
 4 text ;
 4 text ;; inteface node conditions at sliding planes
 4 text int 1 glue kn 102e6 ks 102e6 friction = 31 coh = 0 dil = 10 tbond=0 bslip on ;
geofoam/soil
 4 text int 2 kn 102e6 ks 102e6 friction = 38 coh = 0 dil = 0 tbond=0 bslip on ; geofoma/geofoam
 4 text int 3 kn 102e6 ks 102e6 friction = 38 coh = 0 dil = 0 tbond=0 bslip on
 4 text int 4 kn 102e6 ks 102e6 friction = 38 coh = 0 dil = 0 tbond=0 bslip on
 4 text int 5 kn 102e6 ks 102e6 friction = 38 coh = 0 dil = 0 tbond=0 bslip on
 4 text int 6 kn 102e6 ks 102e6 friction = 38 coh = 0 dil = 0 tbond=0 bslip on
 4 text int 7 kn 102e6 ks 102e6 friction = 38 coh = 0 dil = 0 tbond=0 bslip on
 4 text int 8 kn 102e6 ks 102e6 friction = 38 coh = 0 dil = 0 tbond=0 bslip on ; geofoam/geofoam
 4 text ;
 4 text ;
```

```
 4 text ; GEOFOAM PROPERTIES
 4 text ;
 4 text prop bulk 4.5e6 shear 4.2e6 den 18 i 22 39 j 12 26
 4 text prop bulk 4.5e6 shear 4.2e6 den 18 i 21 j 12 26
 4 text prop bulk 4.5e6 shear 4.2e6 den 18 i 40 j 12 26
 4 text ;
 4 text ;
 4 text step 2000
 4 text ;
 4 text ;
 4 text ; ADDS IN LDS
 4 text ;
 4 text model mohr i 21 40 j 28
 4 text gen 20 18 20 19 40 19 40 18 i 21 41 j 28 29
 4 text int 9 Aside from 21,27 to 41,27 Bside from 21,28 to 41,28
 4 text int 9 kn 102e6 ks 102e6 friction = 38 coh = 0 dil = 0 tbond=0 bslip on ; geofoam/lds
 4 text prop bulk 15625e6 shear 12712e6 den 2305 friction = 0 cohesion = 25e6 tension = 25e6
dilation = 0 i 21 40 j 27 28 ; lumped properties
 4 text ;
 4 text step 13000
 2 state
 3 file dynamic1up
 3 batch
 4 text ;; DYNAMIC LOADING
 4 text ;
 4 text set dynamic on
 4 text set large
 4 text ;
 4 text ini dy_damp=hyst default -3.156 1.904 j 1 11; CLAY
 4 text ini dy_damp=hyst sig3 1 -0.45 .3 j 12 26; GEOFOAM
 4 text ini dy_damp=rayl 0.05 200
 4 text ;
 4 text ; WAVE DEFINITION
 4 text ;wave 1 is horizontal wave
 4 text ;
 4 text ;def wave1
 4 text ;    for free vibration
 4 text ;      wave1=amp1*sin(2*pi/period1*dytime)
 4 text ;    for forced vibration
 4 text ;      wave1=amp1*sin(2*pi/period1*dytime)
 4 text ;end
 4 text ;set amp1 = 600
 4 text ;set period1 = .5 ; fundamental period of geofoam
 4 text ;
 4 text ;
 4 text ;wave 2 is vertical wave
```

```
4 text ;
4 text ;def wave2
4 text ;    for free vibration
4 text ;      wave2=amp2*sin(2*pi/period2*dytime)
4 text ;    for forced vibration
4 text ;      wave2=amp2*sin(2*pi/period2*dytime)
4 text ;end
4 text ;set amp2 = 50
4 text ;set period2 = .1
4 text ;
4 text ;
4 text ;
4 text def rel1
4 text     rel1 = xdisp(31,14) - xdisp(31,13)
4 text end
4 text def rel2
4 text     rel2 = xdisp(31,16) - xdisp(31,15)
4 text end
4 text def rel3
4 text     rel3 = xdisp(31,18) - xdisp(31,17)
4 text end
4 text def rel4
4 text     rel4 = xdisp(31,20) - xdisp(31,19)
4 text end
4 text def rel5
4 text     rel5 = xdisp(31,22) - xdisp(31,21)
4 text end
4 text def rel6
4 text     rel6 = xdisp(31,24) - xdisp(31,23)
4 text end
4 text def rel7
4 text     rel7 = xdisp(31,26) - xdisp(31,25)
4 text end
4 text def rel8
4 text     rel8 = xdisp(31,28) - xdisp(31,27)
4 text end
4 text def reltotal
4 text     reltotal=rel1+rel2+rel3+rel4+rel5+rel6+rel7+rel8
4 text end
4 text ;
4 text ;
4 text ;BOUNDARIES FOR DYNAMIC CASE
4 text ;
4 text apply ff i 1 j 11
4 text apply xquiet j 1
4 text apply yquiet j 1
```

```
4 text ;
4 text ;
4 text ;
4 text ; HISTORIES
4 text ;
4 text his 1  dytime
4 text ;his 2  wave1
4 text his 3  xvel j 1 i 31
4 text his 4  xdisp j 1 i 31
4 text his 5  xvel j 11 i 31
4 text his 6  xdisp j 11 i 31
4 text his 7  xvel j 29 i 31
4 text his 8  xdisp j 29 i 31
4 text his 9  xacc j 1 i 31; soil base
4 text his 10 xacc j 29 i 31; geofoam top
4 text his 11 xacc j 11 i 31; geofoam base
4 text his 12 yacc j 1 i 31; soil base
4 text his 13 yacc j 29 i 31; geofoam top
4 text his 14 yacc j 11 i 31; geofoam base
4 text ;his 15 wave2
4 text his 16 xacc j 11 i 11; free field x acc
4 text his 17 yacc j 11 i 11; free field y acc
4 text his 160 rel1
4 text his 170 rel2
4 text his 180 rel3
4 text his 190 rel4
4 text his 200 rel5
4 text his 210 rel6
4 text his 220 rel7
4 text his 230 rel8
4 text his 240 reltotal
4 text ;;
4 text ;;FOR SINUSODIAL WAVE ONLY
4 text ;apply sxy -2e3 hist=wave1 j=1
4 text ;apply syy -2e3 hist=wave2 j=1
4 text ;displment to; zero before dynamic model starts
4 text ini xdisp = 0 ydisp=0 ;
4 text ;
4 text ;FOR INPUT VELOCITY RECORD
4 text his read 100 eq1vel.flc
4 text his read 300 eq1upvel.flc
4 text apply sxy -337983 hist=100 j=1
4 text apply syy -430000 hist=300 j=1
4 text ;apply syy 828379 hist=300 j=1
4 text ;
4 text set dytime = 0
```

4 text solve step 100000000 dytime= 18
0 eof

```
; rocking evalutions
0 header
1 code FLAC 5.0
1 source giic v2.0.393
1 date Wed Apr 02 11:20:33 MST 2008
1 type giic-save
0 flac
1 config
2 axisym false
2 gwflow false
2 pstress false
2 cppudm false
2 ats false
2 creep false
2 dynamic true
2 thermal false
2 twophase false
2 extra 5
2 units 0
2 struct false
2 advanced false
2 water false
2 interface false
2 gravity true
2 excludereg false
2 solvefos false
2 record 2
0 plots
1 plot 2
2 display
3 viewport
4 autorange true
2 command plot pen history 20
2 name unbal
2 alias
2 title
2 count 1
2 item
3 name 20
1 plot 0
2 display
3 viewport
4 autorange true
2 command plot pen  apply state block grid displacement
2 name vectors
2 title
```

2 count 4
2 item
3 name apply
3 switch 3
2 item
3 name state
3 switch 12
3 mode 2
2 item
3 name grid
3 switch 2
2 item
3 name displacement
3 switch 3
1 plot 2
2 display
3 viewport
4 xrange -1.0E20,1.0E20
4 yrange -1.0E20,1.0E20
2 command plot pen history 2 vs 1
2 name h wave
2 alias
2 title
2 versus 1
2 count 1
2 item
3 name 2
1 plot 2
2 display
3 viewport
4 autorange true
2 command plot pen history 4 line vs 1
2 name x disp bot
2 alias
2 title
2 versus 1
2 count 1
2 item
3 name 4
3 line
1 plot 2
2 display
3 viewport
4 autorange true
2 command plot pen history 6 line vs 1
2 name x disp geofoam bot

2 alias
2 title
2 versus 1
2 count 1
2 item
3 name 6
3 line
1 plot 2
2 display
3 viewport
4 autorange true
2 command plot pen history 8 line vs 1
2 name x disp geofoam top
2 alias
2 versus 1
2 count 1
2 item
3 name 8
3 line
1 plot 2
2 display
3 viewport
4 autorange true
2 command plot pen history 16 vs 1
2 name x acc ff
2 alias
2 versus 1
2 count 1
2 item
3 name 16
1 plot 2
2 display
3 viewport
4 autorange true
2 command plot pen history 10 line 11 vs 1
2 name x acc geofoam top
2 alias
2 versus 1
2 count 2
2 item
3 name 10
3 line
2 item
3 name 11
1 plot 2
2 display

3 viewport
4 autorange true
2 command plot pen history 11 line vs 1
2 name x acc geofoam base
2 alias
2 versus 1
2 count 1
2 item
3 name 11
3 line
1 plot 2
2 display
3 viewport
4 xrange 0.0,1.0
4 yrange 0.0,1.0
2 command plot pen history 15 line vs 1
2 name v wave
2 alias
2 versus 1
2 count 1
2 item
3 name 15
3 line
1 plot 2
2 display
3 viewport
4 autorange true
2 command plot pen history 12 line vs 1
2 name y acc base
2 alias
2 versus 1
2 count 1
2 item
3 name 12
3 line
1 plot 2
2 display
3 viewport
4 autorange true
2 command plot pen history 13 line vs 1
2 name y acc geofoam top
2 alias
2 versus 1
2 count 1
2 item
3 name 13

3 line
1 plot 2
2 display
3 viewport
4 autorange true
2 command plot pen history 14 line vs 1
2 name y acc geofoam base
2 alias
2 versus 1
2 count 1
2 item
3 name 14
3 line
1 plot 2
2 display
3 viewport
4 autorange true
2 command plot pen history 11 line 14 line vs 1
2 name x & y accel geofoam base
2 alias
2 versus 1
2 count 2
2 item
3 name 11
3 line
2 item
3 name 14
3 line
1 plot 2
2 display
3 viewport
4 autorange true
2 command plot pen history 160 line 170 line 180 line 190 line 200 line 210 line 220 line 230 line 240 line vs 1
2 name reldisp1
2 alias
2 versus 1
2 count 9
2 item
3 name 160
3 line
2 item
3 name 170
3 line
2 item
3 name 180

3 line
2 item
3 name 190
3 line
2 item
3 name 200
3 line
2 item
3 name 210
3 line
2 item
3 name 220
3 line
2 item
3 name 230
3 line
2 item
3 name 240
3 line
1 plot 2
2 display
3 viewport
4 autorange true
2 command plot pen history 17 line vs 1
2 name y acc ff
2 alias
2 versus 1
2 count 1
2 item
3 name 17
3 line
1 plot 2
2 display
3 viewport
4 autorange true
2 command plot pen history 18 line vs 1
2 name relvert1
2 alias
2 versus 1
2 count 1
2 item
3 name 18
3 line
1 plot 2
2 display
3 viewport

4 autorange true
2 command plot pen history 19 vs 1
2 name relvert2
2 alias
2 versus 1
2 count 1
2 item
3 name 19
0 matlist
0 CppModels
0 project tree
1 title sylmar
1 notes
1 tree
2 state
3 file static1rockup
3 batch
4 text ;8 m high by 20 m wide geofoam embankment
4 text ;1 m concrete atop
4 text ;
4 text config dynamic extra 5
4 text ;
4 text ;
4 text ; GENERATION OF GRID
4 text ;
4 text grid 60 33
4 text model elastic j 1 11
4 text model elastic i 21 40 j 12
4 text model elastic i 21 40 j 14
4 text model elastic i 21 40 j 16
4 text model elastic i 21 40 j 18
4 text model elastic i 21 40 j 20
4 text model elastic i 21 40 j 22
4 text model elastic i 21 40 j 24
4 text model elastic i 21 40 j 26
4 text model elastic i 21 40 j 28
4 text model elastic i 21 40 j 30
4 text model elastic i 21 40 j 32
4 text ;
4 text ; NULLS OUT PARTS OF MODEL TO CREATE INTERFACES
4 text ;
4 text model null i 1 20 j 11 33
4 text model null i 41 60 j 11 33
4 text model null i 21 41 j 11
4 text model null i 21 41 j 12 33
4 text ;

```
4 text gen 0 0 0 10 60 10 60 0 j 1 11
4 text ;
4 text ; PROPERTIES FOR FOUNDATION SOIL
4 text ;prop bulk 290e6 shear 62.1e6 den 1840 i 1 60 j 1 10 ;foundation properties
4 text prop bulk 667e6 shear 143e6 den 1840 i 1 60 j 1 10 ;foundation properties
4 text ;
4 text ; GRAVITY ON FOR STATIC FORCES
4 text set grav 9.81
4 text ;
4 text ; BOUNDARY CONDITIONS FOR STATIC CASE
4 text ; fix right side of soil box
4 text fix x i 1 j 1 21
4 text ; fix left side of soil box
4 text fix x i 61 j 1 21
4 text ;fix base
4 text fix y j 1
4 text ; STATIC LOADING
4 text set dyn off
4 text his 20 unbal
4 text ;
4 text ; PLACES FOUNDATION SOIL
4 text ;
4 text step 2000
4 text ;
4 text ; MAPS ELEMENTS TO GRID POINTS FOR EMBANKMENT
4 text ;
4 text ; ADDS IN GEOFOAM
4 text model mohr i 21 40 j 12
4 text model mohr i 21 40 j 14
4 text model mohr i 21 40 j 16
4 text model mohr i 21 40 j 18
4 text model mohr i 21 40 j 20
4 text model mohr i 21 40 j 22
4 text model mohr i 21 40 j 24
4 text model mohr i 21 40 j 26
4 text ;
4 text ;
4 text gen 20 10 20 11 40 11 40 10 i 21 41 j 12 13
4 text gen 20 11 20 12 40 12 40 11 i 21 41 j 14 15
4 text gen 20 12 20 13 40 13 40 12 i 21 41 j 16 17
4 text gen 20 13 20 14 40 14 40 13 i 21 41 j 18 19
4 text gen 20 14 20 15 40 15 40 14 i 21 41 j 20 21
4 text gen 20 15 20 16 40 16 40 15 i 21 41 j 22 23
4 text gen 20 16 20 17 40 17 40 16 i 21 41 j 24 25
4 text gen 20 17 20 18 40 18 40 17 i 21 41 j 26 27
4 text ;
```

```
 4 text ; CREATES INTERFACES FOR SLIDE PLANES
 4 text ;
 4 text int 1 Aside from 21,11 to 41,11 Bside from 21,12 to 41,12
 4 text int 2 Aside from 21,13 to 41,13 Bside from 21,14 to 41,14
 4 text int 3 Aside from 21,15 to 41,15 Bside from 21,16 to 41,16
 4 text int 4 Aside from 21,17 to 41,17 Bside from 21,18 to 41,18
 4 text int 5 Aside from 21,19 to 41,19 Bside from 21,20 to 41,20
 4 text int 6 Aside from 21,21 to 41,21 Bside from 21,22 to 41,22
 4 text int 7 Aside from 21,23 to 41,23 Bside from 21,24 to 41,24
 4 text int 8 Aside from 21,25 to 41,25 Bside from 21,26 to 41,26
 4 text ;
 4 text ; INTERFACE PROPERTIES
 4 text ;
 4 text ;; inteface node conditions at sliding planes
 4 text int 1 kn 102e6 ks 102e6 friction = 89 ; geofoam/soil
 4 text ;int 1 kn 102e6 ks 102e6 friction = 31 ; geofoam/soil
 4 text int 2 kn 102e6 ks 102e6 tbond=117.5e3 sbr = 1.35 bslip off friction = 38 ;
geofoma/geofoam
 4 text int 3 kn 102e6 ks 102e6 tbond=117.5e3 sbr = 1.35 bslip off friction = 38
 4 text int 4 kn 102e6 ks 102e6 tbond=117.5e3 sbr = 1.35 bslip off friction = 38
 4 text int 5 kn 102e6 ks 102e6 tbond=117.5e3 sbr = 1.35 bslip off friction = 38
 4 text int 6 kn 102e6 ks 102e6 tbond=117.5e3 sbr = 1.35 bslip off friction = 38
 4 text int 7 kn 102e6 ks 102e6 tbond=117.5e3 sbr = 1.35 bslip off friction = 38
 4 text int 8 kn 102e6 ks 102e6 tbond=117.5e3 sbr = 1.35 bslip off friction = 38 ;
geofoma/geofoam
 4 text ;
 4 text ;
 4 text ; GEOFOAM PROPERTIES
 4 text ;
 4 text prop bulk 4.5e6 shear 4.2e6 den 18 coh 159e3 ten 117.5e3 i 21 40 j 12 26
 4 text ;
 4 text ;
 4 text ;
 4 text step 2000
 4 text ;
 4 text ;
 4 text ; ADDS IN LDS
 4 text ;
 4 text model mohr i 21 40 j 28
 4 text gen 20 18 20 19 40 19 40 18 i 21 41 j 28 29
 4 text int 9 Aside from 21,27 to 41,27 Bside from 21,28 to 41,28
 4 text int 9 kn 102e6 ks 102e6 tbond=117e3 sbr = 0.6 bslip off friction = 38 ; geofoam/lds
 4 text prop bulk 15625e6 shear 12712e6 den 2305 friction = 0 cohesion = 25e6 tension = 25e6 i
21 40 j 27 28 ; lumped properties
 4 text ;
 4 text step 13000
```

```
2 state
3 file dynamic1rockup
3 batch
4 text ;; DYNAMIC LOADING
4 text ;
4 text set dynamic on
4 text set large
4 text ;
4 text ini dy_damp=hyst default -3.156 1.904 j 1 11; CLAY
4 text ini dy_damp=hyst sig3 1 -0.45 .3 j 12 26; GEOFOAM
4 text ini dy_damp=rayl 0.05 200
4 text ;
4 text ; WAVE DEFINITION
4 text ;wave 1 is horizontal wave
4 text ;
4 text ;def wave1
4 text ;    for free vibration
4 text ;      wave1=amp1*sin(2*pi/period1*dytime)
4 text ;    for forced vibration
4 text ;      wave1=amp1*sin(2*pi/period1*dytime)
4 text ;end
4 text ;set amp1 = 600
4 text ;set period1 = .5 ; fundamental period of geofoam
4 text ;
4 text ;
4 text ;wave 2 is vertical wave
4 text ;
4 text ;def wave2
4 text ;    for free vibration
4 text ;      wave2=amp2*sin(2*pi/period2*dytime)
4 text ;    for forced vibration
4 text ;      wave2=amp2*sin(2*pi/period2*dytime)
4 text ;end
4 text ;set amp2 = 50
4 text ;set period2 = .1
4 text ;
4 text ;
4 text ;
4 text def rel1
4 text     rel1 = xdisp(31,14) - xdisp(31,13)
4 text end
4 text def rel2
4 text     rel2 = xdisp(31,16) - xdisp(31,15)
4 text end
4 text def rel3
4 text     rel3 = xdisp(31,18) - xdisp(31,17)
```

```
4 text end
4 text def rel4
4 text     rel4 = xdisp(31,20) - xdisp(31,19)
4 text end
4 text def rel5
4 text     rel5 = xdisp(31,22) - xdisp(31,21)
4 text end
4 text def rel6
4 text     rel6 = xdisp(31,24) - xdisp(31,23)
4 text end
4 text def rel7
4 text     rel7 = xdisp(31,26) - xdisp(31,25)
4 text end
4 text def rel8
4 text     rel8 = xdisp(31,28) - xdisp(31,27)
4 text end
4 text def reltotal
4 text     reltotal=rel1+rel2+rel3+rel4+rel5+rel6+rel7+rel8
4 text end
4 text def relvert1
4 text     relvert1 = ydisp(21,12) - ydisp(21,11)
4 text end
4 text def relvert2
4 text     relvert2 = ydisp(41,12) - ydisp(41,11)
4 text end
4 text ;
4 text ;
4 text ;BOUNDARIES FOR DYNAMIC CASE
4 text ;
4 text apply ff i 1 j 11
4 text apply xquiet j 1
4 text apply yquiet j 1
4 text ;
4 text ;
4 text ;
4 text ; HISTORIES
4 text ;
4 text his 1  dytime
4 text ;his 2  wave1
4 text his 3  xvel j 1 i 31
4 text his 4  xdisp j 1 i 31
4 text his 5  xvel j 11 i 31
4 text his 6  xdisp j 11 i 31
4 text his 7  xvel j 29 i 31
4 text his 8  xdisp j 29 i 31
4 text his 9  xacc j 1 i 31; soil base
```

```
4 text his 10 xacc j 29 i 31; geofoam top
4 text his 11 xacc j 11 i 31; geofoam base
4 text his 12 yacc j 1 i 31; soil base
4 text his 13 yacc j 29 i 31; geofoam top
4 text his 14 yacc j 11 i 31; geofoam base
4 text ;his 15 wave2
4 text his 16 xacc j 11 i 11; free field x acc
4 text his 17 yacc j 11 i 11; free field y acc
4 text his 18 relvert1
4 text his 19 relvert2
4 text his 160 rel1
4 text his 170 rel2
4 text his 180 rel3
4 text his 190 rel4
4 text his 200 rel5
4 text his 210 rel6
4 text his 220 rel7
4 text his 230 rel8
4 text his 240 reltotal
4 text ;;
4 text ;;FOR SINUSODIAL WAVE ONLY
4 text ;apply sxy -2e3 hist=wave1 j=1
4 text ;apply syy -2e3 hist=wave2 j=1
4 text ;displment to; zero before dynamic model starts
4 text ini xdisp = 0 ydisp=0 ;
4 text ;FOR INPUT VELOCITY RECORD
4 text his read 100 eq1vel.flc
4 text his read 300 eq1upvel.flc
4 text apply sxy -337983 hist=100 j=1
4 text apply syy -430000 hist=300 j=1
4 text ;apply syy 828379 hist=300 j=1
4 text ;
4 text set dytime = 0
4 text solve step 100000000 dytime= 18
0 eof
```